الجمهورية الجزائرية الديمقراطية الشعبية
People's Democratic Republic of Algeria
وزارة التعـليـم العالي والـبحـث الـعلـمي
Ministry of Higher Education and Scientific Research
جامـعة الشهيد حمة لخضر الوادي
University of Echahid Hamma Lakhdar -El OUED
كلية العلوم الطبيعية الحياة
Faculty of Natural and Life Sciences
قسم البيولوجيا الخلوية والجزيئية
Department of Cellular and Molecular Biology

THESIS

SUBMITTED TO OBTAIN 3rd CYCLE LMD DOCTORATE DEGREE IN

BIOCHEMISTRY

Speciality: Applied Biochemistry

THEME

Green synthesis and characterization of silver nanoparticles based on *Helianthemum lippii* L. extract and evaluation of their biological activities

Presented by: Ms. LAIB Ibtissam

Graduated 09/03/2023

Jury Members:

Mrs. MEDILA Ifriqya	**AP**	**University of El-Oued**	**Presisent**
Mr. DJAHRA Ali Boutlelis	**Professor**	**University of El-Oued**	**Rapportor**
Mr. LAOUINI Salah Eddine	**Professor**	**University of El-Oued**	**Examiner**
Mrs. HAMMOUDI Roukia	**AP**	**University of Ouargla**	**Examiner**
Mr. BENKHERARA Salah	**AP**	**University of Ghardaia**	**Examiner**

2022/2023

Acknowledgements

I thank **God** Almighty, a great, good and blessed thank you, filling the heavens and the earth, for what He has bestowed upon me to complete this humble work, and prayers and peace be upon His Prophet Muhammad, his family and companions.

All thanks and appreciation to my mother for standing with me, for here I am continuing my life's journey and I have reached what I have long dreamed of, and this would not have happened without God's success and the support of my family

At the outset, I would like to thank my supervisor, Pr. DJAHRA Ali Boutelis, for allowing me to conduct my doctoral research under his supervision; for ongoing support, valuable efforts, and scientific guidance and encouragement throughout my research; and for his beneficial comments and discussion, which contributed to the creation and completion of this thesis.

Wish to extend my sincere thanks to Dr. MEDILA Ifriqya, AP at the University of El Oued, for accepting to chair the dissertation of my thesis. I would also like to thank the committee members: Pr.LAOUINI Salah Eddine, Dr.HAMMOUDI Rokia, and Dr.BENKHERARA Salah for agreeing to examine and judge my work.

Success has people who appreciate its meaning, and creativity has people who reap it. Phrases crowd together, to organize the thank you contract for the honorable Dr. MEHDA Ismail. I give you all the praise and appreciation, with the number of raindrops, the color of the blossom, and the fragrance of perfume for your precious and valuable efforts and for your scientific guidance

A salute of honor to those who gave us a lot, Pr. CHOUIKH Atef , Director of the Biology, Environment and Health Laboratory, and for all his efforts to provide the laboratory's requirements.

I do not forget to express my thanks to Dr. HAMIDA Othman for anatomy and pathology cytology for providing assistance.

I do not find in my heart what I carry for you except love, gratitude, and thanks for raising my determination and morale and for all that, you have given me, my dear brother Faissal

My thanks go to my fellow PhD students, and dearest friends GHARAISSA Noura, BOUDABIA Wafaa, Dr. ALIA Fatima, DJAOUIDI Anfal and Dr. BOUSBIA BRAHIM Aida

Ibtissam LAIB

My dear father's soul

To my dear Mather

To my brothers and sister

To all my friends

To all those who are dear to me

ABSTRACT

In this context, The main objective of this work is to green synthesis of AgNPs from *H.lippii* aqueous extract and to evaluate the biological effects of *H.lippii* plant and silver nanoparticles *in vitro* and as well as *in vivo* in order to look into their potential therapeutic effects against the physiological and biochemical changes brought on by sub-chronic exposure to cadmium chloride in rats. For this purpose, quantitative, qualitative, and extraction bioactive compounds standard procedures were applied. While identification and quantification of individual phenolic compounds were performed by HPLC analysis. On the other hand, has been of AgNPs green synthesis and characterization by different methods (UV, FTIR, XRD, and SEM). In addition, *in vitro* activities Evaluation has been done via antioxidant, anti-inflammatory, Hemolytic, and antibacterial activities, Meanwhile, Spectrophotometric, Voltammetric studies of the binding interaction of AgNPs with deoxyribonucleic acid and bovine serum albumin under similar condition. In regards to studying in vivo, 35 Wistar male rats were divided into seven groups (5 rats in each): Control, *H.lippii*, $CdCl_2$, $CdCl_2$+*H.lippii*, AgNPs, $CdCl_2$+AgNPs, and $CdCl_2$+*H.lippii*+AgNPs. $CdCl_2$ (50mg/Kg) was added in drinking water for 35 day. The therapeutic systems were received intragastrically for *H.lippii* (100 mg/kg b.w) and AgNPs were supplemented intraperitoneally at 0.1mg/kg for the last 15 days. Some biochemical, hematological, oxidative stress markers and histopathology were observed

The phytochemical analysis revealed the presence of most of the phenolic compounds, Further, *H. lippii* had high levels of total phenolics (183.12±2.84mg GA eq/g dry Ex) and flavonoid contents (72.00±1.03 mg QE/mg Ex), as well as saponins (82.2± 33.00 mg DO eq/g dry Ex), and of tannins (Total hydrolyzable tannin; 2.818±0.138mgTA eq/g dry Ex, Condensed tannin; (5.88±1.58 mg Ca eq/g dry Ex) and anthocyanins (4.256±0.590 mg C-3-GE/g dry Ex). HPLC analysis identified six phenolic compounds in high concentration, mainly gallic acid and chlorogenic acid. According to, the absorption peak at 428 nm characterized the synthesized silver nanoparticles, the crystalline nature of AgNP was confirmed by XRD patterns, and SEM analysis revealed that the majority of the nanoparticles were spherical in shape. While investigations using FT-IR technique confirmed the presence of many functional groups that are involved in covering and reducing AgNPs. In addition, *H.lippii* and AgNPs demonstrated strong efficiency as antioxidant, and anti-inflammatory, while providing moderate protection for red blood cells. On the other hand, they showed good antibacterial activity against six types of selected bacteria. Moreover, the results show that there is a spontaneous interaction between AgNPs and DNA as well as BSA via electrostatic interactions, translated by parameters K and ΔG. On the other hand, according to the results obtained *in vivo*, there was a decrease in the body weight gain. An increase in the relative weight of the liver, kidneys, heart and brain, with a decrease in the absolute and relative weight of the testicle. Moreover, the findings in cadmium chloride-treated rats induced significant changes in hematological and biochemical, hormonal parameters, hepatic enzyme markers, and renal function compared to the control group. These changes were accompanied by a decrease in antioxidant defense (GSH, SOD, and CAT) and an increase in MDA levels. The data clearly showed the deterioration of the structure of the studied tissues in comparison with the control group, including severe deterioration of liver and kidney cells, while testicular tissues showed severe necrosis. However, the treatment with *H.lippii* and/or AgNPs mitigated most of toxic effects and the restored all previous variable parameters.

Finally, this study demonstrated the promising biological activity of *H.lippii* and AgNPs, Meanwhile, it is worth noting the strong therapeutic potential of *H.lippii* and AgNPs against cadmium chloride-induced toxicity in rats, which opens new avenues for the use of phytotherapy and nanotherapy and enhances their application in approaches medical.

Keywords: *Helianthemum lippii*, silver nanoparticles, green synthesis, biological activities, cadmium chloride, Wistar rats.

الملخص

في هذا السياق ، الهدف الرئيسي من هذا العمل هو تخليق الأخضر لجسيمات الفضة النانوية من مستخلص نبات السمهري وتقييم الآثار البيولوجية لنبات السمهري وجسيمات الفضة النانوية في المختبر وكذلك في الجسم الحي من أجل النظر في التأثيرات العلاجية المحتملة ضد التغيرات الفسيولوجية والكيميائية الحيوية الناجمة عن التعرض شبه المزمن لكلوريد الكادميوم في الفئران. لهذا الغرض ، تم تطبيق الإجراءات القياسية الكمية والنوعية واستخراج المركبات النشطة بيولوجيا. بينما تم إجراء تحديد وتقدير المركبات الفينولية الفردية عن طريق تحليل HPLC. من ناحية أخرى ، تم التوليف الأخضر وتوصيف AgNPs بطرق مختلفة (UV و FTIR و XRD و SEM). بالإضافة إلى ذلك ، تم تقييم النشاط في المختبر عن طريق مضادات الأكسدة ، ومضادات الالتهاب ، وانحلال الدم ، ومضاد البكتيريا ، وفي الوقت نفسه ، دراسات قياس الطيف الضوئي ، الفولتميترية للتفاعل الملزم لـ AgNPs مع الحمض النووي المنقوص الاوكسجين وألبومين المصل البقري تحت ظروف مماثلة.

بالنسبة للدراسة في الجسم الحي، تم تقسيم 35 جرذًا من الجرذان البيضاء إلى سبع مجموعات من 5 فئران لكل منها: الشاهد، *H.lippi*، $CdCl_2$، $CdCl_2$ + *H.lippii*، AgNPs، $CdCl_2$+AgNPs ، و $CdCl_2$+*H.lippii*+AgNPs. تمت إضافة كلوريد الكادميوم (50 ملغ/ كلغ) في ماء الشرب لمدة 5 أسابيع. تم تلقي الأنظمة العلاجية (100 ملغ/كغ من وزن الجسم) داخل المعدة من السمهري وتم استعمال الجسيمات الفضة النانوية داخل الصفاق بجرعة(0.1 ملغ/ كلغ) خلال آخر 15 يومًا. تم تحديد بعض مؤشرات الإجهاد الكيميائي الحيوي، الدموي، والاجهاد التأكسدي. كما تمت الملاحظة المجهرية للانسجة من الكبد الكلى والخصية

أظهر التحليل الكيميائي النباتي وجود معظم المركبات الفينولية ، علاوة على ذلك ، كان لدى السمهري مستويات عالية من إجمالي الفينولات (183.12 ± 2.84 ملغ مكافئ حمض الغاليك/ غ من المادة الجافة) ومحتويات الفلافونويد (72.00 ± 1.03 ملغ مكافئ من الكيرسيتين / غ من المادة الجافة) ، بالإضافة إلى الصابونين (82.2 ± 33.00 ملغ DO مكافئ /غ من المادة الجافة) ، ومستويات منخفضة من التانين (إجمالي التانين المتحلل بالماء ؛ 2.818 ± 0.138 ملغ مكافئ لحمض التانيك/ غ من المادة الجافة ، مكثف التانين ؛ (5.88 ± 1.58ملغ مكافئ كاتيشين / غ من المادة الجافة) والأنثوسيانين (4.256 ± 0.590 ملغ مكافئ من سيانيدين 3 جلوكوزيد C-3-GE /غ من المادة الجافة) . فيما حدد تحليل HPLC ستة مركبات فينولية بتركيز مرتفع، خاصة حمض الجاليك وحمض الكلوروجينيك. بينما تميزت الجسيمات النانوية الفضية المركبة بذروة الامتصاص عند 428 نانومتر، تم تأكيد الطبيعة البلورية لـ AgNP بواسطة أنماط XRD، وكشف تحليل SEM أن غالبية الجسيمات النانوية كانت كروية الشكل. بينما أكدت التحقيقات باستخدام تقنية FT-IR وجود العديد من المجموعات الوظيفية التي تشارك في تغطية وتقليل AgNPs. بالإضافة إلى ذلك، أوضح السمهري و جسيمات الفضة النانوية فعالية قوية كمضاد للأكسدة، ومضاد للالتهابات، بينما يوفر حماية معتدلة لخلايا الدم الحمراء. من ناحية أخرى، أظهرا نشاطًا مضادًا للبكتيريا جيدًا ضد ستة أنواع من البكتيريا المنتقاة. علاوة على ذلك، تظهر النتائج أن هناك تفاعلًا تلقائيًا بين AgNPs والحمض النووي وكذلك BSA عبر التفاعلات الكهروستاتيكية، المترجمة بواسطة معلمات ال ثابت K وطاقة الترابط. من حهة اخرى ووفقًا للنتائج التي تم الحصول عليها في الجسم الحي، كان هناك انخفاض في زيادة وزن الجسم بسبب تلوث الكادميوم وزيادة الوزن النسبي للكبد والكلى والقلب والدماغ، مع انخفاض الوزن المطلق والنسبي للخصية. علاوة على ذلك، فإن النتائج التي توصلت إليها الفئران المعالجة ب كلوريد الكادميوم تسببت في حدوث تغيرات معنوية في المعلمات الدموية والكيميائية الحيوية، المعلمات الهرمونية, وعلامات الإنزيمات الكبدية، ووظيفة الكلى مقارنة بالمجموعة الضابطة. ترافقت هذه التغييرات مع انخفاض في الدفاع المضاد للأكسدة (GSH وSOD وCAT) وزيادة في مستويات MDA. أظهرت البيانات بوضوح تدهور بنية الأنسجة المدروسة بالمقارنة مع المجموعة الضابطة، بما في ذلك تدهور شديد في خلايا الكبد والكلى، بينما أظهرت أنسجة الخصية نخرًا شديدًا. ومع ذلك، فان النظام العلاج مع السمهري و / أو AgNPs خفف من معظم الآثار السمية وأعاد النظام العلاجي جميع المعلمات المتغيرة السابقة.

في الختام، أظهرت هذه الدراسة النشاط البيولوجي الواعد لنبات السمهري و جسيمات الفضة النانوية ، وفي الوقت نفسه، تجدر الإشارة إلى الإمكانات العلاجية القوية ل نبات السمهري وAgNPs ضد السمية المستحثة بواسطة كلوريد الكادميوم في الفئران، مما يفتح آفاقًا جديدة لاستخدام العلاج بالنباتات والعلاج بالنانو ويعزز تطبيقهما في النهج الطبي

الكلمات الدالة: نبات السمهري، الجسيمات الفضة النانوية، التوليف الأخضر، الأنشطة البيولوجية، كلوريد الكادميوم، فئران Wistar

RESUME

L'objectif principal de ce travail est de verdir la synthèse des AgNPs à partir d'extrait aqueux de *Helianthemum lippii* et d'évaluer les effets biologiques de la plante *H.lippii* et des nanoparticules d'argent in vitro et ainsi qu'in vivo afin d'examiner leurs effets thérapeutiques potentiels contre les modifications physiologiques et biochimiques provoquées par une exposition subchronique au chlorure de cadmium chez le rat. À cette fin, des procédures standard quantitatives, qualitatives et d'extraction des composés bioactifs ont été appliquées. Alors que l'identification et la quantification des composés phénoliques individuels ont été effectuées par HPLC. D'autre part, a été la synthèse verte et la caractérisation des AgNPs par différentes méthodes (UV, FTIR, XRD et SEM). En outre, l'évaluation de l'activité in vitro a été réalisée via des études antioxydantes, anti-inflammatoires, hémolytiques et antibactériennes, tandis que des études spectrophotométriques et voltamétriques de l'interaction de liaison des AgNPs avec l'acide désoxyribonucléique et l'albumine sérique bovine dans des conditions similaires. En ce qui concerne l'étude in vivo, 35 rats albinos wistar ont été divisés en sept groupes de 5 rats chacun:Contrôle,*H.lippii*,$CdCl_2$,$CdCl_2$+*H.lippii*,AgNPs,$CdCl_2$+AgNPs et CdCl2+*H.lippii*+AgNPs. CdCl2 (50mg/Kg) a été ajouté dans l'eau physiologie pendant 35 jour. Les systèmes thérapeutiques ont été reçus par voie intragastrique pour *H.lippii* (100 mg/kg de poids corporel) et les AgNPs ont été complétés par voie intrapéritonéale à 0,1 mg/kg pendant les 15 derniers jours. Certains marqueurs de stress biochimiques, hématologiques, oxydatifs ont été déterminés. L'histopathologie du foie, des reins et des testicules a été observée.

L'analyse phytochimique a révélé la présence de la plupart des composés phénoliques. De plus, *H. lippii* avait des niveaux élevés de composés phénoliques totaux (183.12 ± 2.84 mg GA eq / g Ex sec) et de flavonoïdes (72.00 ± 1.03 mg QE / mg Ex), ainsi que des saponines (82.2± 33.00 mg DO eq/g sec Ex), et de faibles teneurs en tanins (Total hydrolysable tannin ; 2,818±0,138mgTA eq/g sec Ex, Condensed tannin ; (5.88±1.58 mg Ca eq/g sec Ex) et des anthocyanes (4.256±0.590 mg C-3-GE/g sec Ex). L'analyse HPLC a identifié six composés phénoliques à forte concentration, principalement l'acide gallique et l'acide chlorogénique. Alors que le pic d'absorption à 428 nm caractérisait les nanoparticules d'argent synthétisées, la nature cristalline de l'AgNP a été confirmée par des modèles XRD, et l'analyse SEM a révélé que la majorité des nanoparticules étaient de forme sphérique. Alors que les enquêtes utilisant la technique FT-IR ont confirmé la présence de nombreux groupes fonctionnels impliqués dans la couverture et la réduction des AgNPs. De plus, *H.lippii* et AgNPs ont démontré une forte efficace comme antioxydant et anti-inflammatoire, tout en assurant une protection modérée des globules rouges. D'autre part, ils ont montré une bonne activité antibactérienne contre six souches de bactéries sélectionnées. De plus, les résultats montrent qu'il existe une interaction spontanée entre les AgNPs et l'ADN ainsi que la BSA via des interactions électrostatiques, traduites par les paramètres K et ΔG. D'autre part, selon les résultats obtenus in vivo, il y a eu une diminution de la prise de poids corporel. Une augmentation du poids relatif du foie, des reins, du cœur et du cerveau, avec une diminution du poids absolu et relatif du testicule. De plus, les résultats chez les rats traités au chlorure de cadmium ont induit des changements significatifs dans les paramètres hématologiques et biochimiques, les paramètres hormonaux, les marqueurs des enzymes hépatiques et la fonction rénale par rapport au groupe témoin. Ces changements se sont accompagnés d'une diminution de la défense antioxydante (GSH, SOD et CAT) et d'une augmentation des niveaux de MDA. Les données ont clairement montré la détérioration de la structure des tissus étudiés par rapport au groupe témoin, y compris une détérioration sévère des cellules hépatiques et rénales, tandis que les tissus testiculaires présentaient une nécrose sévère. Cependant, le traitement avec *H. lippii* et/ou AgNPs a atténué la plupart des effets toxique et restauré tous les paramètres variables précédents.

En fin , cette étude a démontré l'activité biologique prometteuse de la plante et des AgNPs, Parallèlement, il convient de noter le fort potentiel thérapeutique de *H.lippii* et des AgNPs contre la toxicité induite par le chlorure de cadmium chez le rat, ce qui ouvre de nouvelles voies pour l'utilisation de la phytothérapie et la nanothérapie et valorise leur application dans les approches médicales.

Mots clés : *Helianthemum lippii*, nanoparticules d'argent, synthèse verte, activités biologiques, chlorure de cadmium, rats Wistar.

LIST OF FIGURES

LIST OF TABLES

LIST OF ABBREVIATION

ΔG	Free energy
AFM	Atomic force microscopy
Ag^+	Silver ion
AgNPs	Silver nanoparticles
$AlCl_3$	Aluminum chloride
ALP	Alkaline phosphatase
AP-1	Activator protein 1
ATCC	American Type Culture Collection
Au^+	Gold cation
BHT	Butylated Hydroxy Toluene
BSA	Bovin Serum Albumin
CAT	Catalase
$CdCl_2$	Cadmium Chloride
C-JNK	c-Jun N-terminal Kinase
c-Src	Proto-oncogene tyrosine-protein kinase Src
CV	Cyclic voltammetry
DLS	Dynamic light scattering
DMSO	Dimethyl sulfoxide
DNA	Deoxyribonucleic acid
DPPH•	2,2-diphenyl-1-picrylhydrazyl
DTNB	5,5′-Dithiobis-(2-nitrobenzoic acid)
EDS	Energy dispersive spectroscopy
EDTA	Ethylenediaminetetraacetic acid
EDX	Energy Dispersive X-ray
FAK	Focal adhesion kinase
$FeCl_3$	Ferric chloride
FTIR	Fourier Transform Infrared Spectrometer
GPx	Glutathione Peroxidase
GSH	Glutathione
H_2O_2	Hydrogen peroxide
HO•	Hydroxyl radical
IL-1	Interleukin-1
Ipa	Anodic peak current
LDH	Lactate dehydrogenase

LPO	Lipid peroxidation
MAPK	Mitogen-activated protein kinase
MDA	Malondialdehyde
MHB	Mueller Hinton Broth
Mo (VI)	Tetraoxomolybdate
NBT	Nitro-blue tetrazolium chloride
NF-Kb	Nuclear factor kappa-light-chain-enhancer of activated B cells
NO•	Nitric oxide radical
$NO^{\bullet}_2$	Nitrogen dioxide radical
NPs	Nanoparticles
Nrf2	Nuclear factor erythroid 2-related factor 2
$O^{\bullet -}_2$	Superoxide anions
ONOO	Peroxynitrite
PI3K	Phosphoinositide 3-kinases
PLT	Platelet
RBC	Red Blood Cell
RNA	Ribonucleic Acid
RNS	Reactive nitrogen species
RO•	Peroxyl
ROO•	Alkoxyl radicals
ROS	Reactive oxygen species
SDS	Sodium dodecyl Sulfate
SEM	Scanning electron microscopes
SOD	Superoxide dismutase
SPR	surface plasmon resonance
T3	Triiodothyronine
T4	Thyroxine
TBA	Thiobarbituric Acid
TBS	Tris buffer saline solution
TCA	Trichloroacetic Acid
TEM	Transmission Electron Microscop
TNF	Tumor necrosis factor
TSH	Thyroid-stimulating hormone
UV	Ultraviolet
UV-VIS	UV-VIS: Ultraviolet-visible spectroscopy
WBC	White Blood cell
XRD	X-ray diffraction

SUMMARY

CHAPTER III : Cadmium Chloride

SECOND PART

Experimental Study

CHAPTER I : Material & Methods

CHAPTER II :Results

INTRODUCTION

INTRODUCTION

Medicinal plants are both a finished product intended for consumption and raw material for obtaining the bioactive substances which are at the origin of several modern medicines thanks to their richness in secondary metabolites, in particular in phenolic compounds endowed with beneficial biological (Hiba and Thoppil, 2022). Because compounds with a plant origin have come under scrutiny recently and have the potential to affect many processes. Then, by combining a variety of contemporary science inputs, such as synthesizing nanoparticles, these activities can be greatly enhanced (Anbukkarasi *et al*., 2016; Pokhrel *et al*., 2015).

The field of nanotechnology is the most dynamic region of research in material sciences due to its various applications in several fields such as bionanotechnology, chemistry, material science, medicine, etc. Nanoparticles present a highly attractive platform for a diverse array of biological applications. As Nanotechnology has piqued the scientific community's interest since its debut as a powerful tool of basic and applied science (Xu et *al*., 2006). These performances have contributed to sweeping changes in various fields of technology and science (Dawadi et *al*., 2021).

Green synthesis of noble metal-nanoparticles has become a prominent area of interest in the field of nanoscience and technology, as it is a nontoxic, economically viable, and eco-friendly approach and highly focused research area compared to other chemical and physical methods (Vorobyova et *al*., 2020). Among noble metal nanoparticles, AgNPs have received considerable attention due to their unique characteristics like chemical stability, electrical conductivity, catalytic power, sensing ability and antimicrobial activity, anticancer, and antioxidant (Siddharthan et *al*., 2019; Verma et *al*., 2016).

Plant extract contains various phytochemicals such as flavonoids, phenol derivatives, terpenoids, proteins, reducing sugars, and enzymes. These phytochemicals of herbal extracts can act as both the bioreduction as well as capping agent required for the synthesis and stabilization of nanoparticles (Djemam et *al*., 2020; Verma et *al*., 2016)

Helianthemum lippii L is belonging to the Cistaceae family and contains 08 gener and 200 species that are widespread in the Mediterranean regions. Worldwide, this genus includes 70 species in Algeria and Pakistan (Benabdelaziz et *al*., 2015). *H.lippii* is widely used in traditional medicine due to its notable pharmacological effects medicinal and it is the host plant for various species of desert truffles, which are valuable for food, and economic development, as well as the development of rural and local communities (Alsabri et *al*., 2013; Atef et *al*., 2015). Further, it has biological properties that are promising for the treatment of

many diseases and is used as a pain reliever such as menstrual pain and uterine diseases in women (Djemam et *al*., 2020), thanks to properties tremendous as an antioxidant, antimicrobial and anti-inflammatory, Further, this plant is characterized by being rich in secondary metabolites as it has been proven in many studies (Alsabri et *al*., 2013; Plescia et *al*., 2022). Despite the huge potential of *H.lippii*, its medicinal and pharmaceutical applications are still limited. This work, therefore, extends the frontier of *H.lippii* to the domain of nanobiotechnology.

With rapid industrialization, technological advancement, and unprecedented, increase in population, pollutants such as heavy metals are increasing in the environment (Ye et *al*., 2009). Contamination of food and feedstuffs with heavy metals poses health risks to both humans and animals, drawing concern from all over the world. Cadmium is a harmful chemical that is dangerous and widely ingested and is frequently found in soil, air, water, and food (Buha et *al*., 2013; Zhang et *al*., 2014). Medicinal Plants and nanoparticles green synthesis have a wide important role in the elimination of many in body human adverse effects caused by exposure to environmental and food contaminants (Habeeb Rahuman et *al*., 2022). Therefore, the functional effects of *H.lippii* and silver nanoparticles in the areas of antioxidant effects and xenobiotic detoxification provide a possible option in the control of Cd toxicity in light of these concerns.

Based on this fact, the principal goal of our thesis work was to green synthesize and characterize silver nanoparticles from *H.lippii* and study their biological activities in vitro and in vivo against the toxicity of cadmium chloride in Wistar rats.

The first part consists of three chapters; the first chapter includes a bibliographic overview of *Helianthemum lippii* (L.) Dum.Cours. the second chapter presents of silver nanoparticle and the third one are concerned with cadmium chloride. The second part concerns the experimental work;

- Part one: Based on the *In vitro* study; extraction of plant extract, quantitative and qualitative characterization of these compounds, synthesis and characterize of silver nanoparticles, and evaluation of their biological activities via antioxidant, anti-inflammatory, hemolytic activity, and antibacterial assays, in another hand, exceptionally, Using cyclic voltammetry and spectroscopic methods, have been evaluating the interaction between the studied ligand (AgNPs) and (DNA / BSA) by determining the interaction parameters.
- Part two: Based on the *In vivo* study for evaluation of the curative efficiency of *H.lippii* aqueous extract and silver nanoparticles biosynthesized against metabolic,

physiological, and histological alteration induced by experimental cadmium chloride in rats.

FIRST PART

Bibliographic Synthesis

CHAPTER I

Helianthemum lippii L.

1. Generality

Among all medicinal plants, a special focus is placed on *Helianthemum lippii* (L.) Dum, a valuable medicinal herb with several different applications (Lassed et *al*., 2017; Rubio-Moraga et *al*., 2013). It belongs to the family of Cistaceae. *H.lippii* are also used for the treatment of stomach illnesses, injuries, and burns around the world due to their anthelmintic, and anti-inflammatory respectively. Notably, this plant is known by its scientific name; *Helianthemum lippii*. L Pers (Alsabri et *al*., 2013; Hamza et *al*., 2013), *Helianthemum lippii* (L.) Dum. Cours and *Cistus lippii* L (African plant database). *H.lippii* grows on low-lying, sandy limestone gypsum soils in North Africa (Escudero et *al*., 2007). It is found in the bioclimatic semi-arid region of Southern Tunisia, where it is well adapted to harsh climatic circumstances (Pérez-García and González-Benito, 2006). In addition, It has significant ecological, economic, and pastoral value and is essential to the fight against desertification and the stability of sensitive areas (Díez et *al*., 2002). Furthermore, the aerial part's powder or compress is utilized to cure the coetaneous lesion, therefore it has medicinal value. Several types of desert truffles that are interested in food, medicine, and economics as well as the growth of rural and local communities use *H. lippii* as their host plant (Bradai et *al*., 2015; Mandeel and Al-Laith, 2007). There is a continuous gradual decline in *H.lippii* presence. Due to overgrazing, land clearing, and greater pastoral care, this plant is significantly impacted by the shift in its floristic composition. Despite being rare and endangered, the Intenational Union for Conservation of Nature (IUCN) has not placed this species on its red list (Venturella et *al*., 2015).

2. Botanical description

The plant of *H. lippii* is a perennial shrubby are generally 30-60 cm long, has a woody stem, and erect whitish branches because they have numerous starred hairs. The upper leaves alternate with the bottom leaves being opposite, and the leaf blades are lanceolate (5-6 ×15-20 mm), becoming shorter and more linear throughout the dry season (Alsabri et *al*., 2013). The tops are dense, spiciform, and have 6–15 sub-sessile flowers with 1-2 mm sepals and 1-2 mm long yellow petals. The fruit is actually a capsule containing there are numerous seeds. In addition, a nanophanerophyte grows in arid grasslands and maritime sands between 0 and 300 m above sea level. The Mediterranean region's flowering and fruiting seasons run from April through May. Meanwhile, there is no comprehensive information on seed germination, dissemination method, or pollination (Mahmoud and Alshammari, 2022).

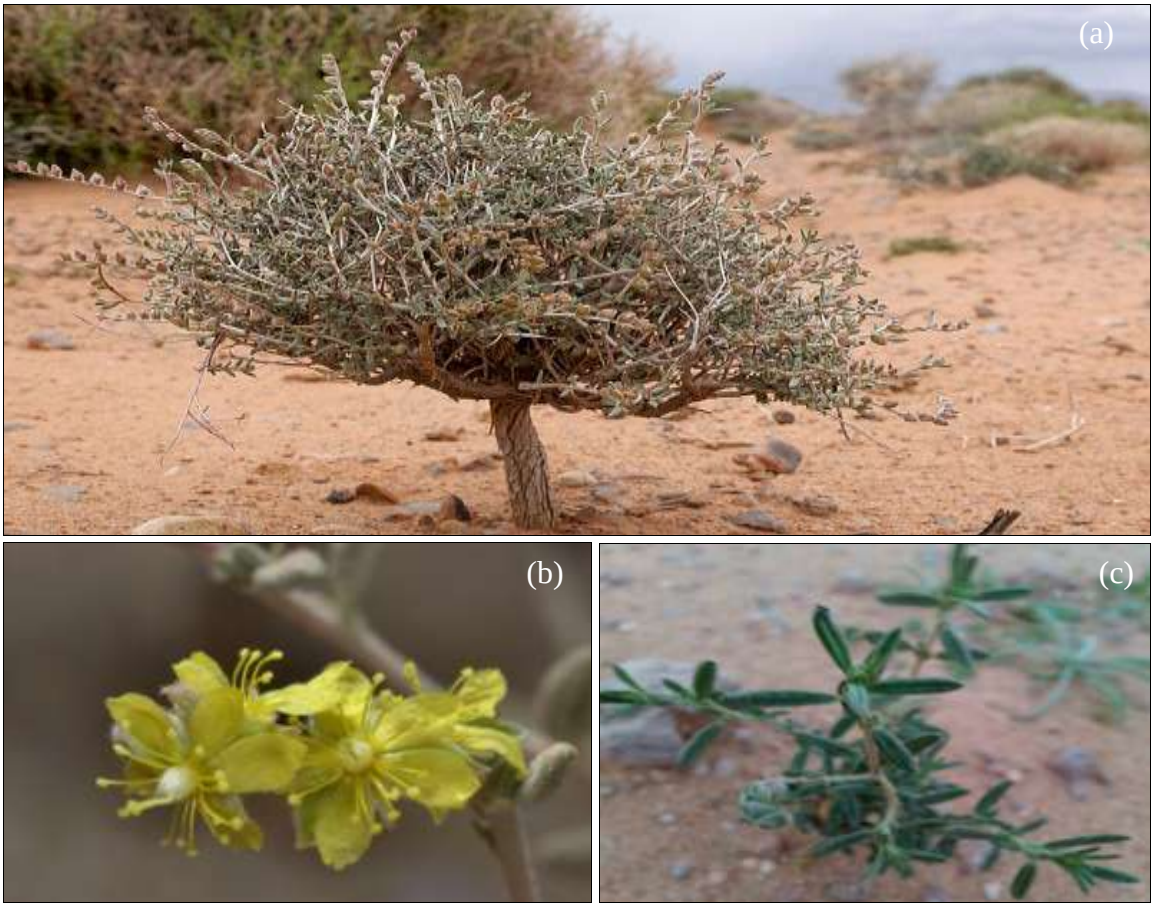

Figure 1 : *Helianthemum lippii (*L.) Dum.Cours: a. Plant of *H.lippii*; b. flowers; c. leaves (www.floraofqatar.com)

3. Geographic distribution

The *H.lippii* plant distributed in many regions of the world. The original home of *H. lippii* is in the Arab desert region (the Arab Maghreb, the Gulf States, the Levant, and Iran), where it prefers light sandy soils and abounds in sandy areas (the arak) as well dry places, roadsides, and fields (African plant database)(Alsabri et *al*., 2013). Additionally, it exists in North Africa (Amina et *al*., 2012). While a current report on *H.lippii* distribution (Cistaceae) was detected both in Iraq, Qatar, Libya, Algeria, Egypt, Greece, Italy, Iran, Malta, Jordan, Morocco, Tunisia, Pakistan, Syria, Kuwait, Lebanon, Spain, Oman, United Arab Emirates, Bulgaria, and Sicily. In addition, is a perennial shrub typical of marine sands and dry grasslands (figure:02) (Fenu et *al*., 2019).

It should be noted a plant's height and general shape vary depending on the region in which it grows, and it branches out a lot in locations with light sand, like areas of race, where it can grow to a height of around a meter. While it grows as a compact mass of tightly overlapping woody branches in areas with hard soil, rarely grows more than 50 cm in these regions.

Figure 2: Map showing the locations of *H.lippii* distribution in the world.

4. Classification

Taxonomic of *H.lippii* is presented in table 01 below according Dupont and Guignard, (2007).

Table 01 : Classification of *H.lippii* (Dupont and Guignard, 2007).

Kingdom	Plantae
Sub-kingdom	Tracheobionta
Division	Magnoliophyta
Class	Magnoliopsida
Order	Malvales
Family	Cistaceae
Gender	Helianthemum
Species	*Helianthemum lippii (*L.) Dum.Cours.

5. Local Nams of *H.lippii*

H.lippii has many common names, and these names vary in different regions and continents, for an example; the name of Al Samhari (in the region of Oued Souf: Southeast of Algeria)(Halis, 2007) ; Tahsowat and Alrjik (in the region of Ouargla: South of Algeria) (South-West of Algeria); Alrkaroq (in Kuwait), Umm Souika (the Arabian Peninsula) (Mandaville, 2013) and Sun Flower (Northeast of Jordan) (Atef et *al*., 2015) are just a few of the local names for this species.

6. Bioactive compounds

Alsabri et *al*. (2013) (Alsabri et *al*., 2013) found that *H.lippii* includes a variety of bioactive compounds. Total phenolic components, tannins, flavonol glycosides, and

flavonoids were detected in the ethyl acetate extract (EtOAc) of *H. lippii (*Badria *et al.*, 2014*)*; (Calzada and Alanís, 2007). Also, Polyphenols (flavonoids, tannins), simple phenolics, glycosides, free reduced sugars were found in the methanolic extract of *H.lippii*, but there were no free anthraquinones, steroids, terpenoids, or alkaloid. The presence of all these bioactive compounds gives the plant tremendous extraordinary therapeutic potential. Furthermore, *H. lippii* was found to have a high concentration of phenolic compounds in a previous study. Vanillic acid (37% rich in gentisic and 4 hydroxybenzoic acids (14 % for both) was the most abundant ingredient in the n-BuOH extract of *H.lippii*, while ferulic, caffeic, and syringic acids (9%, 8%, and 4% respectively) were also significant. The EtOAc extract of *H.lippi*, on the other hand, was predominantly rich in gentisic acid (41%) but also plentiful in gallic and vanillic acids (17% and 11% respectively). The amounts of sinapic acid and catechin in this extract were likewise quite consistent and identical, at 8% and 7%, respectively.

The analysis of the GC-MS chromatogram of the methanolic extract of H. lippii revealed 35 main peaks. Six chemicals that were reported to have biological activity in the study Alshammari et al., 2022 were found in the *H. lippii* extract according to GC-MS analysis (Mahmoud and Alshammari, 2022). These compounds which acts as a liniment counterirritant for relief of deep-seated pain (Rivera et *al*., 2005) and (Tardío et *al*., 2006), Such as Phenethyl alcohol (RT, 19.01) are reported to act as an antiseptic, antimicrobial and disinfectant it is also utilized in pharmaceutics and perfumery as an aromatic essence and preservative (Baudouin, 1976). Oxirane, [4-(1, 1-dimethyl ethyl) phenoxy] methyl], RT (36.94) has an anti-inflammatory, analgesic, and antipyretic). Mebutamate (RT, 41.36) has a sedative and anxiolytic drug with anti-hypertensive activity (Morin et *al*., 1963). Spermatheridine (RT, 46.69) acts as an antimicrobial, Anticancer, and antifungal agent (Shakhatreh et al., 2016). Ethyl isoallocholate (RT, 60.63) was reported to inhibit dihydropteroate synthase (Kargutkar and Brijesh, 2018). Others have found similar findings.

These insights shed light on the plant's potential as a source of cost-effective phytocompounds for the synthesis of complex chemical substances, as well as the plant's true significance. Antibacterial, antioxidant, anti-inflammatory, antifungal, and anticancer elements will need to be investigated further.

7. Therapeutic uses

H.lippii is a valuable medicinal herb with a wide range of uses. Diarrhoeal and epigastric discomfort have been treated with this plant in the past (Rigat et *al*., 2007).

Helianthemum plants had a capacity used for the treatment of stomach illnesses, and injuries around the world due to their anthelmintic, anti-inflammatory, antiulcerogenic, antiparasitic, antibacterial, analgesic, and vasodilating properties (Badria et *al*., 2014). Meanwhile, are used to treat burns, respiratory disorders, and fever (Rigat et *al*., 2007). Additionally, the *H.lippii* is widely used to treat infectious diarrhea, maybe because of its antimicrobial action (Benabdelaziz et *al*., 2015; Calzada and Alanís, 2007; Meckes et *al*., 1999). Moreover, *H. lippii* is widely applied for treating digestive disorders, and hemorrhoids (Calzada et *al*., 1995), most probably as a result of its antibacterial, analgesic, antipyretic, and anti-inflammatory activity (Alsabri et *al*., 2013). As it is worth noting its anti-cancer efficacy which proved it is against HeLa (human cervical cancer) and HT29 (human colorectal cancer) (Djebbari et *al*., 2017), and in the same regard, it showed a very important chemoprotective effect against health degenerations caused by doxorubicin as chemotherapy in rats Wistar (Djebbari et *al*., 2017; Laraba et *al*., 2022; Lassed et *al*., 2017) . Several studies regarding the pharmacological properties of aerial parts of *H.lippii* were reported. However, to date, there is no report that portrays its prospective in nanobiotechnology to synthesize nanoparticles.

CHAPTER II

Silver Nanoparticles

1. Nanotechnology

Nanotechnology is among the most optimistic and new areas of modern material science research. Nanomedicine, an emerging new discipline resulting from the marriage of nanotechnology and medicine, has several uses in a range of research. The physicochemical, optoelectronic, and biological properties of noble-metal nanoparticles are astounding. They are utilized in industrial and pharmaceutical applications for a variety of objectives (Pirtarighat et *al*., 2019). NPs have an extremely small size (less than 100 nm), a large surface area, and a high dispersion rate (Yousaf et *al.*, 2020). As well as, the nanometric scale improves the surface area of contact with the materials, resulting in increased responsiveness (Rather et *al.*, 2022). Because nanoparticles are not simple molecules, they are divided into three layers: (1) the surface layer, which can be stabilized with a variety of special compounds, metal ions, emulsifiers, and polymers; (2) the shell layer, which is chemically and physically distinct from the core and (3) the core, which may be the central component of the NPS (Shin et *al*., 2016).

Chemical and physical processes can both be used to create nanoparticles. The use of laser ablation is one of the physical techniques (Simakin et *al.*, 2004), thermal decomposition (Yang et *al*., 2007), ultrasound irradiation (Abbasi et *al*., 2012), and gamma irradiation (Huang et al., 2009; Stirling et al., 2020),and chemical reduction (Botcha and Prattipati, 2019). The aforementioned methods involve hazardous chemicals, and disposing of these substances is challenging (Kowshik et *al*., 2002; Sadhasivam et *al.*, 2010), Therefore, it is necessary to create eco-friendly processes in order to create NPS. An effective method for connecting nanotechnology and biotechnology is the green synthesis of NPs (Bhattacharya and Gupta, 2005).

2. Silver nanoparticles

Silver (Ag) is the second element in the periodic table's first secondary group (IB) and a more reactive noble metal than gold. The high mechanical resistance of this metal is exploited. It's a soft, white, gleaming transition metal with a great electrical and thermal conductivity that's employed in colloids and lotions (Sathishkumar et *al*., 2016). Otherwise, and due to its great biological potential, including its low-concentration antifungal, antibacterial, antiviral, anti-infectious, wound-healing, and anti-inflammatory capabilities, silver has been referred to as "dynamic" (Aina et *al*., 2019; Lateef et *al*., 2018). Further, about 650 different species of disease-causing microbes can be destroyed by silver, an inorganic antibacterial agent that is non-toxic (Adebayo et *al*., 2019; Bhuyar et *al*., 2020).

Among the many metallic nanoparticles, silver nanoparticles are one of the most significant and interesting nanomaterials, and since they have so many different uses in biomedicine, they are drawing more and more attention.

Due to their remarkable broad-spectrum actions, silver nanoparticles have received the greatest research attention. In the field of nanoscience, research on AgNPs has advanced significantly, particularly in the areas of antimicrobial, antioxidant, antifungal, anti-inflammatory, anticancer, and anti-angiogenic properties (Nagarajan et *al*., 2019; Sondi and Salopek-Sondi, 2004). Noble nanoparticles have extraordinary incredible physicochemical, optoelectronic, and biological capabilities (shape, conductivity, optical activity, high surface area electric, and size) (Habeeb Rahuman et *al*., 2022)

3. Various methods used in the synthesis of metal NPs.

Metallic nanoparticles are frequently prepared and stabilized via a variety of physical and chemical processes, including electrochemical alterations, chemical reduction, and photochemical reduction (Chen et *al*., 2001). However, the majorities of these methods are expensive and employ dangerous substances. Hence, these methods of synthesis produce unfriendly byproducts that pose a major threat to both the environment and human health. It is the main justification for choosing the green route strategy to create nanoparticles because these techniques are generally safe, economical, and eco-friendly (Jamkhande et *al.*, 2019). (Figure 03).

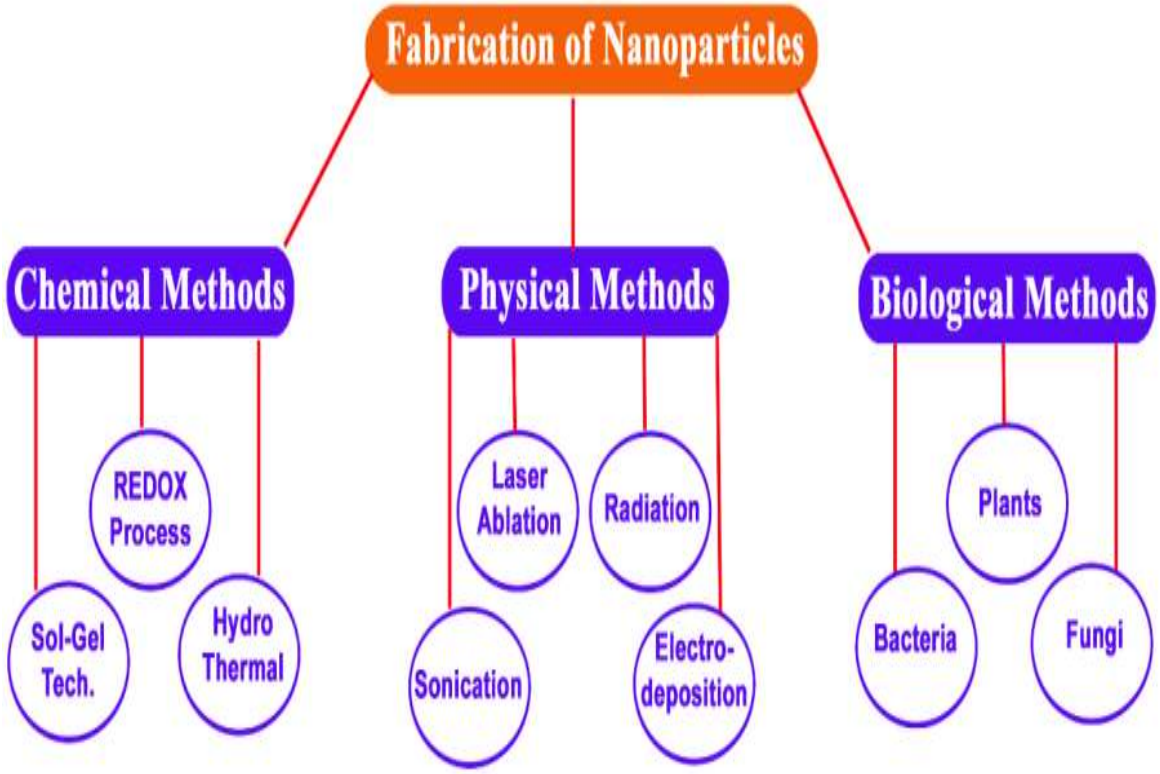

Figure 3 : Methods used in the synthesis of metal NPs (Chung et *al*., 2016).

4. Green synthesis of AgNPs

Using plant extracts including phytochemical agents in the green synthesis of AgNPs has piqued interest. This eco-friendly method is more biocompatible and cost-effective, as well as has the ability to sustain greater synthesis (Arunachalam et *al*., 2013; Mittal et *al*., 2015). The production of AgNPs under various "green" chemical-physical circumstances, as well as by a variety of microbes, has been extensively studied (Chung et *al*., 2016).

Flavonoids, phenolic acid, terpenoids, and alkaloids are new secondary metabolites that are present in crude plant extracts and are principally in charge of reducing ionic metal into bulk metallic nanoparticles (Aromal and Philip, 2012). Secondary metabolites are continuously active in redox processes that produce environmentally friendly nanoparticles. Biosynthesis reactions can be modified.

4.1. Mechanism of Green Synthesis of NPs by Plant Extracts

During the green production of NPs by plant extracts in vitro, a mechanism similar to the one described above could be at work. The production of metallic NPs from the appropriate metal ions is depicted schematically in Figure 04. The cations in metallic salts become saturated and create hydroxyl complexes as the salt disintegrates into cation and anion. The

supersaturation of hydroxyl complexes is followed quickly by the onset of metal-oxygen species crystallization. This causes the creation of crystalline planes with various energy levels. Heat is crucial in supplying energy to the reaction system (Kachlicki et *al*., 2016).

The formation of high-energy atomic growth planes continues until the capping agent is activated by the plant extracts, at which point it stops. This leads to the establishment of certain NP kinds. The reducing agents normally supply the metal ions with electrons during the synthesis, turning them into NPs. Due to their high surface energy; these NPs have a propensity to group together in order to change into their reduced surface energy conformations. More reducing and stabilizing chemicals thus inhibit nanoparticle aggregation and encourage the creation of smaller NP (Khalil et *al*., 2012).

Furthermore, proteins have the capacity to attach metal ions to the surface of their molecules and transform them into the proper nuclei, which can aggregate and create NPs (Makarov et *al*., 2014). Protein amino groups, hydroxyl and carboxyl groups in amino acids and polyphenols, hydroxyl groups in polysaccharides, and carboxyl groups in organic acids bind metal ions and catalyze the production of metallic NPs by preventing the superoxide-driven Fenton process (which is thought to be the most important source of ROS). It has been shown that the protein attached to the surface stabilizes the NPS (Gole et *al*., 2001).

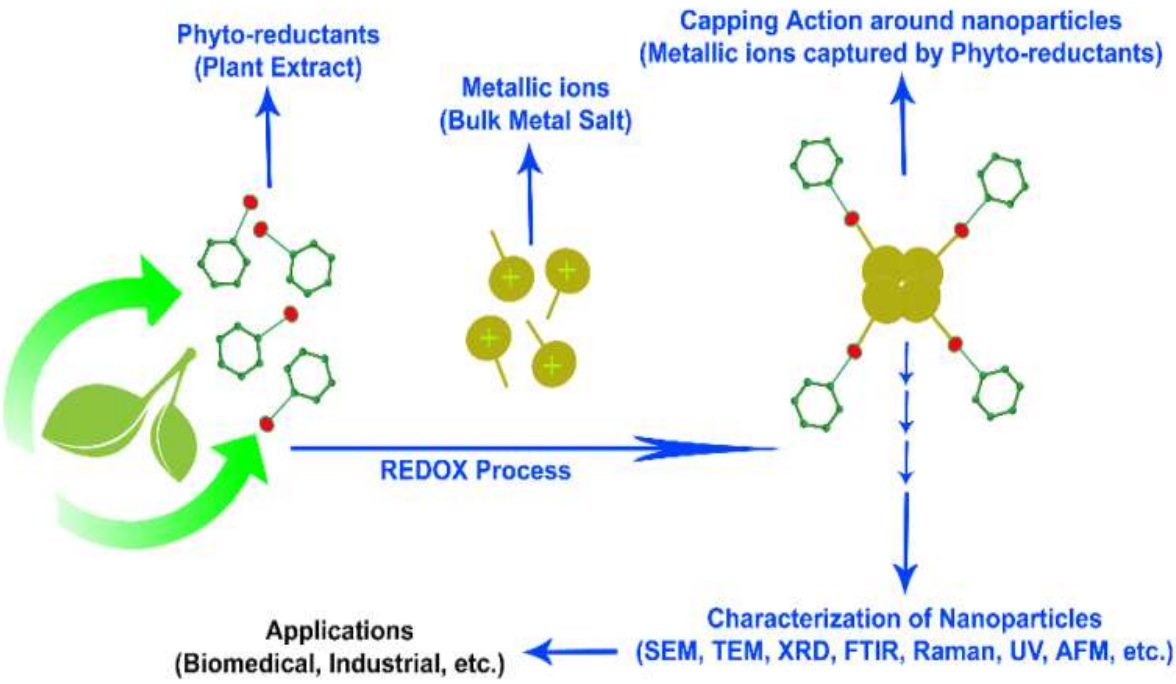

Figure 4 : The mechanism of *in vitro* green synthesis of nanoparticles (Marslin et *al*., 2018).

4.2. Secondary Metabolites in Plant Extract-Mediated Green Synthesis of NPs

Several various plants have been used to synthesize NPs using plant extracts. Proteins, low-molecular-weight substances like terpenoids, alkaloids, amino acids, alcohols, polyphenols (catechin, flavones, taxifolin, procyanidins of different chain lengths formed by catechin and epicatechin units, and phenolic acids), glutathiones, polysaccharides, antioxidants, and organic acids are among the numerous molecules (ascorbic, oxalic, malic, tartaric, and protocatechuate). Proteins, sugars, terpenoids, polyphenols, alkaloids, phenolic acids, and other substances may also aid in the reduction of metal ions into nanoparticles and maintain their stability once they have done so. Further, Flavonoids are the compounds whose involvement in green synthesis has been most extensively studied (Figure 05) (Makarov et *al.*, 2014).

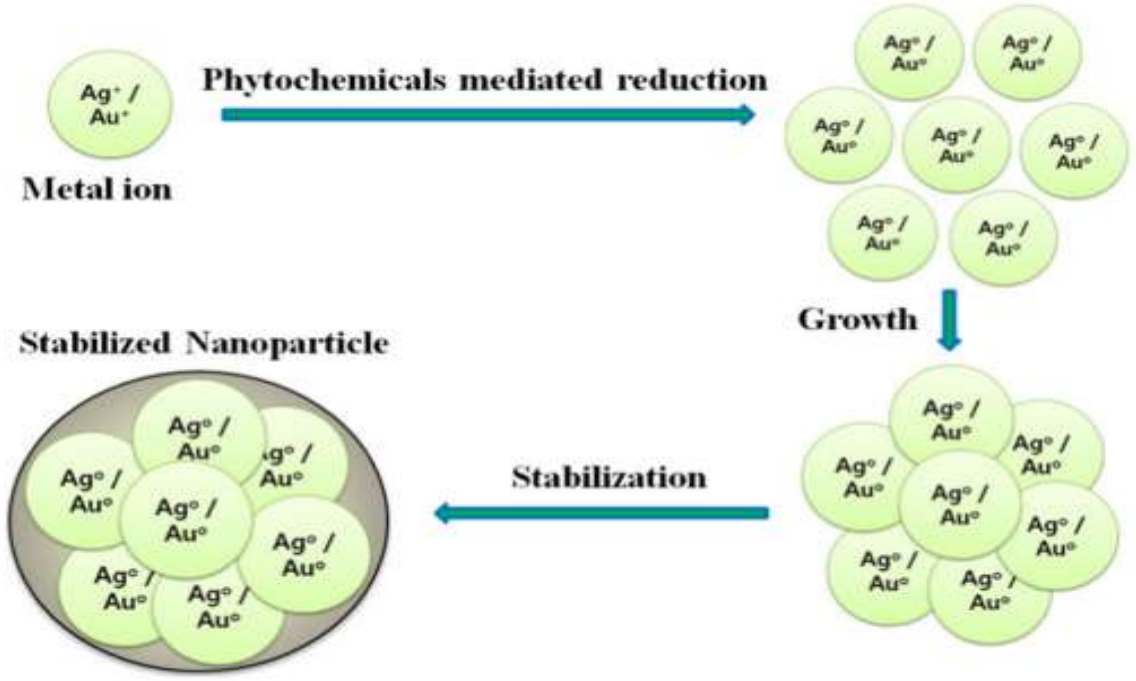

Figure 5 : Mechanism for synthesis of nanoparticles in the presence of phytochemicals as a reducing agent (Patil and Kim, 2017)

5. Operational parameters for the synthesis of silver nanoparticles

A number of important system parameters determine the synthesis of silver nanoparticles. Regardless of the technique used to produce silver nanoparticles, certain operational factors, including the concentration and volume ratio of the reacting components, the time it takes for the reaction to complete, the temperature, and the pH, has an effect on the rate of synthesis, size, and form of the nanoparticles. The size, shape, overall morphology, effectiveness, and applicability of these parameters might all be changed (Makarov et *al.*, 2014).

5.1. Effects of concentration

Investigating this characteristic allowed us to identify the silver ion concentration best suited for creating the silver nanostructure. The concentration of $AgNO_3$ was used in a number of plant-mediated AgNPs manufacturing processes, and it significantly affected the nanoparticles' particle sizes. While maintaining the same values for the other parameters, a range of concentrations of silver ions was generated to study the impact of the initial concentration. The concentration of Ag+ ion is typically changed from 10-3 to 10-2 M. According to reports from the literature, 10-3 M is the concentration that is most suited and ideal for improving surface plasmon resonance and increasing SPR peak intensity (Tarannum and Gautam, 2019).

5.2. Effect pH

The formation of AgNPs is significantly influenced by the reaction's pH value (Gan and Li, 2012). Natural phytochemicals present in an extract may change in charge because of a pH change. This charge change may have an impact on how silver ions are reduced to AgNPs as well as how well silver ions stick to biomolecules. The negative ionizable groups are bound to silver ions because of their positive charge. The studies indicate that pH has an impact on the stability, size, production rate, and form of nanoparticles as well. Zeta potential data demonstrate the stability and surface charge of silver nanoparticles. The zeta potential of AgNPs is typically higher at alkaline pH and lower at strongly acidic pH (Khatoon et *al*., 2017).

5.3. Effect of reaction temperature

The SPR spectra change dramatically as the reaction temperature rises. With an increase in reaction rate, the absorbance peak lowers as the reaction temperature rises, perhaps resulting in smaller nanoparticles (Ibrahim, 2015). The rate of reduction increases as the temperature rises, resulting in a shorter reaction time. Temperature changes may cause a blue shift in wavelength. When the temperature is changed from 10 to 50 degrees Celsius, the maximum wavelength is reduced from 433 to 397 nm. The change in max could be related to AgNPs' surface plasmon resonance localization. Therefore, a temperature increase can lead to smaller AgNPs. There is less opportunity for particle size development and the creation of AgNPs of uniform size as the temperature rises due to the molecules' increased kinetic energy, which also increases the consumption of silver ions (Verma and Mehata, 2016).

5.4. Effect of reaction time

Nanoparticle synthesis is also influenced by how long reducing agents are exposed to metal ions. It has been shown that the synthesis of nanoparticles increases with longer silver-reductant reactions or incubations (Darroudi et *al*., 2011; Krishnaraj et *al*., 2010). According to Khatoon et *al*., (2015) the surface plasmon peak of AgNPs grew from zero to 30 min. later, becoming steady, indicating that the synthesis was successful (Khatoon et *al*., 2015).

5.5. Effect of concentration of reducing precursor

The concentration of reducing and stabilizing precursors has a significant impact on the synthesis of metal nanoparticles. According to White et *al*.,(2012) nanoparticle production changes with the concentration of extract. Higher extract concentrations have also been linked to the formation of polydispersed AgNPs (Von White et *al*., 2012). The concentration fluctuation of olive leaf extract was demonstrated by Khalil et *al*,.(2014) (Khalil et *al*., 2014). They showed that increasing the content of leaf extract causes a blue shirt and a sharpening of the absorbance peak. The decrease in the mean diameter of silver nanoparticles was reflected by this blue shift. According to Krishnaraj et al., AgNP production is higher at 20% A. Indica (Neem) leaves extract than at 40% (Krishnaraj et *al*., 2010). The increasing quantity of bimolecular causes agglomeration, which affects UV-Vis spectroscopy absorption.

Moreover, on the creation of the AgNPs, the impact of the extract amount was examined. 15 mL of 10 mM $AgNO_3$ solutions were incubated with various amounts of seed extract, ranging from 0.4, 0.8, 1.2, 1.6, and 2.0 mL. Visible color changes were observed an hour after combining the extract and $AgNO_3$ solutions, progressing from reddish yellow to deep red with increasing AKSE dosage in each reaction solution. A surprising correlation was found between the absorbance values and the AKSE quantity in the UV-Vis spectrum, which led to the reduction of a larger concentration of AgNPs since more reducing biomolecules were accessible at a higher dose (Krishnaraj et *al*., 2010).

6. Characterization techniques of nanoparticle

Characterization is a crucial step after green nanoparticle synthesis to determine the nanoparticles' form, size, surface area, and dispersity (Jiang et *al*., 2009). Various methods are used to describe nanomaterials (Brongersma et *al*., 2007; Feldheim and Foss Jr, 2002) are employed which are shown below.

6.1. UV-visible spectrophotometer

The primary characterization of produced nanoparticles, as well as the observation of the synthesis and stability of AgNPs, may be accomplished with great validity and effectiveness using UV-vis spectroscopy. Due to unique characteristics, AgNPs can interact strongly with particular light wavelengths. Additionally,UV-vis spectroscopy requires just a brief measurement time, is quick, easy, practical, delicate, specific for many types of NPs, and does not require calibration for the characterization of nanoparticles (Tomaszewska et *al*., 2013). Particle size, dielectric material, and chemical surroundings all have an impact on absorption. As a result of the conduction and valence bands' proximity to one another in AgNPs, electrons can move around the material without any difficulty (Karuppiah and Rajmohan, 2013). As a result of the metallic nanoparticles' collective oscillation, these liberated electrons give rise to the SPR absorption band (Feldheim and Foss, 2002).

6.2. Dynamic light scattering (DLS)

The surface charge, quality, and size distribution of nanoparticles are all characterized using DLS. The generated nanoparticles' polydispersity index is also very helpful (Jiang et *al*., 2009).

6.3. Scanning electron microscopy (SEM) and Transmission

Surface and morphological characterization are one of electron microscopy's most popular uses (TEM). Morphological characterization at the nanoscale to micrometer scale is carried out using scanning electron microscopy (SEM) and transmission electron microscopy (TEM). SEM can provide elemental information on the micron scale and submicron scale, in contrast to TEM, which offers a far higher resolution. The same method is used to evaluate the surface morphology of a sample of newly generated nanoparticles, and TEM is helpful in determining the specific size and form of the particle (Jiang et *al*., 2009).

6.4. Zeta potential measurement

Zeta potential is used to determine how stable a synthesized nanomaterial is; the higher its value, the more stable the sample (Roy and Das, 2015).

6.5. Fourier transforms infrared spectroscopy (FTIR)-

The identification of the organic functional groups adhering to the surface of the particles is made possible by Fourier transform infrared spectroscopy (FTIR), which has significant advantages for surface chemistry (Tamuly et *al*., 2014). FTIR, which also provides accuracy,

consistency, and an excellent transmission ratio, can be used to determine whether biomolecules are directly involved in the production of nanoparticles. The investigation of nanoscaled materials has also been carried out using FTIR, including the confirmation of functional molecules covalently attached to silver. As demonstrated by the prior investigations (Niraimathi et *al*., 2013), Capping involves the use of functional groupings. Peaks show that the NPs were coated with secondary metabolites from plants, including phenols, terpenoids, flavonoids, tannins, and glycosides with function groups like carboxylic acid, ketones, and aldehydes. (Habeeb Rahuman et *al*., 2022).

6.6. X-ray diffraction (XRD)

The analysis method known as X-ray diffractometry (XRD) is popular for analyzing crystal and molecule structures. It may assess particle size, isomorphous substitution, and crystallinity, serving as a qualitative indication of the active ingredients and a qualitative divider of various compounds. The physicochemical characteristics of the crystalline lattice are described by the numerous diffraction peaks that are produced when X-ray light is reflected off of any particles. A wide range of materials, including inorganic catalysts, superconductors, biomolecules, glasses, and polymers, can have their structural properties analyzed using XRD. In evaluating the characteristics of these materials, the diffraction peak structure is crucial. By comparing the diffracted beams to the Joint Committee on Powder Diffraction Standards (JCPDS) reference database, it is possible to ascertain the composition of each material using its unique diffraction lighting.

The underlying principle of XRD is Bragg's law. Using the Scherrer formula, the size of nanoparticles is calculate (Sun et *al*., 2000).

$$\boldsymbol{D} = \frac{K\lambda}{\beta.\theta}$$

Where D is average the crystallite size, k is the so-called shape factor (0.9), λ is the wavelength (0.15418 nm, CuKα), $\boldsymbol{\beta}$ is the Full Width at Half Maximum (FWHM), and $\boldsymbol{\theta}$ is Bragg's angle.

6.7. Energy dispersive spectroscopy

EDS to understand the metal nanoparticles' basic makeup EDS is employed, providing the fundamental understanding of the sample (Brongersma et *al*., 2007).

7. Biological Applications of AgNPs

Silver nanoparticles have many biological uses, including as antibacterial, anticancer, and anti-diabetic agents, as well as in bioimaging, antiangiogenesis, wound healing, biosensing, and neurodegenerative, anti-inflammatory, and anticoagulating activities and biosensing. Some of these uses have also been covered in this section. Due to the aforementioned reasons, including the attachment of biological elements with therapeutic potential, the widespread use of silver nanoparticles inspired the development of biosynthesized silver nanoparticles with enhanced therapeutic effects. The accessibility, bioavailability, and environmental friendliness of nanoparticles also motivate us to focus further on environmentally friendly synthesis methods for the creation of silver nanoparticles (figure 06). Here, we want to highlight how AgNPs are used in diverse biological and biomedical applications (Kotcherlakota et *al*., 2019).

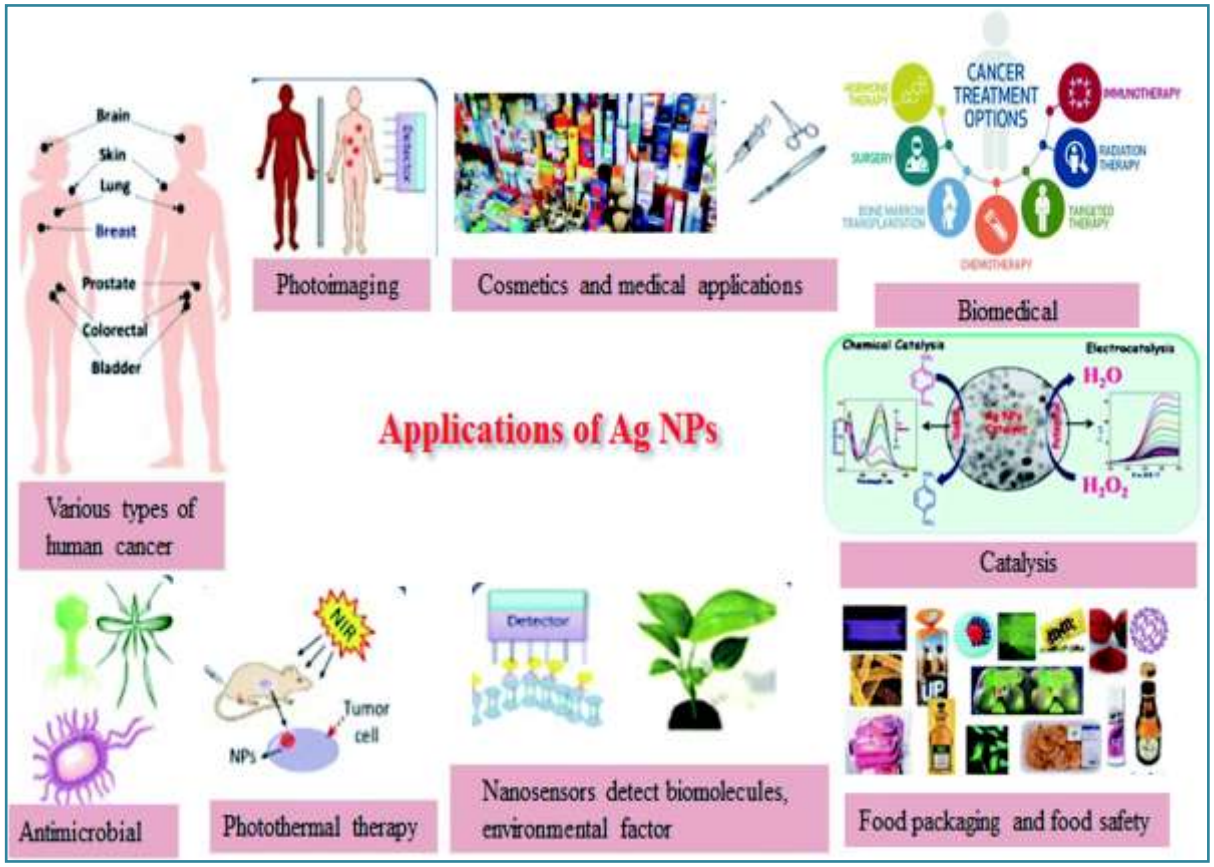

Figure 06: Various applications of silver nanoparticles (Tarannum and Gautam, 2019).

7.1. Antibacterial activity

The development of novel bactericidal medicines is necessary to treat the infection and to establish a platform for learning more powerful anti-microbial treatments that confront multidrug-resistant (MDR) pathogens in the event that an antibiotic-resistant microbe

outbreak occurs on a global scale. The effective biocidal effects of AgNPs on bacteria have long been used to prevent and treat a variety of infections.

Against both Gram-positive and Gram-negative bacteria, AgNPs have a very potent bactericidal effect. The development of cell wall pores that ultimately lead to the leakage of cellular contents may be the cause of AgNPs' antibacterial activity, or the silver ion may enter through ion channels and destabilize the ribosome, which prevents the expression of enzymes and thiol-containing proteins required for the production of ATP or DNA, leading to cell death (figure 07). AgNPs influence the function of membrane-bound enzymes, which is important for the respiratory chain (Ahmad et *al*., 2020).

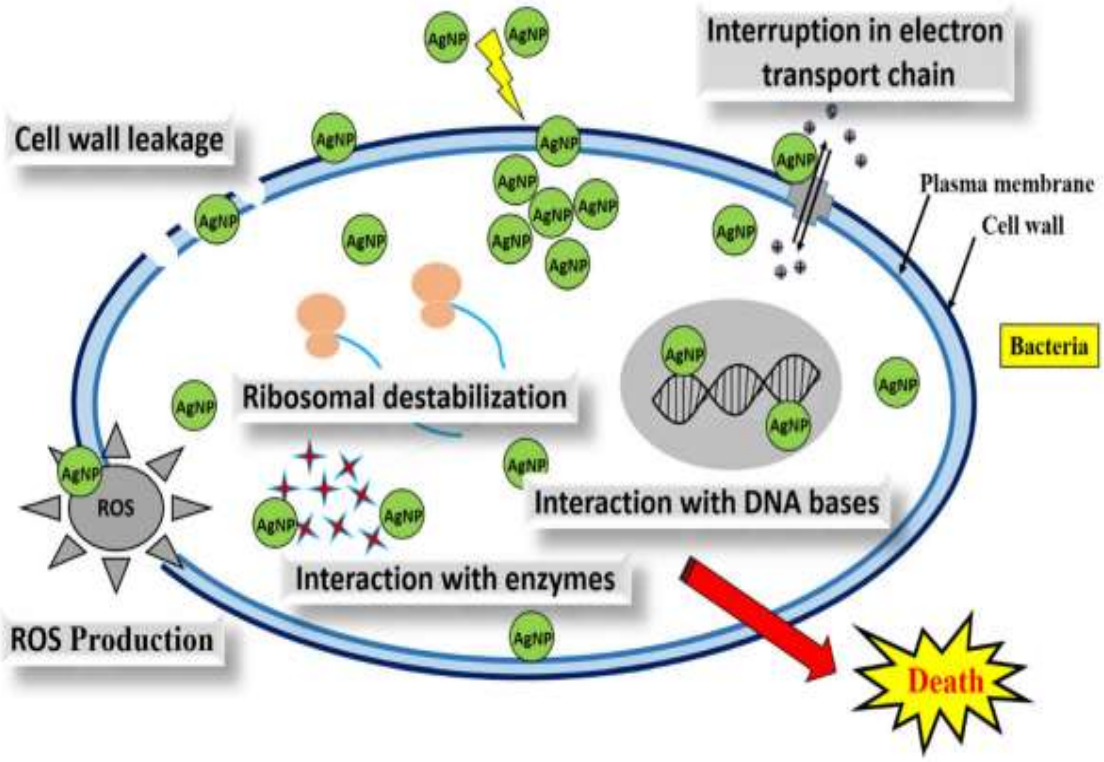

Figure 07: Mechanisms of antibacterial activity for silver nanoparticles (Patil and Kim, 2017)

7.2. Antiviral

Silver's cytoprotective qualities are well recognized, and it has been used to block HIV contact with host cells. AgNPs can also be employed as anti-HIV-1 medicines and to prevent infection following surgery. As a result, the interaction of AgNPs with bacteria and viruses is a burgeoning subject of study (Khatoon et *al*., 2017). AgNPs interact with HIV-1 by binding preferentially to gp120 glycoprotein knobs (figure 08), according to the research. This type of AgNPs interaction prevents viruses from attaching to host cells (Sharmin et *al*., 2021)

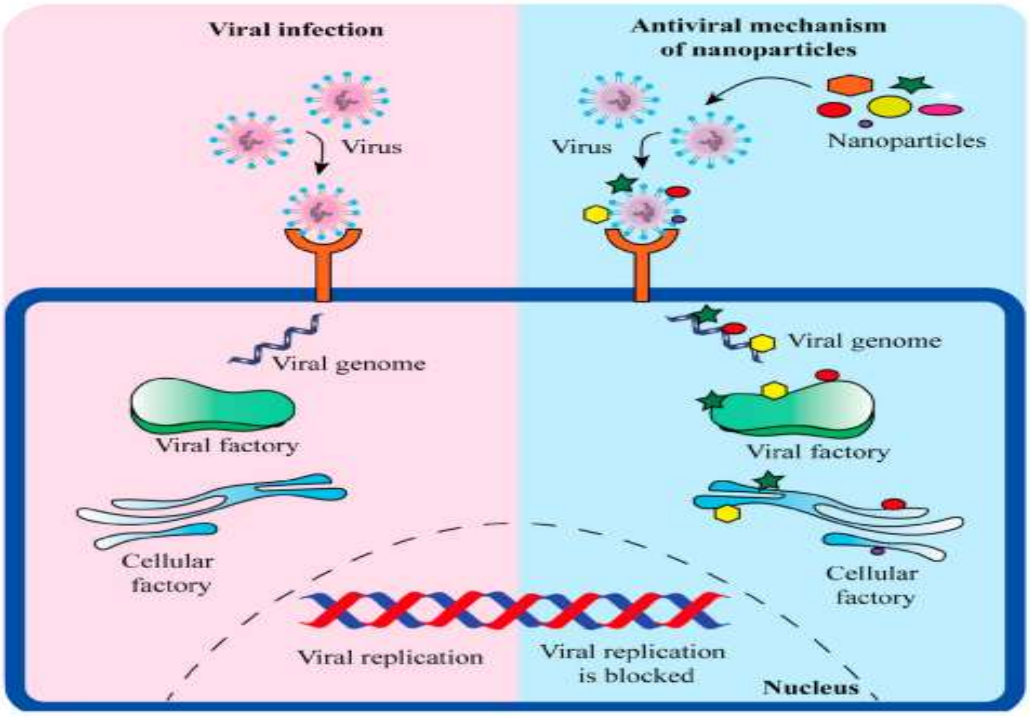

Figure 8: The antiviral mechanism of nanoparticles (Sharmin et *al*., 2021)

7.3. Antioxidant activity

Pevious research showed that silver nanoparticles generated from plant extracts are efficient at scavenging free radicals and serve as a reducing and capping agent (Chang et *al*., 2012). Because of their improved dispersion of AgNPs, the produced AgNPs effectively inhibit the growth of phytopathogens and also produce colloidal nanoparticles that are more stable. In addition, they limit the production of free radicals to prevent cell damage. The AgNPs solution's proton-donating properties may allow it to operate as a free radical scavenger. As a result, it might be applied to both the agricultural and medical fields (Chang et *al*., 2012). It should be mentioned that the flavonoids, alkaloids, tannins, saponins, carbs, phenolic compounds, and glycosides found in the plant extract are actually a valuable root for synthesizing stable AgNPs quickly, and they already play an important role in the reduction and stabilization actions that contribute for the antioxidant activity to AgNPs. (Maruthai et *al*., 2019).

7.4. Anti-Inflammatory Activity of AgNPs

AgNPs have lately gained prominence in the realm of anti-inflammatory medicine. NPS enters the cell through ion channels or pores in the cell membrane. The size of the NP determines this sort of ingression. Although NP uptake does not require membrane receptors, it does require sticky contacts such as electrostatic interactions, Van der Waals forces, and

steric interactions. Different cellular effects are triggered depending on where the NP is located in the cell, which is determined by its size (Ahn et *al*., 2017). Most cellular vesicles readily endocytose some small-sized metal NPs at greater concentrations. Macrophages and neutrophils carry out phagocytosis and macro-pinocytosis. When protein-coated metal NPs engage with macrophages or neutrophils in inflammatory locations, the protein corona that surrounds the nanoparticles is evidently the first to make contact with cell surface receptors (Mahmoudi et *al*., 2011). This protein corona, which is mostly made up of serum proteins, acts as a ligand for M2 macrophage receptors. The anti-inflammatory M2 macrophages are activated as a result of this. In the uptake of NP, these macrophages are essential. When serum proteins are present, M2 macrophages absorb NP quicker and more effectively than M1 macrophages, according to (figure 09). Al-Shmgani et *al*., (2017) (Al-Shmgani et *al*., 2017) used both in vivo and in vitro models to gather more proof of the anti-inflammatory effects of AgNPs. They discovered that AgNPs can down-regulate the amounts of inflammatory markers, suggesting that AgNPs could lessen inflammatory events during the initial stages of wound healing (Jain et *al*., 2021). In a porcine contact dermatitis model, nanosilver therapy accelerated the death of inflammatory cells via apoptosis and decreased the levels of inflammatory cytokines. The amount of edema and cytokines in the tissues of the paws can be reduced by biologically produced AgNPs. They can also stop HaCaT cells from producing cytokines that are caused by UV-B radiation (Agarwal et *al*., 2019).

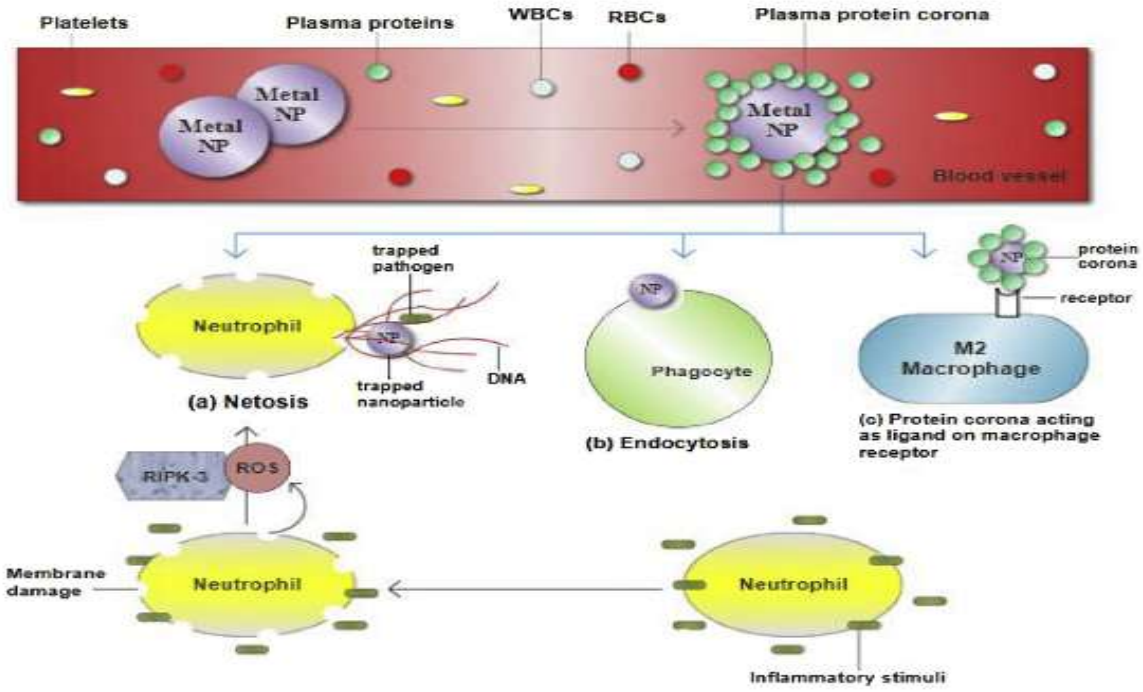

Figure 9 : Anti-inflammatory mechanism adopted by nanoparticles (Agarwal et *al*., 2019)

7.5. Anticancer activity

Numerous studies have shown silver nanoparticles have entered the field of medicine as anti-cancer medicines (Raghunandan et *al*., 2011).

Silver nanoparticles can enter cells via endocytosis, according to several in vitro studies, and their placement inside the cell can be determined in the cytoplasmic perinuclear region and the endolysosomal compartment (Asharani et *al*., 2009). Moreover, due to their ability to enter mitochondria and cause increased oxidative stress, which has an impact on cell respiration, silver nanoparticles can release reactive oxygen species (ROS). In conclusion, AgNPs' hazardous processes can cause DNA damage, apoptosis induction, and mitochondrial damage in cancer cells (Hsin et *al*., 2008; Kim et *al*., 2009). The mechanism of action of silver nanoparticles is depicted (figure 10). Various researches has shown that AgNPs affect how vascular endothelial growth factors operate (VEGF). It is also called the vascular permeability factor, and it is necessary for tumor angiogenesis to take place (Kalishwaralal et *al*., 2009). These findings suggest that AgNPs have anti-cancer effects and could be used as a cancer treatment or angiogenesis inhibitor (Sriram et *al*., 2010). Determining the efficacy of AgNPs as a cancer treatment in a variety of cancer types there is currently a lot of toxicological data being published on nanoparticles. Silver Nanoparticles serve as antitumor agents by decreasing the progressive development of tumor cells. This evidence suggests that Silver Nanoparticles can cause cytotoxicity in cancer cells and halt tumor progression while causing no harm to healthy cells (Sukirtha et *al*., 2012).

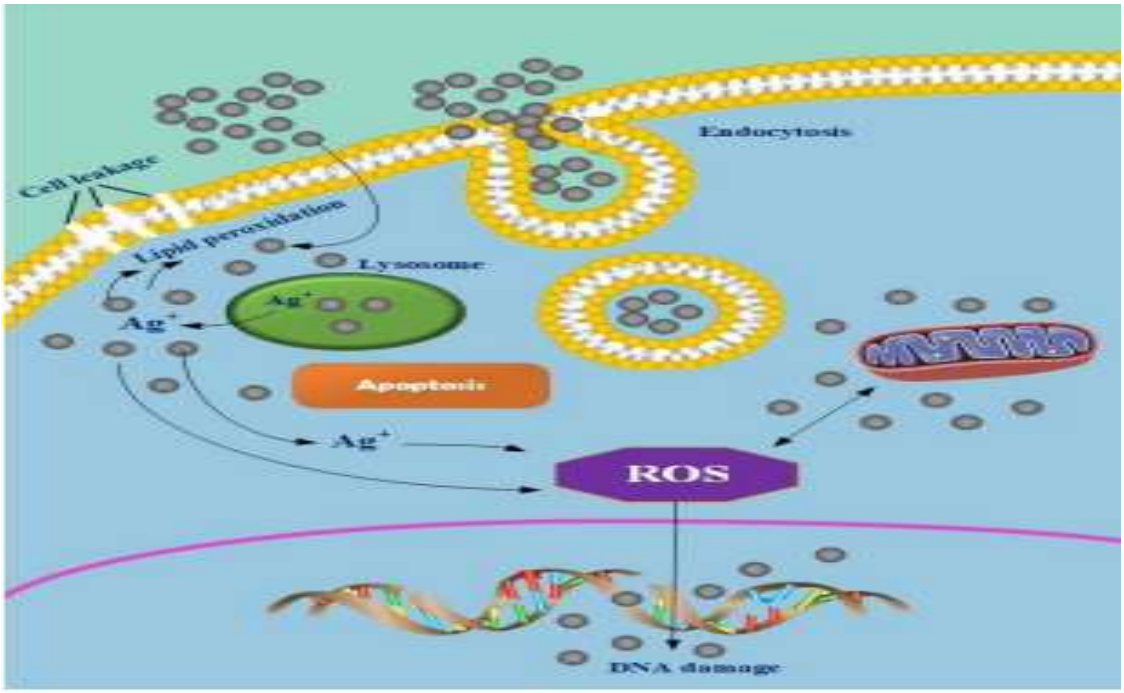

Figure 10: The anticancer mechanism of silver nanoparticles (Yesilot and Aydin, 2019).

7.6. Other applications

Future applications of nanoparticles are quite hopeful given the global threat posed by the excessive spread of microbial contaminations. Nanoelectronics, molecular imaging, diagnostics, and biomedicine are just a few applications of AgNPs in nanomedicine. These novel applications rely on the application of a higher electromagnetic field to the surface and vicinity of AgNPs (Liu et *al*., 2021). AgNPs contain NPs probes with extremely high sensitivity that may be utilized to target and scan DNA, proteins, tiny molecules, cells, tissues, and even tumors. In fact, imaging systems typically use AgNPs with increased plasmon resonance, particularly for cellular imaging with contrasting chemicals stabilized to AgNPs by surface treatment (Heilman and Silva, 2017). Central venous catheters (CVC) are frequently used in bedridden patients to provide access to intravenous fluid administration, hemodynamic monitoring, pharmaceutical delivery systems, and nutritional support. These medical devices are categorized as an outstanding class of equipment sensitive to bacterial contamination and colonization, despite the fact that they are a large contributor to hospital-acquired infections (Heilman and Silva, 2017). The human eye is a vital system with incredible vascularization and connectivity that can be easily polluted by germs (Weng et *al*., 2017) at the right humidity and temperature conditions. AgNPs demonstrated potential activity in the development of cutting-edge, performance-improving therapies for bacterial infections that affect the eyes. The damage to retinal cells was reduced by AgNPs encapsulated with calcium signals, which might be exploited for retinal imaging (Yee et *al*., 2016). Additionally, AgNPs were demonstrated to be efficient as novel nanostructured systems for the detection and treatment of cancer. AgNPs have a broad range of biocompatibilities, making them prospective therapeutics for important cancer and MDR resistance programs as well as anti-infective strategies (Habeeb Rahuman et *al*., 2022; Nithya Deva Krupa and Raghavan, 2014). Therefore, all these properties have made AgNPs one of the most highly recommended bioactive that can be used in pharmaceutical products.

CHAPTER III

Cadmium Chloride

1. Identification

Environmental toxins, such as cadmium, can cause a wide range of clinical symptoms. Several organ systems, including the renal, hepatic, and immunological systems, may be damaged in humans and animals (El-Boshy et *al*., 2015).

Cadmium is a chemical metal silvery-white, soft ductile with atomic number 48. It has been classified as a nonessential element biochemically (Pinot et *al*., 2000). It's naturally present (in low amounts) in a variety of foods and is one of the components of cigarette smoke. Metal plating and the production of Ni-Cd batteries are two of Cd's many applications. High levels of Cd in the body, whether from inhalation or ingestion (eating), can cause a variety of problems, including lung damage and renal illness. Work that involves handling Cd or its salts carries a greater risk of exposure. Because Cd stays in the body, low-level exposure over a lengthy period of time might produce health concerns (Peereboom-Stegeman and Jongstra-Spaapen, 1979).

2. Physical and chemical properties

Group XII of the periodic table contains the chemical element cadmium (Cd, atomic weight 112.41). This soft, silvery-white metal is similar to zinc and mercury in terms of its physical and chemical properties (Table 2). Eight stable isotopes of cadmium make up its atomic weight. With two electrons in the s orbital and a fully filled d orbital, it is a post-transition metal (Fiamegkos et *al*., 2015). Cadmium is also more malleable, ductile, and soft than zinc, and the majority of its compounds favor the oxidation state of +2. Cd is a non-combustible, water-insoluble metal used as a protective plate that resists corrosion. When cadmium is burned in the air, cadmium oxide is produced (Nriagu, 1980).

Cadmium is found in metallic form or in salts (oxide, chloride, sulphate, etc.). Cadmium salts have a very high thermal and chemical stability (Anzum et *al*., 2022). Cadmium chloride ($CdCl_2$), cadmium nitrate ($Cd(NO_3)_2$), and cadmium sulphate ($CdSO_4$) are in the form of colorless crystals, soluble in water and acids. Cadmium sulfide (CdS) exists as lemon-yellow or red crystals depending on the method of preparation. It is insoluble in water. On the other hand, it releases hydrogen sulfide in contact with concentrated acids (Bylishko et *al*., 2021).

Table 02: Physical and chemical properties of cadmium (Nriagu, 1980).

Property	Information
Atomic number	48
Atomic weight	112.41 u
Atomic radius	155pm
Electronic configuration	[Kr]4d105s2
Melting point	321.07 °C
Boiling point	767.3 °C
Density at 20 °C	8.65 g/cm3
Reduction potential $Cd^{2+} + 2e^- \rightarrow Cd(s)$	−0.40 E°
Heat of fusion	6.21 kJ/mol
Heat of vaporization	99.6 kJ/mol
First ionization energy	867.8 kJ/mol
Second ionization energy	1631.4 kJ/mol

3. Sources of exposure and uses

Cadmium is a contaminant that has entered the environment as a result of, as was already mentioned, the quick development of contemporary technology and industry. The earth's crust is where it is primarily found (Drotning, 1984).

Cadmium in the human diet poses a potential long-term health risk. The main source of cadmium consumption in the nonsmoking general population is food. Mollusks and crustaceans have the highest levels of cadmium among fisheries products (Jimoh et *al*., 2015). Cadmium is also abundant in the 'organ meat' of marine mammals. Generally speaking, plant-based diets contain more Cd than meat, dairy, eggs, and other animal-based foods. Green leafy vegetables, potatoes, carrots, and celery can all have higher metal concentrations than other plant-based foods, along with rice and wheat (Chandel and Jain, 2014). Cigarette smoke(approximately 1µg of each cigarette) is another significant cause of cadmium exposure. When cadmium levels in blood samples from smokers were compared to non-smokers, it was discovered that they had 4-5 times the Cd levels in the blood (Schutte et *al*., 2008). As It can also be found in manures and herbicides (Schutte et *al*., 2008).

Because of its physical softness, good corrosion resistance, and other important characteristics in metal usage, such as low melting temperature, cadmium is a very easy metal to form and has a wide variety of uses. Cd is primarily used to make nickel-Cd batteries (Bashir et al., 2016). The PVC and shipbuilding industries favor Cd as a coating material because of its resilience to oxidation (Bashir et al., 2016). Cd sulfur compounds are used as colorants in plastic, glass, ceramics, rubber, paint, and fireworks (figure 11) (Scoullos et *al*.,

2012). In addition, Cd is frequently discovered in fasteners, industrial tools, home products, automobiles, agricultural equipment, and vehicles (screw nuts, bolts, screws, and nails). It is also used in tire and picture repair (Rahman, 2017).

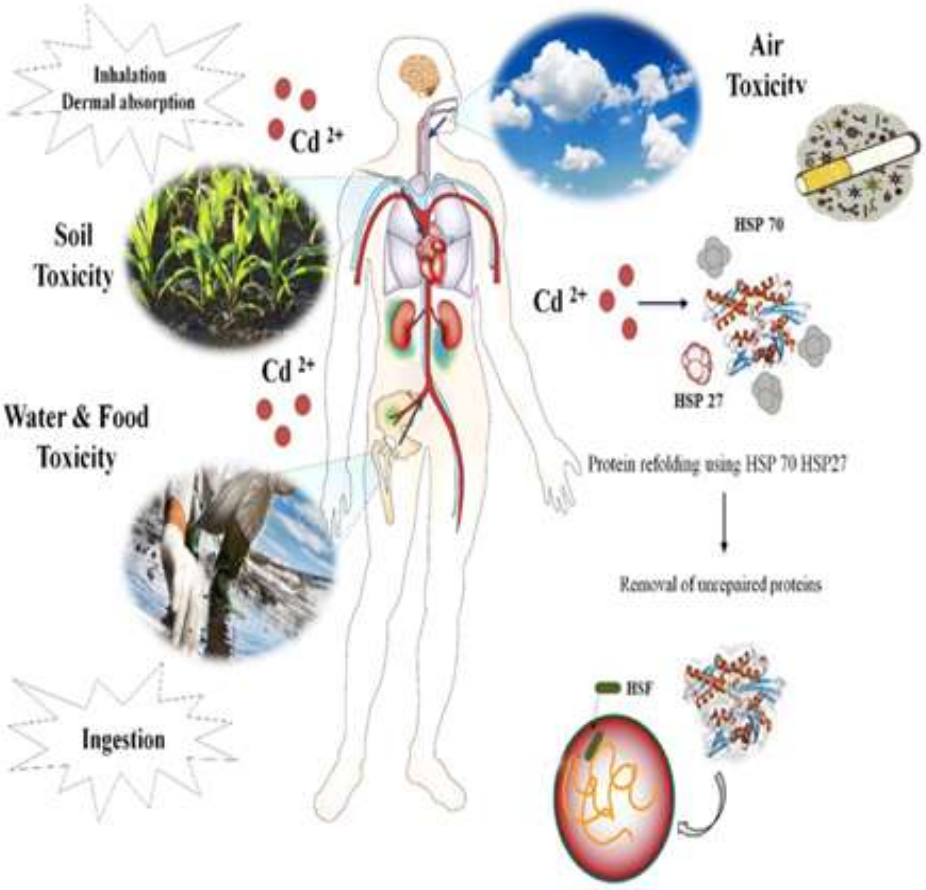

Figure 11 : Different sources exposition of cadmium (Taghavizadeh Yazdi et *al*., 2021)

4. Metabolism

4.1. Absorption

Cadmium is largely absorbed through inhalation and ingestion, with 10 to 50% of inhaled cadmium dust being absorbed, depending on particle size. The respiratory and gastrointestinal (GI) tracts are the main routes of cadmium (Cd) absorption. The skin is only penetrated by a small amount of Cd (Miller and Neathery, 1971; Svartengren et *al*., 1986). The pulmonary absorption of Cd is usually the largest industrial hazard for people and animals. The quantity of inhaled Cd retained varies between 10 and 40%, with the exact amount regulated primarily by mucociliary and alveolar clearance in the lungs (Neathery and Miller, 1975).

4.2. Distribution

Cadmium is absorbed and transported in the blood, primarily in erythrocytes, where it is bound intracellularly to low and high relative molecular mass protein fractions (Nordberg et *al*., 1982). Cadmium coupled to metallo-thionein is rapidly and nearly completely transported from blood to renal tubular cells; however, free cadmium is not taken up to the same amount (Johnson and Foulkes, 1980). Furthermore, cadmium can reach the embryo or fetus early in the pregnancy, and only a little amount of cadmium is transferred across the fully grown placenta (Ahokas and Dilts Jr, 1979) .

Long-term cadmium exposure causes preferential accumulation in the liver and renal cortex, with these organs accounting for up to 75% of the total body burden. About half of the body's load is found in the kidneys, 15% in the liver, and 20% in muscle. While, Brain, bone, and fat have lower concentrations (Sumino et *al*., 1975).

4.3. Metabolism

Cadmium has little or no metabolism, despite the fact that it binds to a variety of macromolecules and protein (Miller, 1973). Unlike the Cd-albumin complex, which does not cross the glomerular barrier due to its high molecular weight, metallothionein is significantly engaged in cadmium binding, which is hypothesized to minimize cadmium toxicity. The cadmium that is bound to metallothionein is released into the bloodstream, where it is removed via glomerular filtration and absorbed by the renal tubules, where the metallothionein is broken down and the cadmium is liberated. Because there is not enough metallothionein produced in the kidney to bind all the free cadmium, there is damage to the tubules or cell membranes due to the activation of oxygen species (Miller et *al*., 1968).

4.4. Elimination

Cadmium is a cumulative toxic substance. Indeed, the biological half-life of cadmium, corresponding to the duration of elimination of half the amount of cadmium present in the organism, is particularly long, since it is approximately 20 to 40 years (Neathery and Miller, 1975). About half of the body's cadmium is in the liver and kidneys. Cadmium excretion is weak and very slow; it is essentially urinary. The appearance of nephrological damage alters the renal elimination capacity of cadmium. A small part of cadmium is excreted via the bile (after conjugation with glutathione), salivary, fecal, and sudoral (Rahimzadeh et *al*., 2017).

5. Toxcicity of cadmium

Cadmium is a toxic metal that targets many levels, perhaps the most prominent of which are the lungs, liver, kidneys, and testicles after acute poisoning. While, it causes renal toxicity, immunotoxicity, ototoxicity, and tumors after prolonged exposure (Genuis et *al*., 2013). In addition, it stimulates cell proliferation, inhibits DNA repair, and prevents apoptosis. On the one hand, it leads to cell death which leads to kidney tissue damage. Further, In cell culture systems, cadmium at low concentration causes apoptosis, and with increasing concentration, it becomes obvious necrosis, and impairment of mitochondrial function stimulates apoptosis (Cannino et *al*., 2009). Moreover, causing inhibition of heme synthesis, cadmium may also impair vitamin D metabolism in the kidney (Kjellström, 1992), with a detrimental effect on the bones. This effect, combined with direct Cd impairment of intestinal calcium absorption and impairment of collagen metabolism, can lead to osteomalacia and/or osteoporosis (Vesey, 2010).

Similarly, Cd-induced dysfunction affects the immune system on multiple levels, including dysregulated thymocyte formation (Hanson et *al*., 2010). In splenocytes, post-natal Cd exposure causes cell cycle arrest and apoptosis. In addition, Cd causes increased autoimmunity, increased nonspecific antibody production, and decreased antigen-specific antibody production (Ohsawa, 2009). Cd also inhibits lymphocyte growth and natural killer cell function (Fortier et *al*., 2008).

Hematopoiesis is negatively impacted, and erythropoietin production is significantly reduced (Horiguchi et *al*., 1994). Meanwhile, Hemolysis may potentially play a role in the development of Cd-associated anemia, which can result in iron deficiency indices despite increased body Fe storage and enhanced duodenal Fe absorption (figure 12).

Otherwise, the 50 percent fatal dose for rats is 500 mg m^3, with 0.02 mg m^3 as the lowest observed adverse impact threshold. The California EPA recommends a public reference level of 0.0001 mg m^3, with a safe level of 0.6 ng m^3 with a 1 millionth lifetime cancer risk (Morselt et *al*., 1983).

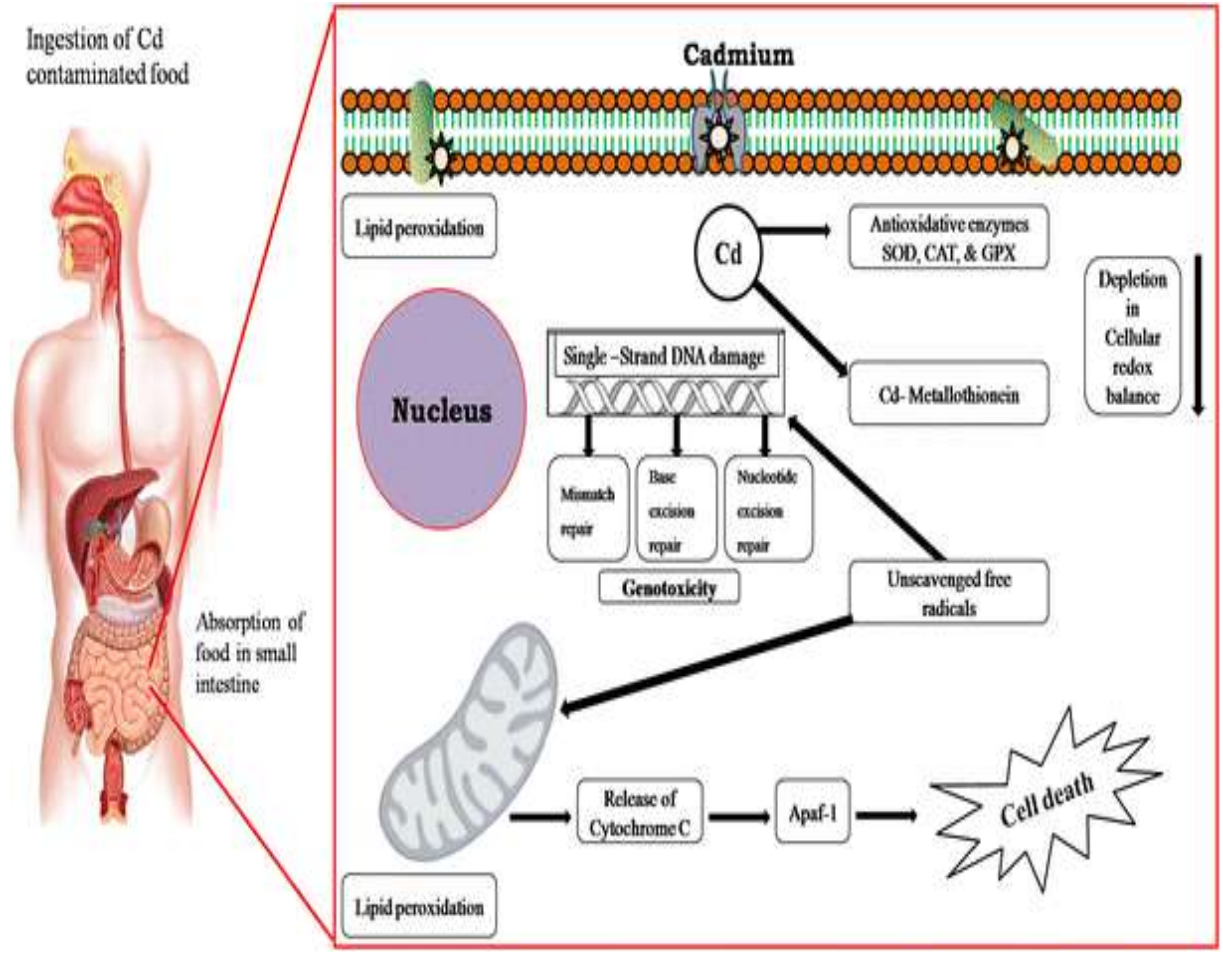

Figure 12 : Mode of cadmium toxicity in human (Kumar et *al*., 2018)

6. Cadmium-Induced Oxidative Stress

Oxidative stress, which is widely acknowledged as one of the major causes of harmful and cancer-causing effects caused by heavy metals, is one of the main mechanisms of these effects (Yiin and Lin, 1995). When oxidative stress occurs, an organ or organism's synthesis of oxidants and antioxidants is out of balance, favoring the former and leading to cellular instability (Knowles and Donaldson, 1990). It has been proposed that this imbalance results from either an excess of reactive oxygen and nitrogen species (ROS and RNS) or from a decrease in the effectiveness of the oxidant defense mechanisms to remove ROS (Lawton and Donaldson, 1991). Normal biological activities such as signal transmission, cell proliferation, gene expression, and immunological defense require physiological quantities of ROS. Hydrogen peroxide (H2O2), hydroxyl radical (HO•), superoxide anions (O_2), peroxyl (RO•), and alkoxyl radicals (ROO•) are examples of reactive oxygen species, whereas reactive nitrogen species (RNS) include nitric oxide radical (NO•), nitrogen dioxide radical (NO2•), and peroxynitrite (ONOO) under normal physiological conditions (ONOO) (Wang et *al*., 2004).

6.1. Mechanism

Depending on the method of exposure, various cellular defense systems are activated in response to Cd exposure to counteract its negative effects. One of the main defense mechanisms is the formation of metallothionein (MT), particularly in the kidney and liver, as well as an increase in cellular glutathione and the activation of the antioxidant transcription factor Nrf_2 (Farant and Wigfield, 1982). These pathways are not "exclusive," but they may function in concert to protect against Cd-induced oxidative damage (Figueiredo-Pereira et *al*., 1998; Patra et *al*., 2007). Once exposure, Cd enters the bloodstream by albumin or erythrocytes, where it undergoes hepatic conjugation with MT to generate Cd-MT, which can be filtered out by the glomerulus and reabsorbed in the proximal and distal tubules (Youngs et *al*., 2000). Lysosomes disrupt the Cd-MT complex when it enters the tubular cell, releasing Cd. As a result of the free Cd, the kidneys are damaged, resulting in oxidative stress. Aside from free Cd, ROS can be formed when Fenton metals (such as iron and copper) are displaced from MT by Cd or when GSH is depleted (Hermes-Lima et *al*., 1991). GSH, which is plentiful in cells, is a free Cd ion target. The disruption of the redox balance caused by Cd-induced depletion of the reduced GSH pool results in an oxidative environment. As a result, Cd-induced oxidative damage is thought to be a key mechanism for causing toxicity in numerous organs by weakening the antioxidant system (Bae et *al*., 2001; Hansen et *al*., 2006). Gene control of proto-oncogene (Hanahan and Weinberg, 2000) , oxidative stress (Ikediobi et *al*., 2004; Othman and El Missiry, 1998; Piqueras et *al*., 1999), disruption of cadherins, suppression of DNA repair, and interference with apoptosis are all basic mechanisms involved in cadmium carcinogenesis. Cadmium is a cell toxin that increases lipid peroxidation and/or alters intracellular glutathione levels, causing oxidative stress. The ubiquitin/ATP-dependent proteolytic pathway is affected. The biological mechanisms underlying cadmium toxicity, however, are largely unknown (Lafuente et *al*., 2000). A significant effect of oxidative stress induced on by Cd is lipid peroxidation (Biswas et *al*., 2001). The transcription factors AP-1 and NF-κB are sensitive to oxidative stress in the cell. The activation of these transcription factors by Cd has been shown in intact animals and in cultured cells. Otherwise, cadmium could obstruct DNA repair, causing a greater buildup of damaged DNA bases and incorrect DNA repair systems malfunctioning (Figueiredo-Pereira et *al*., 1998). A deleterious mutation rate may result from the inability of DNA repair machinery to correct faulty bases. DNA stability genes that are in charge of DNA repair and cell cycle regulation can cause tumor development in higher eukaryotes. The balance between ROS and antioxidant agents (enzymes and antioxidant compounds) in the cells is disturbed by excessive ROS generation.

Cd lowers intracellular GSH levels, which causes cell death brought on by ROS. Another enzyme needed for the antioxidant defense system in cells is glutathione reductase (figure13) (Shih et *al*., 2004).

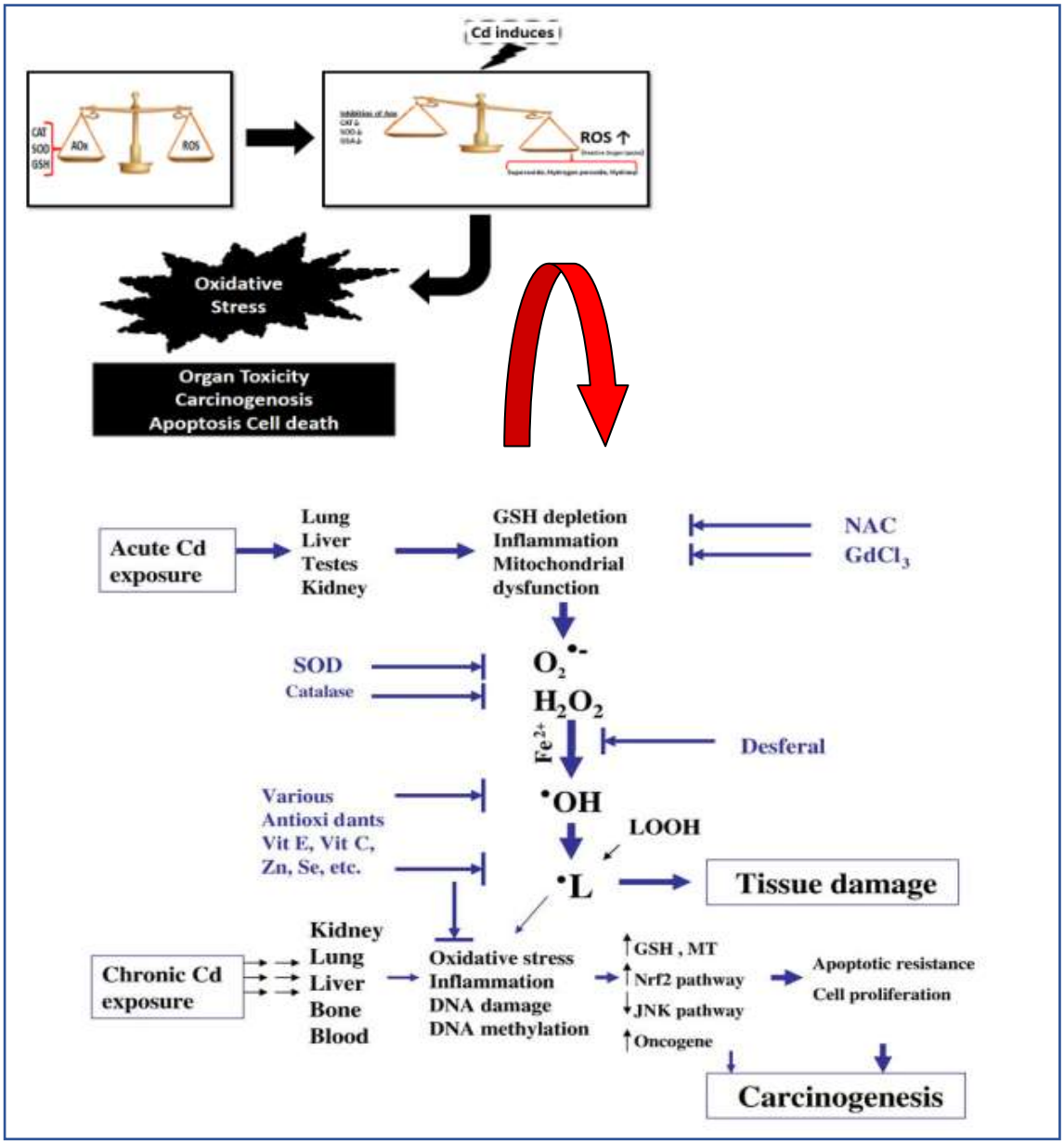

Figure 13 : Proposed pathways for ROS in Cd toxicology and carcinogenesis following acute and chronic exposures (Biswas et *al*., 2001).

SECOND PART

Experimental Study

CHAPTER I

Material & Methods

1. Materials

1.1. Plant material

The aerial parts of the *H. lippii* were collected during the flowering period in March 2020 from Southeastern Algeria exactly in the region of Elhamadin-province (33°35’00’’N6°56’33’’E) of El -Oued, the plant material was identified by Professor CHOUIKH Atef (Faculty of Natural Science and Life, El Oued University). To eliminate dust and other foreign particles, the aerial section was cleaned under running tap water. Then, it was dried, ground, and stored for future use.

Figure 14 : *Helianthemum lippii* (L) Dum. Cours (2020) (Original photo).

1.2. Animals

A total of 35 adult male albino rats, weighing 230.36± 3.81g were obtained from the animal house of Pasteur Institute, Algeria. They were placed and kept in the animal house of the Molecular and Cellular Biology Department, Faculty of Natural and Life Sciences, University of El-Oued, Algeria. Animals were adapted for 2 weeks under the same laboratory conditions of photoperiod (12 h light/12 h dark) with a relative humidity of 64±2% and room temperature of 19±1°C. Standard rat food (Southon et *al*., 1984) and tap water were available libitum for the duration of the experiments. The care and handling of the rats during all experimental procedures followed the local ethics committee's recommended practices.

1.3. Bacterial strains

Samples were tested for their antibacterial efficacy against six bacterial strains obtained from the Pasteur Institute's laboratory in Algeria, including three Gram-positive bacteria (BS: *Bacillus subtilis* ATCC 6633; SA: *Staphylococcus aureus* ATCC 6538; and LI: *Listeria innocua* CIP 74915) and three Gram-negative bacteria (EC: *Escherichia coli* ATCC 8737; PA: *Pseudomonas aeruginosa* ATCC 9027; ST: *Salmonella typhimurium* ATCC 14028).

1.4. Chemicals and reagents

Aluminum chloride ($AlCl_3$), ferric chloride ($FeCl_3$), sodium carbonate (Na_2CO_3), and trichloroacetic acid were obtained from Prolabo (USA). Folin Ciocalteu reagent, Folin-Denis reagent, and hydrogen peroxide (H_2O_2) were obtained from Biochem Chemopharma Co (France). The rest of the chemicals, reagents, and organic solvents were obtained from Sigma-Aldrich (USA). On the other hand were used commercial kits obtained from Spinreact (Barcelona, Spain) for the measurement of biochemical parameters.

1.5. Antibiotics

The antibiotics Amoxicillin and Cephalexin are used because Amoxicillin treats a broad range of gram-positive bacteria as well as some other gram-negative strains, and Cephalexin was used to treat both Gram-positive and many Gram-negative bacteria.

2. Methods

2.1. Phytochemical analysis of *H.lippii*

2.1.1. Extraction of *H.lippii* Aqueous extract

H.lippii dry aerial part powder weighing 10 g was combined with 100 mL of distilled water to create the aqueous extract. After being macerated for 24 hours at room temperature, the mixture was filtered using Whatman paper, and it was then evaporated using a rotary evaporator. The extract was weighed and stored at 4°C in a refrigerator for subsequent analysis (Murugan and Parimelazhagan, 2014).

2.1.2. Extraction of flavonoids.

30 g of the plant were macerated in 300 mL of MeOH for 24 hours, according to Bekkara et *al* (1998). The first extraction was made using 150 mL of hot water and 150 mL of ethyl acetate after filtration and solvent evaporation (2 times). In the aqueous phase of the second extraction, 150 mL of 1-butanol were added twice. In a rotary evaporator, the two organic phases (ethyl acetate and 1-butanol) were evaporated to produce the two flavonoid phases (ethyl acetate and 1-butanol).

2.1.3. Extraction of tannins.

According to Lu et *al* (2007), the dried plant was macerated for 3 days in the dark and at room temperature in 300mL of water/acetone (7V/3V). After filtering, the acetone was

expelled, and the aqueous layer was then extracted using dichloromethane and ethyl acetate. Finally, the organic phase was dried to produce the tannin extract.

2.1.4. Extraction of anthocyanins

H.lippii was extracted in the dark for 20 hours at room temperature using 0.1 % HCl (v/v) in 50 mL of methanol and *H.lippii* was used in the amount of 12 g. The solid residues were rinsed with an additional 50 mL of 0.1 % HCl (v/v) in methanol after the sample was filtered. Filtrates were mixed together and dried at 30°C in a rotary evaporator. The residual particles were dissolved in deionized water containing 0.01 % HCl (v/v) and filtered in stages (Longo et *al*., 2007).

2.1.5. Extraction yield

The extraction yield was calculated as follows equation (1):

$$\text{Yield (\%)} = W1/W2 \times 100 \quad (1)$$

Where W1 is the weight of the extract and W2 is the weight of the dried powder of plant material (Boutennoun et *al*., 2017).

2.1.6. Phytochemical Screening

Phytochemical screening Active constituents in the plant extract of *H.lippii*. Were identified and detected by performing chemical tests as follows:

2.1.6.1. Polyphenols

2 mL of the extract received a few drops of a 2 % (w/v) $FeCl_3$ solution. $FeCl_3$ takes on a greenish or blackish-blue coloring when polyphenol derivatives are present (Sankhalkar and Vernekar, 2016).

2.1.6.2. Alkaloids

In two test tubes, introduce 1 mL of extract for analysis. Acidify the medium with a few drops of HCl and add drops of Mayer's reagent to the first tube and a few drops of Wagner's reagent to the second tube. The appearance of a white or brown precipitate respectively reveals the presence of alkaloids (Gontijo et *al*., 2017)

2.1.6.3. Flavonoids

We added 5mL of the extract to be tested, 5mL of dilute ammonia, and 1mL of H_2SO_4 to the test tube, and the presence of flavonoids is demonstrated by the emergence of yellow color (Ibtissam et *al*., 2021).

2.1.6.4. Terpenoids

In a test tube, we put 5 mL of plant extract along with 2 mL of chloroform and 3 mL of strong sulfuric acid. A reddish-brown colour results from the presence of terpenoids (Harborne, 1998).

2.1.6.5. Saponins

A test tube contains 10 mL of the aqueous extract. After shaking the tube for 15 seconds, it was left to stand for an additional 15 minutes. More than 1 cm of sustained foam height indicated the presence of saponins ((Edeoga et *al*., 2005).

2.1.6.6. Tannins

In a test tube, we combine 5 mL of the extract with 1 mL of a 2% aqueous ferric chloride solution (FeCl3). A greenish or bluish-blackish hue indicated the presence of tannins(Evans, 2009).

2.1.6.7. Cardiac glycosides

2 mL of chloroform were mixed with 1mL of the extract. The interior side of the test tube was then carefully added with H_2SO_4. The existence of a glycone part of a cardiac glycoside is indicated by a reddish-brown color (Yam et *al*., 2009).

2.1.6.8. Mucilages

3 mL of methanol was mixed with 1mL of the aqueous extract at 60 °C. The flocculent precipitate, after stirring, indicates the presence of mucilage (Kiendrebeogo et *al*., 2016)

2.1.6.9. Anthocyanins

The aqueous extract is treated by adding a little amount of hydrochloric acid followed by a small amount of ammonia (NH_4OH). If there are anthocyanins present, the color will alter, and red will show (Wadood et *al*., 2013).

2.1.6.10. Leuco anthocyanins

A volume of 5 mL of the infused is mixed with 4 mL of hydrochloric alcohol (Ethanol / pure HCl 3v /1v). After heating in a water bath at 50°C for a few minutes, the appearance of a cherry red color indicates the presence of leuco anthocyanins (Bate-Smith, 1954).

2.1.6.11. Steroids

1mL of the extract received 5 drops of concentrated H_2SO_4. The presence of steroids is indicated by the color red (Trease and Evans, 1989).

2.1.7. Quantification of phytochemicals compounds

2.1.7.1. Estimation of total phenolics

The total amount of phenolics was determined using the Folin-Ciocalteu method. To 1 mL of 10% Folin-Ciocalteu reagent, 0.2mL of the aqueous extract of H. lippii was added. The addition of 800 L of saturated sodium carbonate (75 g/L) was made after 4 minutes. After 2 hours of incubation at room temperature, the absorbance was measured at 765 nm. To ensure that the results could be replicated, the tests were run three times (Slinkard and Singleton, 1977). From the calibration equation linear of gallic acid used as the standard, the total phenolic content was calculated in mg equivalent of gallic acid per gram of extract.

2.1.7.2. Estimation of total flavonoids

We used the aluminum chloride ($AlCl_3$) colorimetric method for determining the total flavonoid content of *H.lippii* extract (Ahn et *al*., 2007) as follows;

1mL of the $AlCl_3$ solution is mixed with 1mL of the sample, and on the other hand with 1mL of the standard. At 430 nm, the absorbance was measured, after 30 minutes against the prepared reagent blank. In order to determine the results, a linear calibration equation using quercetin as the standard was utilized. The results were represented as milligrams of quercetin per gram of extract.

2.1.7.3. Estimation of total hydrolyzable tannins

The Folin-Ciocalteu colorimetric method was used to calculate the total hydrolyzable tannin concentration. A 10 mL test tube containing 8.4 mL distilled water, 0.5 mL Folin-Ciocalteu reagent, and 0.1 mL sodium carbonate solution (7%) was filled with an aliquot of 1mL tannic acid in distilled water of each concentration. Absorbance was measured at 700 nm against a blank after incubation for 30 minutes. All of the tests were repeated three times. The absorbance was recorded for each concentration of the extract using the same method as

for the standard. The amount of tannic acid equivalents (TAE) per gram of dry extract (mg/g) represents the overall amount of tannin in the extracts (Poudel and Rajbhandari, 2020).

2.1.7.4. Estimation of condensed tannin

The level of tannin in the extract was determined using spectrophotometry, according to Broadhurst and Jones (1978) (Broadhurst and Jones, 1978), Catechin was used to make the calibration curve. The sample was pipetted into an aluminum foil-wrapped tube along with 3.0 mL of newly prepared vanillin reagent (4% w/v vanillin in methanol), and the mixture was properly mixed before 1.5 mL of strong hydrochloric acid was added. After 15 minutes at 20 to 2°C, the reaction's absorbance was assessed against water at 500 nm.

2.1.7.5. Estimation of total Saponin content

The sample aqueous solution was completely combined with 5.0 mL of 72% (v/v) sulfuric acid in an ice-water bath before 0.5 mL of an 8% (w/v) vanillin solution was added. After that, the mixture was heated in a bath at 60°C. The absorbance at 535 nm was then measured after was cooled in cold water for 10 minutes (V. Le et *al*., 2018).

2.1.7.6. Total anthocyanin content (TAC)

The amount of total anthocyanins was determined using the pH differential method, according to Brito et *al*. (2014) (Brito et *al*., 2014), 400 µL of our sample, which had a concentration of 1 mg/mL in water, was diluted using two different buffers—0.4 M sodium acetate buffer, pH = 4.5, and 0.025 M potassium chloride buffer, pH = 1.0. Measurements of the absorbance at 510 and 700 nm were made following 30 minutes of incubation. The anthocyanin content, which is expressed as mg cyanidin 3-glucoside equivalents per gram of fraction (C3GE/g fraction) (equation 02), is calculated using the formula as follows:

$$TAC = (A \times MW \times DF \times 100)/MA \qquad (2)$$

Where; $A = (A_{510} - A_{700})\ pH1 - (A_{510} - A_{700})\ pH_{4,5}$; MW: molar weight (449,2g/mol); DF: dilution factor (10); MA; Molar apsorptivity of cyanidin 3-glucoside (26,9l/mol.cm).

2.1.8. Analyze qualitative by HPLC

Using scanning equipment and high-performance liquid chromatography, the active components were discovered (HPLC). For the investigation of phenolic chemicals in crude extract, we utilized HPLC with UV-Vis type Shimadzu LC20 AL equipped with the universal

injector (Hamilton 25l), an analytical column was a Shim-pack VP-ODSC18 (4,6mm250mm, 5m), and UV-VIS detector SPD 20A type (Shimadzu). The reverse-phase chromatography studies were conducted using non-polar aliphatic residues, and the mobile phase comprised of gradient elution of a combination of acetonitrile and acetic acid (0.1%). The injection volume was 0, 45µL and the flow rate was 1mL/min. The monitoring wavelength was 268nm, and the sample and standard injection volume were 20µL.

The retention duration and UV absorbance of various compounds were compared to those of the standards to identify them.

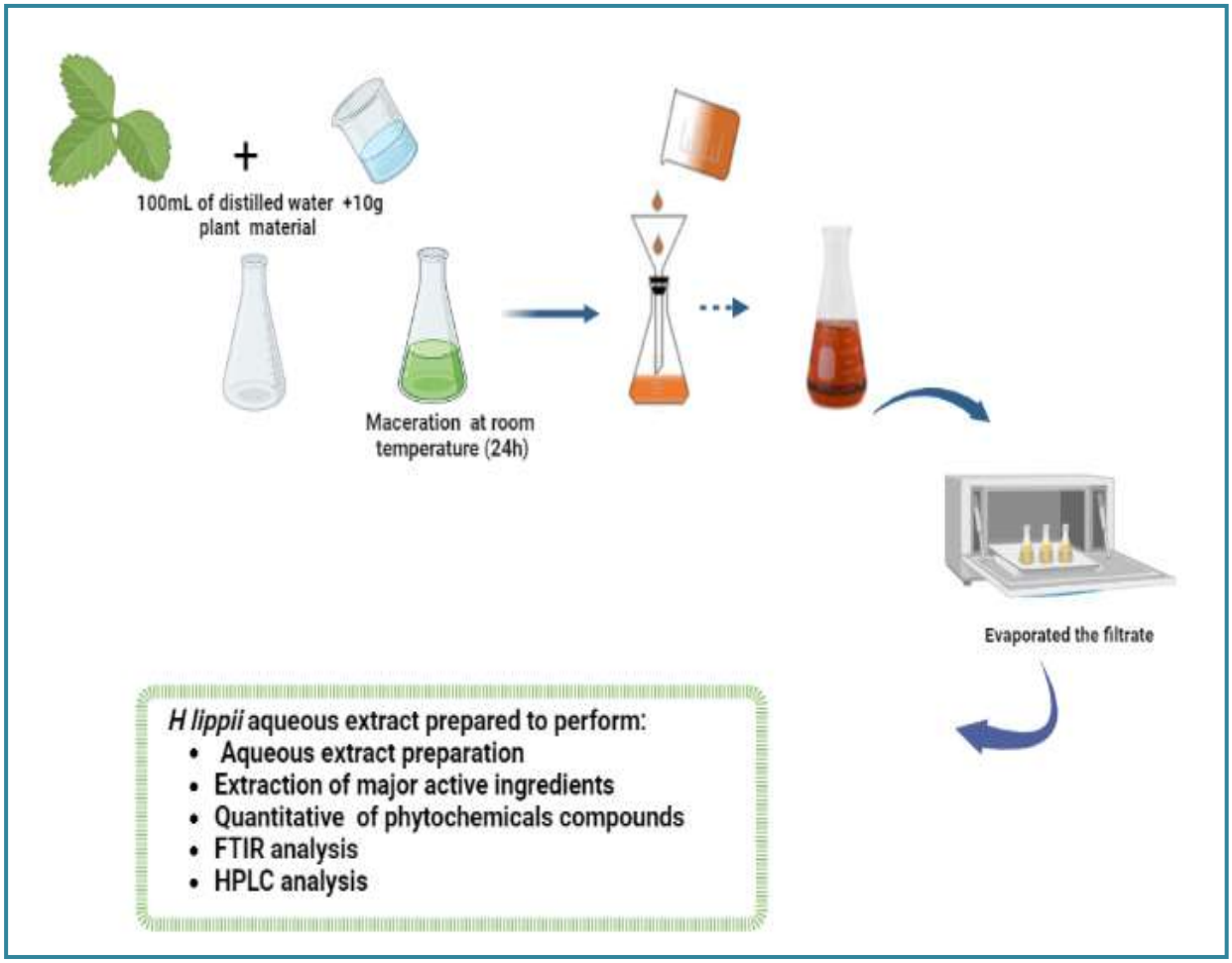

Figure 15 : *H.lippii* aqueous extract preparation

2.2. Green synthesis of Silver Nanoparticles

AgNPs were synthesized by mixing 10 mL of aerial part of *H.lippii* with 90 mL of a 1 mM AgNO3 solution. A brownish tint appears a short while later, indicating the synthesis of AgNPs. For 24 hours, the combinations were incubated in the dark and heated to 60°C. After AgNPs' production was confirmed by UV-vis spectra, it was centrifuged to ensure full separation and, it was then many times washed with distilled water and ethanol. The final

precipitate was carefully collected and dried to obtain the final nanoparticles of AgNPs for additional future experiments and characterizations (Jha and Shimpi, 2018).

2.2.1. Characterization of AgNPs

The methods UV-Vis, FT-IR, XRD, SEM, and EDX were used to characterize silver nanoparticles.

2.2.1.1. UV-visible spectrophotometer

A UV-Vis spectrophotometer was used to measure the optical characteristics of AgNPs (the device is Shimadzu UV-1800, Japan UV–Vis Spectrophotometer). Data were recorded in the 200 to 800 nm wavelength range.

2.2.1.2. Fourier transforms infrared spectroscopy (FTIR)

The bonding characteristic of AgNPs was analyzed using a Fourier transform infrared spectrometer (FTIR, the Agilent Cary 630 type (Agilent Technologies)). The sample was placed directly on the platform, uniform pressure was applied, and the spectra were recorded as the average of 8 scans at 16 Cm^{-1} resolution in the region of (4000-400) Cm^{-1}.

2.2.1.3. X-ray diffraction (XRD)

The crystalline structure of AgNPs was examined by using X-Ray Powder Diffraction (PROTO AXRD Benchtop) using CuKα radiation (30 kV and 20 mA) with a wavelength of 0.154281 nm and scanning speed of 0.05°. In a 2θ range of 20–80°, we managed to conduct the X-ray analysis of distinctly mixed solids. The crystallite size was calculated using the Scherrer formula (equation 03), by selecting the dominating peak of the highest intensity.

$$D = \frac{K.\lambda}{\beta.\theta} \qquad (3)$$

Where **D** is the crystallite size, **k** is the so-called shape factor (0.9), $\boldsymbol{\lambda}$ is the wavelength (0.154281nm, CuKα), $\boldsymbol{\beta}$ is the Full Width at Half Maximum (FWHM), and $\boldsymbol{\theta}$ is the diffraction angle.

2.2.1.4. Scanning electron microscopy (SEM) and Energy dispersive spectroscopy (EDX)

The scanning electron microscopy makes it possible to scan part of the surface of the sample using an electron beam with a diameter of a few nanometers. This method allows visualization of morphological features with high magnification created between the electron

beam and the atomic envelopes of the elements of the material to be analyzed. During scanning, X-ray fluorescence radiation is created which can be recorded by an energy dispersive spectroscopy (EDX) and used for analysis.

The particle size and shape of silver nanoparticles were determined by the phenom Pro Desktop scanning electron microscopic (SEM) with an optical magnification range of 20-134×, an electron magnification range of 160-150,000×, maximum digital zoom of 12×, acceleration voltages of 5, 10, and 15 kV, a backscattered electron detector. Backscattered electron detector (BSD) and energy dispersive spectroscopy (EDX), with a nominal resolution of 6nm or less. The microscope is equipped with a temperature-controlled sample holder (temperature range -20°C to 50°C).

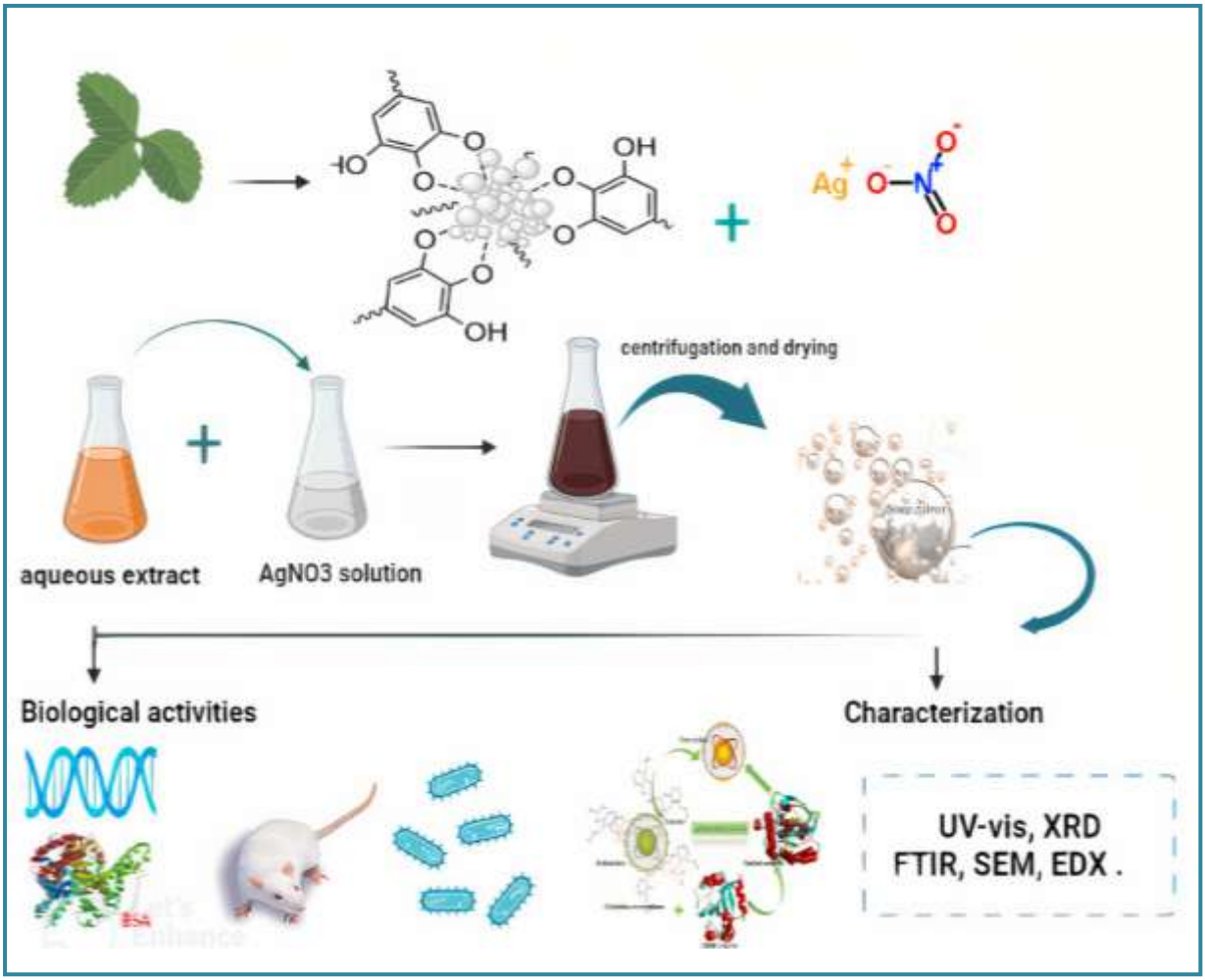

Figure 16 : The green synthesis method of silver nanoparticles

2.3. *In Vitro* Activity of the aqueous extract of *H lippii,* silver nanoparticles, and the fractions obtained from this plant

2.3.1. Antioxidant activity

2.3.1.1. DPPH free-radical scavenging activity (DPPH)

1 mL of the DPPH• solution is mixed with 1 mL of each extract (or ascorbic acid as a control). To complete the reaction, the reaction mixture is stirred briefly and then kept at room temperature for 30 minutes in the dark. At 517 nm, the reaction medium's absorbance is measuredb (Equation 04)(Mansouri *et al*., 2005).

Percent inhibition (PI) = [(Abs control - Abs sample) / Abs control) × 100] (4)

Where Abs control is the absorbance of the control (containing all reagents except the sample) and Abs sample is the absorbance of the sample.

2.3.1.2. Reducing Power Assay (RP)

Oyaizu's methods were used to calculate the extract's reducing power. The samples was combined with phosphate buffer (2.5 mL, 0.2 M, pH 6.6) and 1% potassium ferricyanide water solution (2.5 mL, K3 [Fe (CN) 6]) at various concentrations (mg/mL) in distilled water. After aliquots of trichloracetic acid (2.5mL, 10% aqueous solution) were added, the mixture was incubated at 50°C for 20 minutes before centrifuging for 10 minutes at 3000 rpm. The supernatant (2.5mL) and filtered water were mixed with freshly manufactured $FeCl_3$ (0.5mL, 0.1%) solution (2.5mL) the absorbance was determined at a wavelength of 700 nm. The use of ascorbic acid as a positive control was used (Oraiza, 1986).

2.3.1.3. Phosphomolybdate assay (Total Antioxidant Capacity)

The assay is based on the capacity of the extract to reduce Mo (VI)-Mo (V) and then form a green phosphate/Mo (V) complex at an acidic pH. An aliquot of 0.3 mL extract was combined with 3 mL of reagent solution (0.6 M sulfuric acid, 28 mM sodium phosphate, and 4 mM ammonium molybdate). The reaction mixture was incubated in tubes for 90 minutes at 95°C. After the samples cooled to room temperature, the absorbance of the solution at 695 nm was measured using a spectrophotometer in comparison to a blank. 0.3 mL of distilled water is used as the blank in place of the extract (Islam et *al*., 2013).

A standard AA graph was used to estimate the ascorbic acid equivalents. The experiment was done three times, and the results are expressed as mg per g of extract that is equivalent to ascorbic acid.

2.3.1.4. Linoleic acid/b-carotene bleaching assay (BCB)

The linoleic acid/b-carotene method was used to assess the samples' anti-lipid peroxidation abilities (Islam et *al*., 2013). A stock solution of b-carotene and linoleic acid was created by mixing two milligrams of b-carotene with 45 µL of linoleic acid, 10 mL of chloroform, and

400 mg of Tween 40. Vacuum was used to evaporate the chloroform, and the residue was blended with aerated 100 mL of pure water. Separate test tubes containing the sample were filled with the aforementioned combination after it had been produced in distilled water at varied concentrations (mg/mL).

A spectrophotometer was used to measure the zero time absorbance at 470 nm as soon as the sample was added to each tube. After that, the tubes were then incubated at 50°C in a hot water bath. The absorbance levels were measured at 470 nm again after 2 hours. As a positive control, gallic acid was utilized. For background subtraction, a blank devoid of b-carotene was created.

The following equation (05) was used to obtain the inhibition percentage of bleaching (Ibleaching percent):

$$I_{\text{bleaching}}\,(\%) = \frac{Absorbance\ after\ 2h\ of\ assay}{Initial\ absorbance} \times 100 \qquad (5)$$

2.3.2. Hemolytic activity

The Hemolysis experiment is conducted as described below, according to Vinjamuri et *al*. (2015); 5mL of blood was centrifuged at 1000 rpm for 10 minutes at 40°C in tubes containing 5.4 mg of EDTA to stop coagulation. The hemolytic assay was carried out on washed erythrocytes that were kept at 40°C for 6 hours. 100 µL of test samples (containing an *H.lippii* component, silver nanoparticles, and various fractions) and 50 µL of erythrocyte suspension in 10 dilutions were employed. The positive and negative controls, 100 µL each of 1XPBS and 100 µL each of 1% SDS, were utilized. After that, incubate for 60 minutes in a water bath at 37 °C (Vinjamuri et *al*., 2015). 850 µL of XPB were added to the reaction mixture to bring the volume up to 1 mL. After centrifuging it for 3 minutes at 300 rpm, the hemoglobin concentration was calculated by measuring the resulting amount of hemoglobin in the supernatant with a spectrophotometer at 540 nm.

The following formula was used to compute the percentage of hemolysis (equation 06):

$$\%\ Hemolysis\ Inhibition = 100 - \frac{OD\ Sample}{OD\ Control} \times 100 \qquad (6)$$

2.3.3. Anti-inflammatory activity

The egg albumin denaturation inhibition method was used to investigate the anti-inflammatory potential of crude aqueous extract, silver nanoparticles, and fractions from *H.*

lippii. The reaction mixture (5 mL) contained 200 µL of hen's egg albumin (fresh), 2.8 mL of phosphate buffer (pH 6.4), and was added 2 mL of various concentrations of our sample standard drug diclofenac sodium, also, 2 mL of distilled water was used instead of extract or diclofenac to prepare the control. Following a 15-minute incubation period at 37°C in a water bath, the reaction mixtures underwent a 5-minute heating period at 70°C. The reaction mixtures' absorbance was measured at 660 nm using a UV-visible spectrophotometer after cooling, with the buffer serving as the blank (Dharmadeva et *al*., 2018).

The following equation was used to get the egg albumin denaturation inhibition percentage (equation 07):

$$\text{Inhibition percentage} = \frac{A\ Control - A\ sample}{A\ control} \times 100 \quad (7)$$

2.3.4. Antibacterial activity assays

Firstly, the susceptibility of the bacterial strains of the crude aqueous extract, silver nanoparticles, and fractions from *H.lippii*, was determined by the agar diffusion method cited by Belhaoues et *al*., 2020 (Belhaoues et *al*., 2020).

2.3.4.1. Antibacterial test using the agar diffusion method

As noted before, the agar diffusion method was used to assess the materials' antibacterial activity. Prior to usage, the bacterial strains were grown on nutrient agar for 24 hours at 37°C while in the stationary phase of growth. The suspension of bacterial cells is another factor (10^6 colony-forming units per mL). were applied to Petri dishes containing Mueller Hinton agar (using sterile swabs). The discs (6 mm in diameter) were then immersed in 10 microliters of various plant extracts, AgNPs, and *H. lippii* fractions that were all dissolved in DMSO (5%, v/v) at different concentrations. Amoxicillin (10 µg/mL), Cephalexin (30 µg/mL), and (DMSO 5%, v/v) were used as a positive and negative control, respectively, and incubated for 24 hours at 37 °C.

2.3.4.2. Determination of minimal inhibitory concentration (MIC)

MIC of AgNPs, *H. lippii*, and its fractions against the previous six bacteria was determined by an amended broth macro-dilution method. For MIC estimation, stock solutions of five different concentrations of each one of our samples and ranging from 1mg/mL to 30 µg/mL of silver nanoparticles, 15mg/mL to 0,973mg/mL and 5 to 0,156 mg/mL of crude extract and its fractions respectively. Additionally, were made in MHB broth that had been autoclaved. For

each bacterial strain, two sets of sterile test tubes (13 x 100 mm) with cotton plugs and 0.2 mL of bacterial inoculum were set up. The ultimate volume of media in the flasks was 4 mL as a result of individually inoculating each test tube with 2 mL of each concentration of samples. As positive and negative controls, MHB with bacterial inoculum and MHB with all of the prior samples but without bacterial inoculum, respectively, were used. All test tubes were kept at 37°C for 24 hours (Verma et *al*., 2016).

2.3.5. Anticancer Activity of silver nanoparticles

Electrochemical methods based on cyclic voltammetry and spectroscopic methods based on UV spectroscopy were used to experimentally evaluate the binding free energy and the binding constant of the interaction of this AgNPs synthesized with DNA and BSA in the VTRS Laboratory at the University of El Oued.

2.3.5.1. DNA interaction study

In order to understand the mechanism behind acting as AgNPs an anticancer agent, basic understanding of anticancer agents is required. However, despite the extensive usage of AgNPs, very few reports on the interaction of AgNPs with DNA are available.

2.3.5.1.1. DNA extraction

Isolation of DNA from blood can be performed using a variety of techniques, differing protocols and a large number of commercially available kits. The DNA extraction technique chosen should be able to deliver pure DNA samples ready to be used for the studying the anticancer activity of AgNPs.

In this study, we utilized a simple and non-toxic DNA extraction technique called the salting-out (Carpi et *al*., 2011), This procedure has the advantage of avoiding the use of toxic and corrosive organic solvents by using just conventional chemicals that can be bought from any commercial supplier, as well as requiring no specialist equipment or biochemical understanding (Boom et *al*., 1990; Price et *al*., 2009).

- **Blood sample**

Blood samples from chickens were collected into blood collection tubes containing EDTA as an anticoagulant, maintained stored at 4°C.

- **Extraction procedure of DNA**

1. We placed 5 mL of whole chicken blood sample in a 20 mL flacon tube, after that 10 mL of RBC lysis buffer was added to the blood and the resultant mixture is allowed to cool for 20 minutes in an ice bath. Following that, it was centrifuged for 15 minutes at room temperature at 2500 rpm. This procedure was carried out 3 to 4 times until the blood's red color vanished, the flacon tube was left to dray for 5 minutes.

2. were removed the white blood cells by addition 2mL of WCLB (White Cell Lysis Buffer), then vortexing for 3 minutes.

3. We added 150 µL of sodium dodecyl sulfate solution for cell lysis and was undertaken centrifuging at 172 for 90 minutes at 55°C.

4. 3 mL of 6M sodium chloride solution was added after centrifugation and followed by a 6-minute vortex followed by 10-minute centrifugation at 1300 for the final mixture.

5. After recovering the liquid phase, two volumes of cold absolute ethanol were added, and centrifugation at 1300 for 30 minutes at room temperature was completed. In addition, at the end of this step, we note the appearance of the thin white filament within the tubes containing a mixture.

6. The obtained DNA was washed by 70% ethanol (must be cold) then centrifuged for 2 min at 1500 rpm.

7. Finally, the obtained DNA dried in ambient experimental conditions and was characterized using spectroscopy technique.

- **Estimation of DNA concentration and control of its quality.**

Following its extraction, estimation of the DNA's quantity and quality was crucial. Maximum UV absorption for nucleic acids occurs at 260 nm. This report gives information on the level of DNA purity and potential protein contamination by estimating the optical density (OD) versus distilled water at 260 and 280 nm in a quartz cell. The DNA is clear, according to a report with a value between 1.6 and 2 (Sirajuddin et *al*., 2013). Beer Lambert's law estimated that DNA concentrations were at 260 nm.

2.3.5.1.2. Electrochemical DNA interaction study

Cyclic voltammetry is performed using a Galvanostat Model PGZ301 potentiostat (Radiometer Analytical SAS) connected to an electrochemical cell with three electrodes.

- ✓ A vitreous carbon electrode surface 3 mm2.
- ✓ A saturated Hg/Hg2Cl2/KCl reference electrode.
- ✓ An auxiliary platinum electrode. Diameter 3 mm².

Everything is controlled by a Pentium IV microcomputer (4.0 GHz CPU and 2 GB RAM) equipped with VoltaMaster4 software, version 7.08.

The reaction between the silver nanoparticle and DNA takes place in an electrochemical cell. The reaction medium is a 0.1 M phosphate buffer (KH_2PO_4 /K_2HPO_4) at pH = 7.2. Polishing of the working electrode using the p4000 sandpaper is carried out before each manipulation; the electrodes are then rinsed with ultra-pure water and wiped with absorbent paper. The electrochemical cell is filled with 25 mL of a solution consisting of the buffer containing the silver nanoparticles then it is equipped with the reference electrode and the auxiliary electrode, and also the working electrode. The voltammogram and tracing in the absence and in the presence of an increasing concentration of DNA.

A variable potential is imposed at a fixed scanning speed, and the voltammogram obtained is used to access the interaction parameters between the silver nanoparticles and DNA (Lanez et *al*., 2020).

2.3.5.1.3. UV visible spectroscopic DNA interaction study

❖ **Procedure**

The electron spectrum of silver nanoparticles AgNPs solubilized in a phosphate buffer (KH_2PO_4 / K_2HPO_4) 0.1 M at pH = 7.2 was carried out, after the addition of the different concentrations of DNA, the spectra are recorded in order to determine λ max and calculate the interaction parameters (Lanez et *al*., 2019b).

2.3.5.2. BSA interaction study

2.3.5.2.1. Electrochemical BSA interaction study

In order effectively recognize the overall pharmacokinetic profile of our studied compound; it is important studying the reversible behavior of AgNPs in the presence of BSA. The used mediums of these assays are 0.1 M buffer phosphate solution at pH = 7.2. The experiments were performed in the same steps previously mentioned for DNA. The voltammograms of AgNPs were recorded in similar experimental conditions of speed scan (100 $mV.s^{-1}$) and temperature (T=298 k) with silver nanoparticles (AgNPs), with and without the increasing concentration of BSA (Benamara et *al*., 2020).

2.3.5.2.2. UV visible spectroscopic BSA interaction study.

Electronic spectroscopy experiments were conducted to study the interaction of AgNPs with BSA in buffer phosphate solution (KH_2PO_4/K_2HPO_4) at pH = 7.2 in the absence and presence of a gradually increasing quantity of BSA stock solution (Khennoufa et *al*., 2021).

2.4. *In vivo* activity of aqueous extract *of H.lippii* and AgNPs

2.4.1. Sub-acute toxicity study

Investigation on the acute toxicity of silver nanoparticles and the aqueous extract of *H. lippii* according to the rules established by the organization for economic cooperation and development OECD 425: Six groups of three male albino rats to each were created as follows: Group 1 (control group) received normal water; Group 2, 3, 4, were administered intragastrically once with different doses (100, 1000, 4000 mg/kg) of *H.lippii* aqueous extract and Group 5, 6 were administered intraperitoneal once with different doses (2, 10 mg/Kg) of silver nanoparticles. Signs of toxicity, body weight change, adverse effects and mortality were monitored for 24 h, 72 h, and a follow-up period of 14 days.

2.4.2. Experimental design

After two weeks of acclimatization, the adult Wistar albino rats were randomly divided into seven groups, each containing five rats (n=5) as follow:

- **Group I:** was serving as a control and received normal water;
- **Group II:** was treated orally by gavage 100 mg/kg, b.w (days/week) of aqueous extract of *H. lippii* for 05 weeks;
- **Group III:** received in drinking water 50 mg/kg, b.w/day of Cadmium chloride ($CdCl_2$) daily for 05 weeks;
- **Group IV**: was firstly received in drinking water 50 mg/kg, b.w/day of $CdCl_2$ only for 05 weeks then treated curatively by 100 mg/kg, b. w/day of *H. lippii* for the last 15 days;
- **Group V**: was treated intraperitoneally 0.1mg/kg, b.w/day of silver nanoparticles (Ag NPs) for 05 weeks (Singh et *al*., 2018);
- **Group VI:** was firstly received in drinking water 50 mg/kg, b.w/day of $CdCl_2$ only for 05 weeks then treated curatively by 0.1 mg/kg, b.w/day of Ag NPs for the last 15 days;
- **Group VII:** was firstly received in drinking water 50 mg/kg, b.w/day of $CdCl_2$ only for 05 weeks then treated curatively by 100 mg/kg, b. w/day of *H. lippii* and AgNPs 0.1 mg/kg, b.w/day ($CdCl_{2+}$ *H. lippii*$_+$ Ag NPs) for the last 15 days.

Body weight was recorded periodically during the experiment weeks.

2.4.3. Samples preparation

2.4.3.1. Sacrifice and Blood collection

After 16 hours of fasting and at the end of each treatment, rats were decapitated under a light anesthetic of 94% chloroform, and blood samples were transferred into tubes EDTA that had been previously marked and numbered for each rat. The serum obtained after centrifuging the blood at a speed of 2500 rpm for 10 minutes was stored at -20°C until it was needed for biochemical analysis. A glucometer was used to measure the fasting blood glucose levels of each rat.

2.4.3.2. Preparation of tissues samples

The sacrificed animals were opened ventrally for the removal of certain organs. The liver, kidneys, heart, brain, and testes were weighed after being washed in normal saline, and stored at -20°C for the determination of oxidative stress parameters (MDA, SOD, GSH, and CAT). In addition, a piece of the liver, kidneys, and testis of the other half was fixed in formaldehyde (10%) for histopathological examination.

2.4.4. Hematological parameters analysis

Using Coulter's technique and a Medonic automatic hematological analyzer, hematological parameters are calculated (Coulter Beckman -USA-).

2.4.5. Biochemical parameters analysis

Serum glucose, urea, uric acid, creatinine, and serum lipid (Cholesterol and Triglyceride) levels were determined for each one using the commercial kit from Spinreact, Spain (ref: glucose-1001200, urea-20141, uric acid-20091, creatinine-20151, cholesterol-20111, and triglyceride-20131). In addition, were measured albumin, calcium, and total protein serum using another commercial kit from Spinreact, Spain (ref: albumin-1001020, calcium-1001060, and total protein- 1001290). Further, enzymatic activities of Lactate dehydrogenase (LDH), Glutamate-pyruvate-transaminase (GPT), Glutamate-oxaloacetate-transaminase (GOT), and alkaline phosphatase (ALP) were measured using commercial kits (Spinreact) (ref: LDH-1001260, GPT-1001171, GOT-1001161, and ALP-MX41233) (Annex 04).

2.4.6. Hormonal parameters

2.4.6.1. Tri-iodothyronine, Thyroxine and Thyroid-stimulating Hormone

FT3, FT4, and TSH hormone parameters were measured using Vitros ECIQ 2's automated immunoassay by chimiluminescence procedure.

2.4.6.2. Testosterone (Serum)

Specifically designed Enzyme linked Immuno Sorbant Assay (ELISA) kits were used to measure testosterone levels (Biocheck, Inc, USA) (Jahan et *al*., 2014).

2.4.7. Oxidative stress parameters

2.4.7.1. Homogenates preparation

The liver, kidney, brain, heart, and testicles, each weighing 1g, were all homogenized in 9 mL of Tris buffer saline (Tris 50 mM, NaCl 150 mM; pH 7.4). After homogenates were centrifuged at 3900 rpm for 20 minutes, the produced supernatants were used to determine the presence of oxidative stress indicators.

2.4.7.2. Determination of tissue proteins

❖ **Principle**

Using Coomassie blue as a reagent, which reacts with the amine group (NH_2) of the proteins to generate a blue complex, the tissue proteins were identified using a colorimetric technique by a spectrophotometer**.** The intensity of the blue color is correlated with the amount of proteins present, and its appearance indicates how ionized the acid medium is. At At 595 n, the absorbance is measured nm (Bradford, 1976).

❖ **Preparation of Bradford's reagent**

100 mg of Coomassie blue really be dissolved in 50 mL of ethanol (95%), and the mixture then needs to be shaken for two hours in the dark before 100 mL of orthophosphoric acid (H3PO4) (85%) is added. Additionally, distilled water was used to fill the capacity to 1 liter, and then filter paper was used to purify the resultant solution.

Note: For two weeks at 4°C, this reagent is stable.

- **Procedure**

We added 5 mL of Coomassie blue to 1 mL of the homogenate, and after five minutes, we read the optical densities at 595 nm in comparison to a blank.

When determining whether or not there is protein present, the protein concentration is compared to a standard range of bovine serum albumin (0.1-0.2-0.4-0.6-0.8-1mg/mL) that has been carried out under comparable conditions.

2.4.7.3. Determination of malondialdehyde (MDA) level

200 µL of sample and 800 µL of TBA reagent into the glass test tubes in the glass vise, and then tightly cap the tubes. For 15 minutes, the mixture will be heated at 100°C in a water bath. 30 minutes after being frozen in a cold water bath, leave the tubes open to let the reaction's gases escape. Use a spectrophotometer to measure the supernatant's absorbance at 532 nm after 5 minutes of centrifuging at 3000 rpm (Yaki, 1976).

- **Expression of results**

Using the molecular extinction coefficient of MDA (å= $1.53.10^5$ M^{-1}.cm-1), the concentration

of thiobarbituric acid reactive compounds (TBARS) was calculated. The outcomes were presented as nmol /mg of prot (equation 08).

$$\mathbf{MDA\ (nmol\ /mg\ of\ prot)} = \frac{OD\ Sample}{1{,}53.10^5.mg\ of\ prot} \quad (8)$$

2.4.7.4. Determination of reduced glutathione level

The optical density of 2-nitro-5-mercocapturic acid (TNB), a short-lived Ellman reagent with SH groups present in GSH, which is generated from the reduction of dithio-bis-2-nitrobenzoic acid (DTNB), is used to calculate the amount of reduced glutathione, according to Weckbecker and Cory (1988)(Weckbecker and Cory, 1988).

- **Procedure**

200 µL of salicylic acid (0.25%) are mixed with 800 µL of homogenate samples. The mixture was then centrifuged for five minutes at a speed of 1000 rpm. Additionally, 25 µL of DTNB (0.01 mol/L) and 500 µL of supernatant were combined with 1000 µL of tris buffer (tris 0.4mol, 0.02mol NaCl, pH = 8.9). After 5 min of incubation, the absorbance of the reaction medium is measured at 412 nm.

❖ **Expression of results**

According to the following equation (equation 09), the concentration of GSH is expressed in nanomoles per milligram of protein (nmol/mg of prot):

$$GSH(nM/Mg\ de\ prot) = \frac{DO \times 1 \times 1.525}{13133 \times 0.8 \times 0.5 \times mg\ de\ prot} \times d \quad (9)$$

- OD: Optical Density.
- 1.525: total volume of blend an mL.
- 13133: Absorption constant of SH groups at 412 nm.
- 0.5: Volume of the supernatant
- 1: volume of protein mixture.
- 0.8: volume of homogeneous solution without protein exists in 1 mL.

2.4.7.5. Determination of Super Oxide Dismutase (SOD) activity

Super Oxide Dismutase is detected by evaluating the spectrophotometrically measured absorbance at 560 nm utilizing the test technique of SOD activity using the NBT by the superoxide anion (O2.-) (Beauchamp and Fridovich, 1971).

❖ **Procedure**

The reaction was initiated by mixing 50µL of the sample with 1000µL of EDTA-Met (0.1mM, 13mM) followed by 1800µL of Phosphate buffer (50Mm) and added 85 µL of NBT and 22.6µL of Riboflavin. The same protocol used for blank, exceptionally an additional 50 µL of phosphate buffer has been added in place of the sample. The Absorption is measured at 560nm.

❖ **Expression of results**

According to equation (10) Inhibition percentage of NBT reduction by SOD was calculated:

$$SOD = \frac{DO\ blanc - DO\ Echantion}{DO\ blanc} \times 100 \qquad (10)$$

2.4.7.6. Determination of Catalase activity

The Aebi (1984) (Aebi, 1984) approach was used to assess CAT activity. The reaction was initiated by mixing 20 µL of supernatant with 780 µL of phosphate buffer and 200µL of H_2O_2 (0.030 M) (KH_2PO_4, 0.1 M; pH 7.5). The drop in absorbance at 240 nm was observed every 30 seconds for 2 minutes in order to track the breakdown of H_2O_2. International units per minute and per gram of protein (IU/min/g of protein) were used to express the enzymatic activity (equation 10).

$$\text{Catalase (UI/min) /g)} = \frac{(2.3033/T).(Log A1/A2)}{DF.g\ pro} \qquad (11)$$

A1: Absorbance at the first minute.

A2: Absorbance at the second minute.

T: Time interval in minutes.

2.4.8. Histopathological study of liver, Kidney and Testicle tissues

The part of the liver, kidney, and testicles was removed from the rats after they were killed and placed in fixative (10% formaldehyde) until it was time to prepare the slices for analysis. The samples were dehydrated in ascending graded series of ethanol (60%, 70%, 80% and 100%), cleaned with xylene, and immersed in paraffin. Sections of 4~6 µm were prepared from paraffin blocks using a Histoline Rotary Microtome (Thermo Scientific (Micron HM 325)). Hematoxylin and eosin were used to color the image. Using a light microscope, histopathological observation was performed.

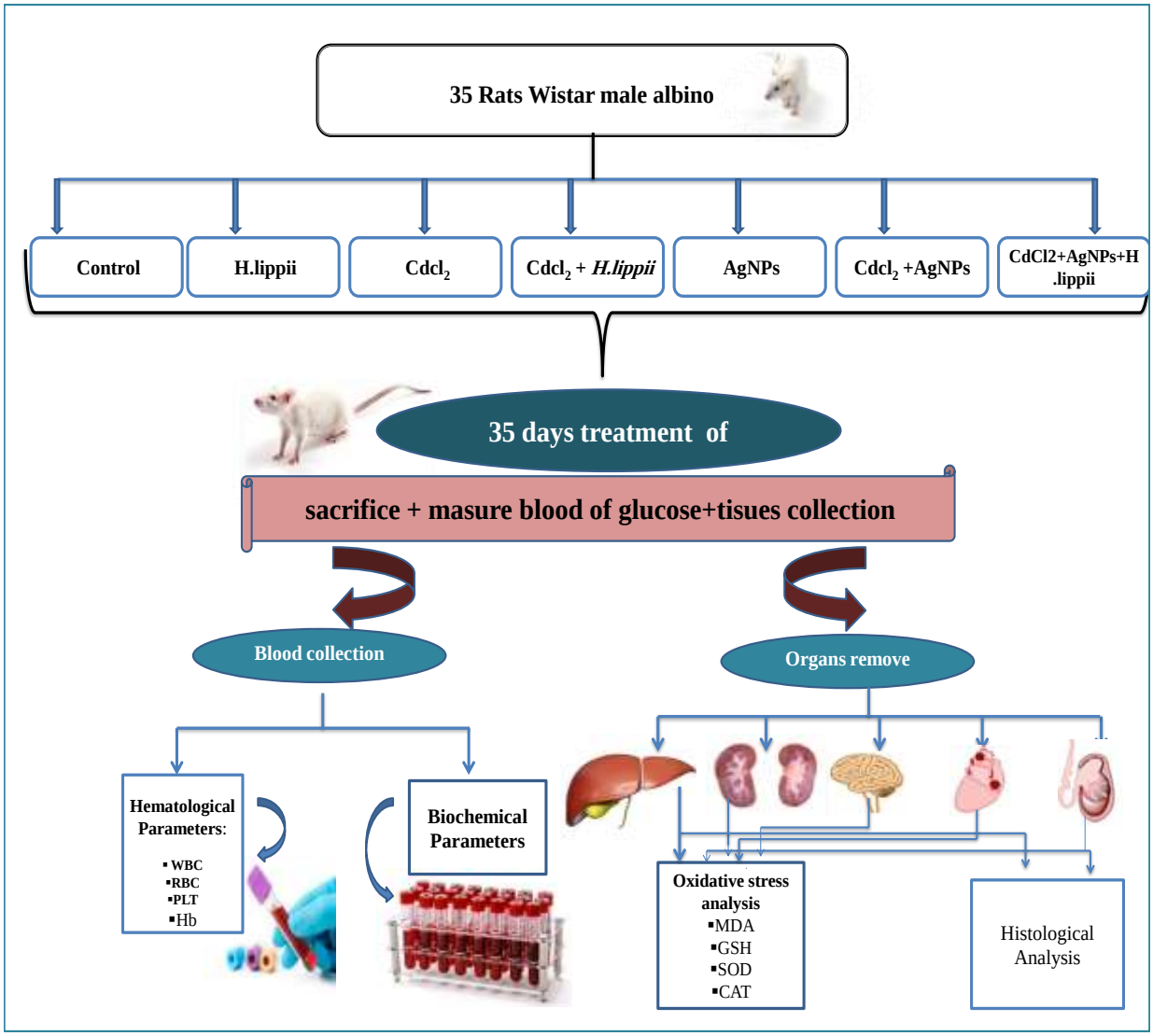

Figure 17 **:** Summary schema of the experimental protocol of in vivo study.

2.5. Statistical analysis

The results obtained are expressed as the mean ± standard error of the mean (Mean ± SEM). The comparison between the different groups is carried out after a Student T-test. Statistical analysis of the data was carried out using the MINITAB (Version 13Fr), EXCEL (version 2007), and significant differences between means were calculated using Duncan's multiple range test (DMRT) at p=0.05 using the SPSS (Statistical Package for Social Sciences) version 26 software. Differences were considered significant at $p \leq 0.05$.

- ✓ Significant (* $P \leq 0.05$).
- ✓ Highly significant compared with the control (** $P \leq 0.01$).
- ✓ Very highly significant compared with the control (*** $P \leq 0.001$).

CHAPTER II

Results

CHAPTER III

Discussion

Conclusion

CONCLUSION

The current study documented the synthesis and characterization of silver nanoparticles using *Helianthemum lippii* L extract. In this work, the biological activity of *Helianthemum lippii* and greenly synthesized silver nanoparticles were evaluated *in vitro* and *in vivo* against toxicity induced by cadmium chloride in Wister rats', depending on to the obtained results we can be conclude that:

H.lippii is extremely rich in bioactive components both qualitatively and quantitatively through various analyzes including HPLC, This enables us to identify a new source of bioactive molecules that may be utilized to treat a variety of diseases.

Silver nanoparticles were successfully synthesized, as shown by FT-IR, UV-Vis, EDX, XRD, and SEM analyses. This indicates that *H.lippii*'s aerial portions contain bioactive compounds that are in charge of reducing and capping silver nitrate into silver nanoparticles.

Also, we may classify these compounds (*H.lippii* and AgNPs) as important biological and medical molecules due to their powerful *in vitro* anti-oxidant, anti-inflammatory activity, and protection for red blood cells. All of this opens promising hopes that they may be presented as medicines or treatments against health relapses associated with these mechanisms.

AgNPs and *H.lippii* exhibit good antibacterial activity against the select bacteria; hence, these two treatments approaches-especially AgNPs, which were the most effective-can be employed in the future as nanoantibiotics against bacterial pathogens that affect humans.

The anticancer activity was evaluated based on the interaction of DNA and BSA with exceptionally AgNPs. As a result, the obtained results provide insight into how nanoparticles interact with DNA and BSA via electrostatic interactions. These interactions are beneficial because they can alter the structure of DNA and slow down the process of cell proliferation. Therefore, the nanoparticles are candidates for use as treatments for various cancers and, on the other hand, in the potential development of drugs with enhanced or more selective activity.

Thanks to the sub-acute toxicity investigation the aqueous extract of *Helianthemum lippii* and the green-synthesized silver nanoparticles can be used safely and therapeutically

As physiological aspect parameters, our therapy with *H.lippii* and AgNPs ameliorates the body weight and relative weights of the organs, which clearly supports the efficacy of therapeutic compounds against the accumulation of cadmium chloride into the body.

As Notably, *H.lippii* and AgNPs mainly curative treatment has potential protective effects against hematotoxicity induced by cadmium chloride.

The beneficial effect of H. lippii and AgNPs approaches on restoring lipid profiles and biochemical markers demonstrate the benefit of treatment against the toxicity of cadmium, which is characterized by a metabolic imbalance and altered liver and renal function in several biological systems related to our study data. Therapy systems also have strong hepatoprotective and nephroprotective effects against this toxicity.

AgNPs and *H.lippii* treatments significantly improved thyroid function and halted the fall of testosterone levels.

Our findings demonstrate that treatment with *H.lippii* and AgNPs lowers the level of oxidative stress brought on by exposure to cadmium chloride by restricting radical phenomena, repairing oxidative damage by lowering lipid peroxidation in the studied tissues (liver, kidney, heart, testicles, and brain), and by improving the mobility of the antioxidant defense, which also demonstrates another way that these treatments are protective against pathologies connected to cadmium chloride exposure.

Our treatment has excellent protection capabilities that go beyond biological factors to the microscopic level, demonstrating its strong protection in cell stability against oxidative stress-induced liver, kidney, and testicular harm. This gives us the opportunity to make assumptions about how these treatments would reduce any degradation that may be caused by cadmium or another substance.

Finally, based on all of the above, we can conclude that *H.lippii* and AgNPs have proven highly biologically effective at different levels, which opens promising hopes and promotes their use in the medical field against various health problems.

Perspective

Given the importance of these results, they open experimental perspectives and other in depth studies that should allow us to clearly identify:

- ✓ Dependence *H.lippii* is an excellent source for the synthesis of various nanoparticles.
- ✓ Evaluation of the protective effect of plant and AgNPs against certain chronic diseases (such as cancer).
- ✓ Interaction study of silver nanoparticles with reverse transcriptase enzyme for inhibition development VIH and Covid 19.
- ✓ Exploitation of the results for the formation of a start-up after obtaining the Patented.

References

REFERENCES

1. Abbasi, A. R., Kalantary, H., Yousefi, M., Ramazani, A., & Morsali, A. (2012). Synthesis and characterization of Ag nanoparticles polyethylene fibers under ultrasound irradiation. *Ultrasonics sonochemistry*, *19*(4), 853-857.

2. Abdel-Aziz, M. S., Shaheen, M. S., El-Nekeety, A. A., & Abdel-Wahhab, M. A. (2014). Antioxidant and antibacterial activity of silver nanoparticles biosynthesized using Chenopodium murale leaf extract. *Journal of Saudi Chemical Society*, *18*(4), 356-363.

3. Adebayo, A. E., Oke, A. M., Lateef, A., Oyatokun, A. A., Abisoye, O. D., Adiji, I. P., Fagbenro, D. O., Amusan, T. V., Badmus, J., & Asafa, T. (2019). Biosynthesis of silver, gold and silver–gold alloy nanoparticles using Persea americana fruit peel aqueous extract for their biomedical properties. *Nanotechnology for Environmental Engineering*, *4*(1), 1-15.

4. Adi, P. J., Burra, S. P., Vataparti, A. R., & Matcha, B. (2016). Calcium, zinc and vitamin E ameliorate cadmium-induced renal oxidative damage in albino Wistar rats. *Toxicology reports*, *3*, 591-597.

5. Aebi, H. (1984). Catalase in vitro. In *Methods in enzymology*. Academic Press (Vol. 105, pp. 121-126).

6. Afsar, T., Razak, S., Khan, M. R., Mawash, S., Almajwal, A., Shabir, M., & Haq, I. U. (2016). Evaluation of antioxidant, anti-hemolytic and anticancer activity of various solvent extracts of Acacia hydaspica R. Parker aerial parts. *BMC complementary and alternative medicine*, *16*(1), 1-16.

7. Agarwal, H., Nakara, A., & Shanmugam, V. K. (2019). Anti-inflammatory mechanism of various metal and metal oxide nanoparticles synthesized using plant extracts: A review. *Biomedicine & Pharmacotherapy*, *109*, 2561-2572.

8. Ahmad, F., Khan, R. A., & Rasheed, S. (1992). Study of analgesic and anti-inflammatory activity from plant extracts of Lactuca scariola and Artemisia absinthium. *Journal of Islamic Academy of Sciences*, *5*(2), 111-114.

9. Ahmad, S. A., Das, S. S., Khatoon, A., Ansari, M. T., Afzal, M., Hasnain, M. S., & Nayak, A. K. (2020). Bactericidal activity of silver nanoparticles: A mechanistic review. *Materials Science for Energy Technologies*, *3*, 756-769.

10. Ahn, M.-R., Kumazawa, S., Usui, Y., Nakamura, J., Matsuka, M., Zhu, F., & Nakayama, T. (2007). Antioxidant activity and constituents of propolis collected in various areas of China. *Food Chemistry*, *101*(4), 1383-1392.

11. Ahn, S., Singh, P., Castro-Aceituno, V., Yesmin Simu, S., Kim, Y.-J., Mathiyalagan, R., & Yang, D.-C. (2017). Gold nanoparticles synthesized using Panax ginseng leaves suppress inflammatory-mediators production via blockade of NF-κB activation in macrophages. *Artificial cells, nanomedicine, and biotechnology*, *45*(2), 270-276.

12. Ahokas, R. A., & Dilts Jr, P. (1979). Cadmium uptake by the rat embryo as a function of gestational age. *American journal of obstetrics and gynecology*, *135*(2), 219-222.

13. Aina, D. A., Owolo, O., Lateef, A., Aina, F. O., & Hakeem, A. S. (2019). Biomedical Applications ofChasmanthera dependens stem extract mediated silver nanoparticles as

Antimicrobial, Antioxidant, Anticoagulant, thrombolytic, and Larvicidal agents. *Karbala Int. J. Mod. Sci., 5*, 71-80.

14. Al-Azemi, M., Omu, F. E., Kehinde, E. O., Anim, J. T., Oriowo, M. A., & Omu, A. E. (2010). Lithium protects against toxic effects of cadmium in the rat testes. *Journal of Assisted Reproduction and Genetics, 27*(8), 469-476.

15. Al-Shmgani, H. S., Mohammed, W. H., Sulaiman, G. M., & Saadoon, A. H. (2017). Biosynthesis of silver nanoparticles from Catharanthus roseus leaf extract and assessing their antioxidant, antimicrobial, and wound-healing activities. *Artificial cells, nanomedicine, and biotechnology, 45*(6), 1234-1240.

16. Alghasham, A., Salem, T. A., & Meki, A.-R. M. (2013). Effect of cadmium-polluted water on plasma levels of tumor necrosis factor-α, interleukin-6 and oxidative status biomarkers in rats: protective effect of curcumin. *Food and Chemical Toxicology, 59*, 160-164.

17. Ali-Rachedi, F., Meraghni, S., Touaibia, N., & Mohamed, S. (2018). Quantitative analysis of phenolic compounds of an algerian endemic Scabiosa atropurpurea sub. Maritima L. *Bull Company R Sci Liège, 87*, 13-21.

18. Ali, S., Bashir, S., Mumtaz, S., Shakir, H. A., Ara, C., Ahmad, F., Tahir, H. M., Faheem, M., Irfan, M., & Masih, A. (2021). Evaluation of cadmium chloride-induced toxicity in chicks via hematological, biochemical parameters, and cadmium level in tissues. *Biological trace element research, 199*(9), 3457-3469.

19. Alsabri, S. G., Rmeli, N. B., Zetrini, A. A., Mohamed, S. B., Meshri, M. I., Aburas, K. M., Bensaber, S. M., Mrema, I. A., Mosbah, A. A., & Allahresh, K. A. (2013). Phytochemical, anti-oxidant, anti-microbial, anti-inflammatory and anti-ulcer properties of Helianthemum lippii. *Journal of Pharmacognosy and Phytochemistry, 2*(2).

20. Alsabri, S. G., Zetrini, A., Fitouri, S., & Hermann, A. (2012). Screening of analgesic and anti-inflammatory activities for two Libyan medicinal plants: Helianthemum lippii and Launaea residifolia. *Journal of Chemical and Pharmaceutical Research, 4*(9), 4201-4205.

21. Amamou, F., Nemmiche, S., kaouthar Meziane, R., Didi, A., Yazit, S. M., & Chabane-Sari, D. (2015). Protective effect of olive oil and colocynth oil against cadmium-induced oxidative stress in the liver of Wistar rats. *Food and Chemical Toxicology, 78*, 177-184.

22. Amina, H., Lamia, H., Mohsen, H., Foued, H., Gtari, M., & Mohamed, N. (2012). In vitro micropropagation of Helianthemum lippii L. var Sessiliforuim (Cistaceae): a valuable pastoral plant. *Middle East Journal of Scientific Research, 11*(5), 652-655.

23. Anand, K. K. H., & Mandal, B. K. (2015). Activity study of biogenic spherical silver nanoparticles towards microbes and oxidants. *Spectrochimica Acta Part A: Molecular and Biomolecular Spectroscopy, 135*, 639-645.

24. Anbukkarasi, M., Thomas, P. A., Sundararajan, M., & Geraldine, P. (2016). Gas chromatography-mass spectrometry analysis and in vitro antioxidant activity of the ethanolic extract of the leaves of Tabernaemontana divaricata. *Pharmacognosy Journal, 8*(5).

25. Anzum, R., Alawamleh, H. S. K., Bokov, D. O., Jalil, A. T., Hoi, H. T., Abdelbasset, W. K., Thoi, N. T., Widjaja, G., & Kurochkin, A. (2022). A review on separation and detection of

copper, cadmium, and chromium in food based on cloud point extraction technology. *Food Science and Technology*, *42*.

26. Argun, H., & Dao, S. (2018). Hydrogen gas production from waste peach pulp by natural microflora. *Waste and Biomass Valorization*, *9*(11), 2117-2124.

27. Aromal, S. A., & Philip, D. (2012). Green synthesis of gold nanoparticles using Trigonella foenum-graecum and its size-dependent catalytic activity. *Spectrochimica Acta Part A: Molecular and Biomolecular Spectroscopy*, *97*, 1-5.

28. Arunachalam, K. D., Annamalai, S. K., & Hari, S. (2013). One-step green synthesis and characterization of leaf extract-mediated biocompatible silver and gold nanoparticles from Memecylon umbellatum. *International journal of nanomedicine*, *8*, 1307.

29. Asagba, S., Isamah, G., Ossai, E., & Ekakitie, A. (2002). Effect of oral exposure to cadmium on the levels of vitamin A and lipid peroxidation in the eye. *Bulletin of environmental contamination and toxicology*, *68*(1), 18-21.

30. Asharani, P., Hande, M. P., & Valiyaveettil, S. (2009). Anti-proliferative activity of silver nanoparticles. *BMC cell biology*, *10*(1), 1-14.

31. Atef, C., Anouar, F., El-Hadda, A., & Azzedine, C. (2015). Phytochemicals study, antioxidant and antimicrobial activities of Helianthemum lippii (L.) pers. in different stages of growth (somatic, flowering and fruiting). *World J Pharm Pharm Sci*, *4*, 338-349.

32. Aughey, E., Fell, G., Scott, R., & Black, M. (1984). Histopathology of early effects of oral cadmium in the rat kidney. *Environmental health perspectives*, *54*, 153-161.

33. Badria, F., Hetta, M., Sarhan, R. M., & El-Din, M. E. (2014). Lethal effects of Helianthemum lippii (L.) on Acanthamoeba castellanii cysts in vitro. *The Korean Journal of Parasitology*, *52*(3), 243.

34. Bae, D.-S., Gennings, C., Carter Jr, W. H., Yang, R. S., & Campain, J. A. (2001). Toxicological interactions among arsenic, cadmium, chromium, and lead in human keratinocytes. *Toxicological Sciences*, *63*(1), 132-142.

35. Bagchi, D., Bagchi, M., Hassoun, E., & Stohs, S. (1996). Cadmium-induced excretion of urinary lipid metabolites, DNA damage, glutathione depletion, and hepatic lipid peroxidation in Sprague-Dawley rats. *Biological trace element research*, *52*(2), 143-154.

36. Balasundram, N., Sundram, K., & Samman, S. (2006). Phenolic compounds in plants and agri-industrial by-products: Antioxidant activity, occurrence, and potential uses. *Food Chemistry*, *99*(1), 191-203.

37. BarathManiKanth, S., Kalishwaralal, K., Sriram, M., Pandian, S. R. K., Youn, H.-s., Eom, S., & Gurunathan, S. (2010). Anti-oxidant effect of gold nanoparticles restrains hyperglycemic conditions in diabetic mice. *Journal of nanobiotechnology*, *8*(1), 1-15.

38. Barghout, B., El-Sayed, S., & El-Said, E.-S. (2020). Protective effect of green tea extract against cadmium-induced testicular damage in rats in respect of oxidant/antioxidant equilibrium and androgen production. *Mansoura Veterinary Medical Journal*, *21*(1), 31-35.

39. Bashir, N., Manoharan, V., & Miltonprabu, S. (2016). Grape seed proanthocyanidins protects against cadmium induced oxidative pancreatitis in rats by attenuating oxidative

stress, inflammation and apoptosis via Nrf-2/HO-1 signaling. *The Journal of Nutritional Biochemistry*, *32*, 128-141.

40. Bate-Smith, E. (1954). Leuco-anthocyanins. 1. Detection and identification of anthocyanidins formed from leuco-anthocyanins in plant tissues. *Biochemical Journal*, *58*(1), 122.

41. Baudouin, M. (1976). 2-Phenylethanol. *National Center for Biotechnology Information. PubChem Compound Database, US National Library of Medicine. pubchem. ncbi. nlm. nih. gov/compound/2-phenylethanol*.

42. Baydar, N. G., Özkan, G., & Sağdiç, O. (2004). Total phenolic contents and antibacterial activities of grape (Vitis vinifera L.) extracts. *Food control*, *15*(5), 335-339.

43. Beauchamp, C., & Fridovich, I. (1971). Superoxide dismutase: improved assays and an assay applicable to acrylamide gels. *Analytical biochemistry*, *44*(1), 276-287.

44. Bekkara, F., Jay, M., Viricel, M. R., & Rome, S. (1998). Distribution of phenolic compounds within seed and seedlings of two Vicia faba cvs differing in their seed tannin content, and study of their seed and root phenolic exudations. *Plant and Soil*, *203*(1), 27-36.

45. Belhaoues, S., Amri, S., & Bensouilah, M. (2020). Major phenolic compounds, antioxidant and antibacterial activities of Anthemis praecox Link aerial parts. *South African Journal of Botany*, *131*, 200-205.

46. Bem, E. M., Piotrowski, J. K., Sobczak-Kozlowska, M., & Dmuchowski, C. (1988). Cadmium, zinc, copper and metallothionein levels in human liver. *International archives of occupational and environmental health*, *60*(6), 413-417.

47. Benabdelaziz, I., Haba, H., Lavaud, C., Harakat, D., & Benkhaled, M. (2015). Lignans and other constituents from Helianthemum sessiliflorum Pers. *Records of Natural Products*, *9*(3), 342.

48. Benamara, H., Lanez, T., & Lanez, E. (2020). BSA-binding studies of 2-and 4-ferrocenylbenzonitrile: voltammetric, spectroscopic and molecular docking investigations. *Journal of Electrochemical Science and Engineering*, *10*(4), 335-346.

49. Benhammou, N., Bekkara, F. A., & Panovska, T. K. (2009). Antioxidant activity of methanolic extracts and some bioactive compounds of Atriplex halimus. *Comptes Rendus Chimie*, *12*(12), 1259-1266.

50. Bhattacharya, D., & Gupta, R. K. (2005). Nanotechnology and potential of microorganisms. *Critical reviews in biotechnology*, *25*(4), 199-204.

51. Bhuyar, P., Rahim, M. H. A., Sundararaju, S., Ramaraj, R., Maniam, G. P., & Govindan, N. (2020). Synthesis of silver nanoparticles using marine macroalgae Padina sp. and its antibacterial activity towards pathogenic bacteria. *Beni-Suef University Journal of Basic and Applied Sciences*, *9*(1), 1-15.

52. Bindhu, M., & Umadevi, M. (2013). Synthesis of monodispersed silver nanoparticles using Hibiscus cannabinus leaf extract and its antimicrobial activity. *Spectrochimica Acta Part A: Molecular and Biomolecular Spectroscopy*, *101*, 184-190.

53. Biswas, N. M., Gupta, R. S., Chattopadhyay, A., Choudhury, G. R., & Sarkar, M. (2001). Effect of atenolol on cadmium-induced testicular toxicity in male rats. *Reproductive Toxicology, 15*(6), 699-704.

54. Boom, R., Sol, C., Salimans, M., Jansen, C., Wertheim-van Dillen, P., & Van der Noordaa, J. (1990). Rapid and simple method for purification of nucleic acids. *Journal of clinical microbiology, 28*(3), 495-503.

55. Botcha, S., & Prattipati, S. D. (2019). Green synthesis of silver nanoparticles using Hyptis suaveolens (L.) Poit leaf extracts, their characterization and cytotoxicity evaluation against PC-3 and MDA-MB 231 cells. *Biologia, 74*(7), 783-793.

56. Boutennoun, H., Boussouf, L., Rawashdeh, A., Al-Qaoud, K., Abdelhafez, S., Kebieche, M., & Madani, K. (2017). In vitro cytotoxic and antioxidant activities of phenolic components of Algerian Achillea odorata leaves. *Arabian Journal of Chemistry, 10*(3), 403-409.

57. Bradai, L., Neffar, S., Amrani, K., Bissati, S., & Chenchouni, H. (2015). Ethnomycological survey of traditional usage and indigenous knowledge on desert truffles among the native Sahara Desert people of Algeria. *Journal of Ethnopharmacology, 162*, 31-38.

58. Bradford, M. M. (1976). A rapid and sensitive method for the quantitation of microgram quantities of protein utilizing the principle of protein-dye binding. *Analytical biochemistry, 72*(1-2), 248-254.

59. Brito, A., Areche, C., Sepúlveda, B., Kennelly, E. J., & Simirgiotis, M. J. (2014). Anthocyanin characterization, total phenolic quantification and antioxidant features of some Chilean edible berry extracts. *Molecules, 19*(8), 10936-10955.

60. Broadhurst, R. B., & Jones, W. T. (1978). Analysis of condensed tannins using acidified vanillin. *Journal of the Science of Food and Agriculture, 29*(9), 788-794.

61. Brongersma, H. H., Draxler, M., De Ridder, M., & Bauer, P. (2007). Surface composition analysis by low-energy ion scattering. *Surface Science Reports, 62*(3), 63-109.

62. Brzóska, M. M., Kamiński, M., Supernak-Bobko, D., Zwierz, K., & Moniuszko-Jakoniuk, J. (2003). Changes in the structure and function of the kidney of rats chronically exposed to cadmium. I. Biochemical and histopathological studies. *Archives of toxicology, 77*(6), 344-352.

63. Buha, A., Antonijević, B., Bulat, Z., Jaćević, V., Milovanović, V., & Matović, V. (2013). The impact of prolonged cadmium exposure and co-exposure with polychlorinated biphenyls on thyroid function in rats. *Toxicology letters, 221*(2), 83-90.

64. Bunghez, I., Barbinta Patrascu, M., Badea, N., Doncea, S., Popescu, A., & Ion, R. (2012). Antioxidant silver nanoparticles green synthesized using ornamental plants. *Journal of optoelectronics and advanced materials, 14*(11), 1016.

65. Burukoğlu, D., & Bayçu, C. (2008). Protective effects of zinc on testes of cadmium-treated rats. *Bulletin of environmental contamination and toxicology, 81*(6), 521-524.

66. Bylishko, D., Shevchenko, I., Ostretsova, S., & Halperin, O. (2021). EXPERIMENTAL DETERMINATION OF CHRONIC INFLUENCE OF CADMIUM SALTS ON RAT HEPATOGENESIS. *Bulletin of problems biology and medicine,* 230-235.

67. Calzada, F., & Alanís, A. D. (2007). Additional antiprotozoal flavonol glycosides of the aerial parts of Helianthemum glomeratum. *Phytotherapy Research: An International Journal Devoted to Pharmacological and Toxicological Evaluation of Natural Product Derivatives, 21*(1), 78-80.

68. Calzada, F., Lopéz, R., Meckes, M., & Cedillo-Rivera, R. (1995). Flavonoids of the aerial parts of Helianthemum glomeratum. *International journal of pharmacognosy, 33*(4), 351-352.

69. Cannino, G., Ferruggia, E., Luparello, C., & Rinaldi, A. M. (2009). Cadmium and mitochondria. *Mitochondrion, 9*(6), 377-384.

70. Casalino, E., Calzaretti, G., Sblano, C., & Landriscina, C. (2000). Cadmium-dependent enzyme activity alteration is not imputable to lipid peroxidation. *Archives of Biochemistry and Biophysics, 383*(2), 288-295.

71. Catts, V. S. (2010). Oxidative Stress. Australian And New Zealand Journal Of Psychiatry,

72. Chandel, M., & Jain, G. C. (2014). Toxic effects of transition metals on male reproductive system: A review. *J. Env. Occup. Sci, 3*, 205.

73. Chang, C. L., Lin, C. S., & Lai, G. H. (2012). Phytochemical characteristics, free radical scavenging activities, and neuroprotection of five medicinal plant extracts. *Evidence-Based Complementary and Alternative Medicine, 2012*.

74. Chater, S., Douki, T., Favier, A., Sakly, M., & Abdelmelek, H. (2009). Changes in antioxidant status and biochemical parameters after orally cadmium administration in females rats. *Acta Biologica Hungarica, 60*(1), 79-88.

75. Chen, L. Q., Fang, L., Ling, J., Ding, C. Z., Kang, B., & Huang, C. Z. (2015). Nanotoxicity of silver nanoparticles to red blood cells: size dependent adsorption, uptake, and hemolytic activity. *Chemical research in toxicology, 28*(3), 501-509.

76. Chen, W., Cai, W., Zhang, L., Wang, G., & Zhang, L. (2001). Sonochemical processes and formation of gold nanoparticles within pores of mesoporous silica. *Journal of colloid and interface science, 238*(2), 291-295.

77. Chen, Y., Hu, Y., Liu, S., Zheng, H., Wu, X., Huang, Z., Li, H., Peng, B., Long, J., & Pan, B. (2016). Whole-body aerosol exposure of cadmium chloride (CdCl2) and tetrabromobisphenol A (TBBPA) induced hepatic changes in CD-1 male mice. *Journal of hazardous materials, 318*, 109-116.

78. Choi, Y.-J., Kang, J.-S., Park, J. H. Y., Lee, Y.-J., Choi, J.-S., & Kang, Y.-H. (2003). Polyphenolic flavonoids differ in their antiapoptotic efficacy in hydrogen peroxide–treated human vascular endothelial cells. *The Journal of nutrition, 133*(4), 985-991.

79. Chung, I.-M., Park, I., Seung-Hyun, K., Thiruvengadam, M., & Rajakumar, G. (2016). Plant-mediated synthesis of silver nanoparticles: their characteristic properties and therapeutic applications. *Nanoscale research letters, 11*(1), 1-14.

80. Darroudi, M., Ahmad, M. B., Abdullah, A. H., & Ibrahim, N. A. (2011). Green synthesis and characterization of gelatin-based and sugar-reduced silver nanoparticles. *International journal of nanomedicine, 6*, 569.

81. Das, P., Ghosal, K., Jana, N. K., Mukherjee, A., & Basak, P. (2019). Green synthesis and characterization of silver nanoparticles using belladonna mother tincture and its efficacy as a potential antibacterial and anti-inflammatory agent. *Materials Chemistry and Physics, 228*, 310-317.

82. Dawadi, S., Katuwal, S., Gupta, A., Lamichhane, U., Thapa, R., Jaisi, S., Lamichhane, G., Bhattarai, D. P., & Parajuli, N. (2021). Current research on silver nanoparticles: Synthesis, characterization, and applications. *Journal of nanomaterials, 2021*.

83. de Souza Predes, F., Diamante, M. A. S., & Dolder, H. (2010). Testis response to low doses of cadmium in Wistar rats. *International journal of experimental pathology, 91*(2), 125-131.

84. Dharmadeva, S., Galgamuwa, L. S., Prasadinie, C., & Kumarasinghe, N. (2018). In vitro anti-inflammatory activity of Ficus racemosa L. bark using albumin denaturation method. *Ayu, 39*(4), 239.

85. Di Giulio, R. T., & Scanlon, P. F. (1985). Effects of cadmium ingestion and food restriction on energy metabolism and tissue metal concentrations in mallard ducks (Anas platyrhynchos). *Environmental research, 37*(2), 433-444.

86. Díez, J., Manjón, J. L., & Martin, F. (2002). Molecular phylogeny of the mycorrhizal desert truffles (Terfezia and Tirmania), host specificity and edaphic tolerance. *Mycologia, 94*(2), 247-259.

87. Djebbari, R., Chemam, Y., Boubekri, N., Lakroun, Z., Kebieche, M., Amrani, A., Benayache, F., Benayache, S., & Zama, D. (2017). Chemoprotective potential of Helianthemum confertum against the loss of molecular and functional integrity of the liver cell in doxorubicin-treated rats. *IJPPR, 9*(7), 903-910.

88. Djebbari, R., & Zama, D. *L'effet protecteur des extraits des plantes Helianthemum confertum et Helianthemum ruficomum vis-à-vis de la toxicité induite par la Doxorubicine* [جامعة الإخوة منتوري قسنطينة].

89. Djemam, N., Lassed, S., Gül, F., Altun, M., Monteiro, M., Menezes-Pinto, D., Benayache, S., Benayache, F., Zama, D., & Demirtas, I. (2020). Characterization of ethyl acetate and n-butanol extracts of Cymbopogon schoenanthus and Helianthemum lippii and their effect on the smooth muscle of the rat distal colon. *Journal of Ethnopharmacology, 252*, 112613.

90. Dkhil, M. A., Diab, M. S., Lokman, M. S., El-Sayed, H., Aljawdah, H. M., Al-Quraishy, S., & Bauomy, A. A. (2020). Hepato-protective effect of Pleurotus ostreatus extracts in cadmium-intoxicated rats. *Journal of King Saud University-Science, 32*(8), 3432-3436.

91. Dkhil, M. A., Diab, M. S., Lokman, M. S., El-Sayed, H., Bauomy, A. A., Al-Shaebi, E. M., & Al-Quraishy, S. (2020). Nephroprotective effect of Pleurotus ostreatus extract against cadmium chloride toxicity in rats. *Anais da Academia Brasileira de Ciências, 92*.

92. Donmez, H., Donmez, N., Kısadere, I., & Undag, I. (2019). Protective effect of quercetin on some hematological parameters in rats exposed to cadmium. *Biotechnic & Histochemistry, 94*(5), 381-386.

93. Drotning, W. (1984). Thermal expansion of the group IIb liquid metals zinc, cadmium and mercury. *Journal of the Less Common Metals*, *96*, 223-227.

94. Dupont, F., & Guignard, J.-L. (2007). *Botanique: systématique moléculaire*. Elsevier masson.

95. Edeoga, H. O., Okwu, D., & Mbaebie, B. (2005). Phytochemical constituents of some Nigerian medicinal plants. *African Journal of Biotechnology*, *4*(7), 685-688.

96. El-Boshy, M. E., Risha, E. F., Abdelhamid, F. M., Mubarak, M. S., & Hadda, T. B. (2015). Protective effects of selenium against cadmium induced hematological disturbances, immunosuppressive, oxidative stress and hepatorenal damage in rats. *Journal of Trace Elements in Medicine and Biology*, *29*, 104-110.

97. El-Demerdash, F. M., Yousef, M. I., Kedwany, F. S., & Baghdadi, H. H. (2004). Cadmium-induced changes in lipid peroxidation, blood hematology, biochemical parameters and semen quality of male rats: protective role of vitamin E and β-carotene. *Food and Chemical Toxicology*, *42*(10), 1563-1571.

98. El-Refaiy, A. I., & Eissa, F. I. (2013). Histopathology and cytotoxicity as biomarkers in treated rats with cadmium and some therapeutic agents. *Saudi Journal of Biological Sciences*, *20*(3), 265-280.

99. El-Sharaky, A., Newairy, A., Badreldeen, M., Eweda, S., & Sheweita, S. (2007). Protective role of selenium against renal toxicity induced by cadmium in rats. *Toxicology*, *235*(3), 185-193.

100. El Jemli, M., Kamal, R., Marmouzi, I., Zerrouki, A., Cherrah, Y., & Alaoui, K. (2016). Radical-scavenging activity and ferric reducing ability of Juniperus thurifera (L.), J. oxycedrus (L.), J. phoenicea (L.) and Tetraclinis articulata (L.). *Advances in pharmacological sciences*, *2016*.

101. El Muayed, M., Raja, M. R., Zhang, X., MacRenaris, K. W., Bhatt, S., Chen, X., Urbanek, M., O'halloran, T. V., & Lowe, J., William L. (2012). Accumulation of cadmium in insulin-producing β cells. *Islets*, *4*(6), 405-416.

102. Elkhadragy, M. F., Al-Olayan, E. M., Al-Amiery, A. A., & Abdel Moneim, A. E. (2018). Protective effects of Fragaria ananassa extract against cadmium chloride-induced acute renal toxicity in rats. *Biological trace element research*, *181*(2), 378-387.

103. Erdogan, Z., Erdogan, S., Celik, S., & Unlu, A. (2005). Effects of ascorbic acid on cadmium-induced oxidative stress and performance of broilers. *Biological trace element research*, *104*(1), 19-31.

104. Escudero, A., Martínez, I., De la Cruz, A., Otálora, M., & Maestre, F. (2007). Soil lichens have species-specific effects on the seedling emergence of three gypsophile plant species. *Journal of Arid Environments*, *70*(1), 18-28.

105. Eswaran, A., Muthukrishnan, S., Mathaiyan, M., Pradeepkumar, S., Mari, K. R., & Manogaran, P. (2021). Green synthesis, characterization and hepatoprotective activity of silver nanoparticles synthesized from pre-formulated Liv-Pro-08 poly-herbal formulation. *Applied Nanoscience*, 1-13.

106. Farant, J.-P., & Wigfield, D. (1982). Biomonitoring lead exposure with δ-aminolevulinate dehydratase (ALA-D) activity ratios. *International archives of occupational and environmental health, 51*(1), 15-24.

107. Feldheim, D. L., & Foss Jr, C. (2002). Metal nanoparticles: synthesis, characterization, and applications. *Marcel! Dekker, Inc, 270 Madison Avenue, New York, NY 10016, USA, 2002. 338*.

108. Feng, Q. L., Wu, J., Chen, G. Q., Cui, F., Kim, T., & Kim, J. (2000). A mechanistic study of the antibacterial effect of silver ions on Escherichia coli and Staphylococcus aureus. *Journal of biomedical materials research, 52*(4), 662-668.

109. Fenu, G., Bernardo, L., Calvo, R., Cortis, P., De Agostini, A., Gangale, C., Gargano, D., Gargano, M. L., Lussu, M., & Medagli, P. (2019). Global and regional IUCN Red List assessments: 8. *Italian Botanist, 8*, 17.

110. Fiamegkos, I., Cordeiro, F., Devesa, V., Vélez, D., Robouch, P., Emteborg, H., Leys, H., Cizek-Stroh, A., & de la Calle, B. (2015). IMEP-41: determination of inorganic As in food. *Int J Environ Res Public Health, 17*.

111. Figueiredo-Pereira, M. E., Yakushin, S., & Cohen, G. (1998). Disruption of the intracellular sulfhydryl homeostasis by cadmium-induced oxidative stress leads to protein thiolation and ubiquitination in neuronal cells. *Journal of Biological Chemistry, 273*(21), 12703-12709.

112. Fortier, M., Omara, F., Bernier, J., Brousseau, P., & Fournier, M. (2008). Effects of physiological concentrations of heavy metals both individually and in mixtures on the viability and function of peripheral blood human leukocytes in vitro. *Journal of Toxicology and Environmental Health, Part A, 71*(19), 1327-1337.

113. Gabr, S. A., Alghadir, A. H., & Ghoniem, G. A. (2019). Biological activities of ginger against cadmium-induced renal toxicity. *Saudi Journal of Biological Sciences, 26*(2), 382-389.

114. Gan, P. P., & Li, S. F. Y. (2012). Potential of plant as a biological factory to synthesize gold and silver nanoparticles and their applications. *Reviews in Environmental Science and Bio/Technology, 11*(2), 169-206.

115. Gao, L., Yue, R., Xu, J., Liu, Z., & Chai, J. (2018). Pt-PEDOT/rGO nanocomposites: One-pot preparation and superior electrochemical sensing performance for caffeic acid in tea. *Journal of Electroanalytical Chemistry, 816*, 14-20.

116. Geethalakshmi, R., & Sarada, D. (2012). Gold and silver nanoparticles from Trianthema decandra: synthesis, characterization, and antimicrobial properties. *International journal of nanomedicine, 7*, 5375.

117. Ghosh, P., Das, C., & Biswas, S. (2020). Phytochemical composition analysis and evaluation of in vitro. medicinal properties and cytotoxicity of five wild weeds: A comparative study [version 1; peer review: 1 approved, 2 approved with reservations]. F1000Res. 2020; 9: 493. *PubMed Abstract*| *Publisher Full Text*| *Free Full Text*.

118. Gobe, G., & Crane, D. (2010). Mitochondria, reactive oxygen species and cadmium toxicity in the kidney. *Toxicology letters, 198*(1), 49-55.

119. Gole, A., Dash, C., Ramakrishnan, V., Sainkar, S., Mandale, A., Rao, M., & Sastry, M. (2001). Pepsin− gold colloid conjugates: preparation, characterization, and enzymatic activity. *Langmuir*, *17*(5), 1674-1679.

120. Gong, Z.-G., Wang, X.-Y., Wang, J.-H., Fan, R.-F., & Wang, L. (2019). Trehalose prevents cadmium-induced hepatotoxicity by blocking Nrf2 pathway, restoring autophagy and inhibiting apoptosis. *Journal of inorganic biochemistry*, *192*, 62-71.

121. Gontijo, D. C., Brandão, G. C., Gontijo, P. C., de Oliveira, A. B., Diaz, M. A. N., Fietto, L. G., & Leite, J. P. V. (2017). Identification of phenolic compounds and biologically related activities from Ocotea odorifera aqueous extract leaves. *Food Chemistry*, *230*, 618-626.

122. Habeeb Rahuman, H. B., Dhandapani, R., Narayanan, S., Palanivel, V., Paramasivam, R., Subbarayalu, R., Thangavelu, S., & Muthupandian, S. (2022). Medicinal plants mediated the green synthesis of silver nanoparticles and their biomedical applications. *IET nanobiotechnology*, *16*(4), 115-144.

123. Hajian, N., Rezayatmand, Z., & Shahanipur, K. (2018). Preventive effects of Allium hirtifolium Boiss methanolic and aqueous extracts on renal injury induced by lead in rats. *Journal of Herbmed Pharmacology*, *7*(3).

124. Halis, Y. (2007). Plant Encyclopedia in area Oued Souf: desert plants common in the Big East race. *El Oued, Algeria: El Walid*, 154-155.

125. Hamad, S. M., Shnawa, B. H., Jalil, P. J., & Ahmed, M. H. (2022). Assessment of the Therapeutic Efficacy of Silver Nanoparticles against Secondary Cystic Echinococcosis in BALB/c Mice. *Surfaces*, *5*(1), 91-112.

126. Hamed, M. A., Ali, S. A., & Saba El-Rigal, N. (2012). Therapeutic potential of ginger against renal injury induced by carbon tetrachloride in rats. *The Scientific World Journal*, *2012*.

127. Hamza, A., Gtari, M., & Mohamed, N. (2013). Micropropagation of Helianthemum lippii L. var Sessiliforuim (Cistaceae) an important pastoral plant of North African arid areas. *African Journal of Biotechnology*, *12*(46), 6468-6473.

128. Hanahan, D., & Weinberg, R. A. (2000). The hallmarks of cancer. *cell*, *100*(1), 57-70.

129. Hansen, J. M., Zhang, H., & Jones, D. P. (2006). Differential oxidation of thioredoxin-1, thioredoxin-2, and glutathione by metal ions. *Free Radical Biology and Medicine*, *40*(1), 138-145.

130. Hanson, M. L., Brundage, K. M., Schafer, R., Tou, J. C., & Barnett, J. B. (2010). Prenatal cadmium exposure dysregulates sonic hedgehog and Wnt/β-catenin signaling in the thymus resulting in altered thymocyte development. *Toxicology and applied pharmacology*, *242*(2), 136-145.

131. Harborne, A. (1998). *Phytochemical methods a guide to modern techniques of plant analysis*. springer science & business media.

132. Heilman, S., & Silva, L. (2017). Silver and titanium nanoparticles used as coating on polyurethane catheters. Journal of Nano Research,

133. Heim, K. E., Tagliaferro, A. R., & Bobilya, D. J. (2002). Flavonoid antioxidants: chemistry, metabolism and structure-activity relationships. *The Journal of Nutritional Biochemistry, 13*(10), 572-584.

134. Hejazy, M., & Koohi, M. K. (2017). Effects of nano-zinc on biochemical parameters in cadmium-exposed rats. *Biological trace element research, 180*(2), 265-274.

135. Hermes-Lima, M., Valle, V. G., Vercesi, A. E., & Bechara, E. J. (1991). Damage to rat liver mitochondria promoted by δ-aminolevulinic acid-generated reactive oxygen species: connections with acute intermittent porphyria and lead-poisoning. *Biochimica et Biophysica Acta (BBA)-Bioenergetics, 1056*(1), 57-63.

136. Hiba, H., & Thoppil, J. E. (2022). Medicinal herbs as a panacea for biogenic silver nanoparticles. *Bulletin of the National Research Centre, 46*(1), 1-15.

137. Hoffmann, E., Cook, J., Di Luzio, N., & Coover, J. (1975). The effects of acute cadmium administration in the liver and kidney of the rat. Light and electron microscopic studies. *Laboratory Investigation; a Journal of Technical Methods and Pathology, 32*(5), 655-664.

138. Hooper, D., Spitsin, S., Kean, R., Champion, J., Dickson, G., Chaudhry, I., & Koprowski, H. (1998). Uric acid, a natural scavenger of peroxynitrite, in experimental allergic encephalomyelitis and multiple sclerosis. *Proceedings of the National Academy of Sciences, 95*(2), 675-680.

139. Horiguchi, H., Sato, M., Konno, N., & Fukushima, M. (1996). Long-term cadmium exposure induces anemia in rats through hypoinduction of erythropoietin in the kidneys. *Archives of toxicology, 71*(1), 11-19.

140. Horiguchi, H., Teranishi, H., Niiya, K., Aoshima, K., Katoh, T., Sakuragawa, N., & Kasuya, M. (1994). Hypoproduction of erythropoietin contributes to anemia in chronic cadmium intoxication: clinical study on Itai-itai disease in Japan. *Archives of toxicology, 68*(10), 632-636.

141. Hsin, Y.-H., Chen, C.-F., Huang, S., Shih, T.-S., Lai, P.-S., & Chueh, P. J. (2008). The apoptotic effect of nanosilver is mediated by a ROS-and JNK-dependent mechanism involving the mitochondrial pathway in NIH3T3 cells. *Toxicology letters, 179*(3), 130-139.

142. Huang, N., Radiman, S., Lim, H., Khiew, P., Chiu, W., Lee, K., Syahida, A., Hashim, R., & Chia, C. (2009). γ-Ray assisted synthesis of silver nanoparticles in chitosan solution and the antibacterial properties. *Chemical Engineering Journal, 155*(1-2), 499-507.

143. Ibrahim, H. M. (2015). Green synthesis and characterization of silver nanoparticles using banana peel extract and their antimicrobial activity against representative microorganisms. *Journal of radiation research and applied sciences, 8*(3), 265-275.

144. Ibtissam, L., Samir, D., & Wiam, Z. (2021). Aristolochia longa (Aristolochiaceae) Spice Alleviates Nickel-Induced Oxidative Stress and Biochemical Alterations in Rats. *Austin J Pharmacol Ther, 9*(6), 1151.

145. Ijaz, M. U., Batool, M., Batool, A., Al-Ghanimd, K., Zafar, S., Ashraf, A., Al-Misned, F., Ahmed, Z., Shahzadi, S., & Samad, A. (2021). Protective effects of vitexin on cadmium-induced renal toxicity in rats. *Saudi Journal of Biological Sciences, 28*(10), 5860-5864.

146. Ikediobi, C. O., Badisa, V. L., Ayuk-Takem, L. T., Latinwo, L. M., & West, J. (2004). Response of antioxidant enzymes and redox metabolites to cadmium-induced oxidative stress in CRL-1439 normal rat liver cells. *International journal of molecular medicine, 14*(1), 87-92.

147. Imed, M., Fatima, H., & Abdelhamid, K. (2008). Protective effects of selenium (Se) and zinc (Zn) on cadmium (Cd) toxicity in the liver and kidney of the rat: histology and Cd accumulation. *Food and Chemical Toxicology, 46*(11), 3522-3527.

148. Islam, E., Islam, R., Rahman, A. A., Alam, A., Khondkar, P., Rashid, M., & Parvin, S. (2013). Estimation of total phenol and in vitro antioxidant activity of Albizia procera leaves. *BMC research notes, 6*(1), 1-7.

149. Ismail, A., Ktari, L., Ahmed, M., Bolhuis, H., Boudabbous, A., Stal, L. J., Cretoiu, M. S., & El Bour, M. (2016). Antimicrobial activities of bacteria associated with the brown alga Padina pavonica. *Frontiers in Microbiology, 7*, 1072.

150. Jahan, S., Khan, M., Ahmed, S., & Ullah, H. (2014). Comparative analysis of antioxidants against cadmium induced reproductive toxicity in adult male rats. *Systems biology in reproductive medicine, 60*(1), 28-34.

151. Jain, N., Jain, P., Rajput, D., & Patil, U. K. (2021). Green synthesized plant-based silver nanoparticles: Therapeutic prospective for anticancer and antiviral activity. *Micro and Nano Systems Letters, 9*(1), 1-24.

152. Jamkhande, P. G., Ghule, N. W., Bamer, A. H., & Kalaskar, M. G. (2019). Metal nanoparticles synthesis: An overview on methods of preparation, advantages and disadvantages, and applications. *Journal of drug delivery science and technology, 53*, 101174.

153. Jha, M., & Shimpi, N. G. (2018). Green synthesis of zero valent colloidal nanosilver targeting A549 lung cancer cell: in vitro cytotoxicity. *Journal of Genetic Engineering and Biotechnology, 16*(1), 115-124.

154. Jiang, J., Oberdörster, G., & Biswas, P. (2009). Characterization of size, surface charge, and agglomeration state of nanoparticle dispersions for toxicological studies. *Journal of Nanoparticle Research, 11*(1), 77-89.

155. Jimoh, A., Adebayo, G., Otun, K., Ajiboye, A., Bale, A., Jamiu, W., & Alao, F. (2015). Sorption study of Cd (II) from aqueous solution using activated carbon prepared from Vitellaria paradoxa shell. *Journal of Bioremediation & Biodegredation, 6*(3), 1.

156. Jin, T., Nordberg, M., Frech, W., Dumont, X., Bernard, A., Ye, T.-t., Kong, Q., Wang, Z., Li, P., & Lundström, N.-G. (2002). Cadmium biomonitoring and renal dysfunction among a population environmentally exposed to cadmium from smelting in China (ChinaCad). *Biometals, 15*(4), 397-410.

157. Johnson, D., & Foulkes, E. (1980). On the proposed role of metallothionein in the transport of cadmium. *Environmental research, 21*(2), 360-365.

158. Kachlicki, P., Piasecka, A., Stobiecki, M., & Marczak, Ł. (2016). Structural characterization of flavonoid glycoconjugates and their derivatives with mass spectrometric techniques. *Molecules, 21*(11), 1494.

159. Kalishwaralal, K., Banumathi, E., Pandian, S. R. K., Deepak, V., Muniyandi, J., Eom, S. H., & Gurunathan, S. (2009). Silver nanoparticles inhibit VEGF induced cell proliferation and

migration in bovine retinal endothelial cells. *Colloids and Surfaces B: Biointerfaces, 73*(1), 51-57.

160. Kargutkar, S., & Brijesh, S. (2018). Anti-inflammatory evaluation and characterization of leaf extract of Ananas comosus. *Inflammopharmacology, 26*(2), 469-477.

161. Karthikesan, K., Pari, L., & Menon, V. P. (2010). Protective effect of tetrahydrocurcumin and chlorogenic acid against streptozotocin–nicotinamide generated oxidative stress induced diabetes. *Journal of Functional Foods, 2*(2), 134-142.

162. Karuppiah, M., & Rajmohan, R. (2013). Green synthesis of silver nanoparticles using Ixora coccinea leaves extract. *Materials Letters, 97*, 141-143.

163. Kathirvel, A., & Sujatha, V. (2016). Phytochemical studies, antioxidant activities and identification of active compounds using GC–MS of Dryopteris cochleata leaves. *Arabian Journal of Chemistry, 9*, S1435-S1442.

164. Keshari, A. K., Srivastava, R., Singh, P., Yadav, V. B., & Nath, G. (2020). Antioxidant and antibacterial activity of silver nanoparticles synthesized by Cestrum nocturnum. *Journal of Ayurveda and integrative medicine, 11*(1), 37-44.

165. Khalil, M. M., Ismail, E. H., El-Baghdady, K. Z., & Mohamed, D. (2014). Green synthesis of silver nanoparticles using olive leaf extract and its antibacterial activity. *Arabian Journal of Chemistry, 7*(6), 1131-1139.

166. Khalil, M. M., Ismail, E. H., & El-Magdoub, F. (2012). Biosynthesis of Au nanoparticles using olive leaf extract: 1st nano updates. *Arabian Journal of Chemistry, 5*(4), 431-437.

167. Kharat, S. N., & Mendhulkar, V. D. (2016). Synthesis, characterization and studies on antioxidant activity of silver nanoparticles using Elephantopus scaber leaf extract. *Materials Science and Engineering: C, 62*, 719-724.

168. Khatoon, N., Mazumder, J. A., & Sardar, M. (2017). Biotechnological applications of green synthesized silver nanoparticles. *J. Nanosci. Curr. Res, 2*(107), 2572-0813.1000107.

169. Khatoon, N., Mishra, A., Alam, H., Manzoor, N., & Sardar, M. (2015). Biosynthesis, characterization, and antifungal activity of the silver nanoparticles against pathogenic Candida species. *BioNanoScience, 5*(2), 65-74.

170. Khennoufa, A., Bechki, L., Lanez, T., Lanez, E., & Zegheb, N. (2021). Spectrophotometric, voltammetric and molecular docking studies of binding interaction of N-ferrocenylmethylnitroanilines with bovine serum albumin. *Journal of Molecular Structure, 1224*, 129052.

171. Kiendrebeogo, M., Coulibaly, K., Sanogo, R., & Kone-Bamba, D. (2016). Mineral salt composition and secondary metabolites of Ocimum gratissimum L., an antihyperglycemic plant. *Journal of Pharmacognosy and Phytochemistry, 5*(5), 425.

172. Kim, S., Choi, J. E., Choi, J., Chung, K.-H., Park, K., Yi, J., & Ryu, D.-Y. (2009). Oxidative stress-dependent toxicity of silver nanoparticles in human hepatoma cells. *Toxicology in vitro, 23*(6), 1076-1084.

173. Kim, T., Lee, C.-H., Joo, S.-W., & Lee, K. (2008). Kinetics of gold nanoparticle aggregation: experiments and modeling. *Journal of colloid and interface science*, *318*(2), 238-243.

174. Kini, R. D., Tripathi, Y., Raghuveer, C., Pai, S. R., Ramswamy, C., Nayanatara, A., Vinodhini, N., & Ranade, A. (2009). Protective role of vitamin E against cadmium chloride induced testicular damage in rats. *J Physiol Biomed Sci*, *22*, 12-16.

175.Kısadere, İ., Aydın, M. F., & Ündağ, İ. (2022). Partial protective effects of melatonin on cadmium-induced changes in hematological characteristics in rats. *Biotechnic & Histochemistry*, *97*(3), 192-198.

176. Kjellström, T. (1992). Mechanism and epidemiology of bone effects of cadmium. *IARC Scientific publications*(118), 301-310.

177. Knowles, S. O., & Donaldson, W. (1990). Dietary modification of lead toxicity: effects on fatty acid and eicosanoid metabolism in chicks. *Comparative biochemistry and physiology. C, Comparative pharmacology and toxicology*, *95*(1), 99-104.

178. Koriem, K. M., Fathi, G. E., Salem, H. A., Akram, N. H., & Gamil, S. A. (2013). Protective role of pectin against cadmium-induced testicular toxicity and oxidative stress in rats. *Toxicology mechanisms and methods*, *23*(4), 263-272.

179. Kotcherlakota, R., Das, S., & Patra, C. R. (2019). Therapeutic applications of green-synthesized silver nanoparticles. In *Green synthesis, characterization and applications of nanoparticles* (pp. 389-428). Elsevier.

180. Kowalczyk, E., Kopff, A., Fijałkowski, P., Kopff, M., Niedworok, J., Błaszczyk, J., Kêdziora, J., & Tyślerowicz, P. (2003). Effect of anthocyanins on selected biochemical parameters in rats exposed to cadmium. *Acta Biochimica Polonica*, *50*(2), 543-548.

181. Kowshik, M., Ashtaputre, S., Kharrazi, S., Vogel, W., Urban, J., Kulkarni, S. K., & Paknikar, K. M. (2002). Extracellular synthesis of silver nanoparticles by a silver-tolerant yeast strain MKY3. *Nanotechnology*, *14*(1), 95.

182. Koyu, A., Gokcimen, A., Ozguner, F., Bayram, D. S., & Kocak, A. (2006). Evaluation of the effects of cadmium on rat liver. *Molecular and cellular biochemistry*, *284*(1), 81-85.

183. Krishnaraj, C., Jagan, E., Rajasekar, S., Selvakumar, P., Kalaichelvan, P., & Mohan, N. (2010). Synthesis of silver nanoparticles using Acalypha indica leaf extracts and its antibacterial activity against water borne pathogens. *Colloids and Surfaces B: Biointerfaces*, *76*(1), 50-56.

184. Ksouri, R., Megdiche, W., Falleh, H., Trabelsi, N., Boulaaba, M., Smaoui, A., & Abdelly, C. (2008). Influence of biological, environmental and technical factors on phenolic content and antioxidant activities of Tunisian halophytes. *Comptes Rendus Biologies*, *331*(11), 865-873.

185. Kumar, D., Kumar, G., & Agrawal, V. (2018). Green synthesis of silver nanoparticles using Holarrhena antidysenterica (L.) Wall. bark extract and their larvicidal activity against dengue and filariasis vectors. *Parasitology research*, *117*(2), 377-389.

186. Kumar, N., Kumari, V., Ram, C., Thakur, K., & Tomar, S. K. (2018). Bio-prospectus of cadmium bioadsorption by lactic acid bacteria to mitigate health and environmental impacts. *Applied microbiology and biotechnology*, *102*(4), 1599-1615.

187. Kumar, P. V., Pammi, S., Kollu, P., Satyanarayana, K., & Shameem, U. (2014). Green synthesis and characterization of silver nanoparticles using Boerhaavia diffusa plant extract and their anti bacterial activity. *Industrial Crops and Products, 52*, 562-566.

188. Kuppusamy, P., Yusoff, M. M., Maniam, G. P., & Govindan, N. (2016). Biosynthesis of metallic nanoparticles using plant derivatives and their new avenues in pharmacological applications–An updated report. *Saudi Pharmaceutical Journal, 24*(4), 473-484.

189. Kutzman, R., Drew, R., Shiotsuka, R., & Cockrell, B. (1986). Pulmonary changes resulting from subchronic exposure to cadmium chloride aerosol. *Journal of Toxicology and Environmental Health, Part A Current Issues, 17*(2-3), 175-189.

190. Lafuente, A., Márquez, N., Pérez-Lorenzo, M., Pazo, D., & Esquifino, A. (2000). Pubertal and postpubertal cadmium exposure differentially affects the hypothalamic–pituitary–testicular axis function in the rat. *Food and Chemical Toxicology, 38*(10), 913-923.

191. Lanez, E., Bechki, L., & Lanez, T. (2019a). Computational molecular docking, voltammetric and spectroscopic DNA interaction studies of 9N-(ferrocenylmethyl) adenine. *Chemistry & Chemical Technology, 1 (13), 2019*(1), 11-17.

192. Lanez, E., Bechki, L., & Lanez, T. (2019b). Computational molecular docking, voltammetric and spectroscopic DNA interaction studies of 9n-(ferrocenylmethyl) adenine Chem. *Chem. Technol, 13*(1), 11-17.

193. Lanez, E., Bechki, L., & Lanez, T. (2020). Ferrocenylmethylnucleobases: Synthesis, dft calculations, electrochemical and spectroscopic characterisation. *Chemistry, 14*(2), 146-153.

194. Laraba, M., Tachour, S. H., Belbache, H., Boubekri, N., Djebbari, R., Benayache, F., Benayache, S., & Zama, D. (2022). Hepatoprotective potential of the n-butanol extract of Moricandia arvensis from Algeria against doxorubicin induced toxicity in Wistar albino rats. *Advances in Traditional Medicine*, 1-12.

195. Lassed, S., Deus, C. M., Djebbari, R., Zama, D., Oliveira, P. J., Rizvanov, A. A., Dahdouh, A., Benayache, F., & Benayache, S. (2017). Protective effect of green tea (Camellia sinensis (L.) Kuntze) against prostate cancer: from in vitro data to Algerian patients. *Evidence-Based Complementary and Alternative Medicine, 2017*.

196. Lateef, A., Folarin, B. I., Oladejo, S. M., Akinola, P. O., Beukes, L. S., & Gueguim-Kana, E. B. (2018). Characterization, antimicrobial, antioxidant, and anticoagulant activities of silver nanoparticles synthesized from Petiveria alliacea L. leaf extract. *Preparative Biochemistry and Biotechnology, 48*(7), 646-652.

197. Lawton, L. J., & Donaldson, W. (1991). Lead-induced tissue fatty acid alterations and lipid peroxidation. *Biological trace element research, 28*(2), 83-97.

198. Li, W.-R., Xie, X.-B., Shi, Q.-S., Zeng, H.-Y., Ou-Yang, Y.-S., & Chen, Y.-B. (2010). Antibacterial activity and mechanism of silver nanoparticles on Escherichia coli. *Applied microbiology and biotechnology, 85*(4), 1115-1122.

199. Liu, J., Habeebu, S. S., Liu, Y., & Klaassen, C. D. (1998). Acute CdMT Injection Is Not a Good Model to Study Chronic Cd Nephropathy: Comparison of Chronic CdCl2and CdMT Exposure with Acute CdMT Injection in Rats. *Toxicology and applied pharmacology, 153*(1), 48-58.

200. Liu, X., Shan, K., Shao, X., Shi, X., He, Y., Liu, Z., Jacob, J. A., & Deng, L. (2021). Nanotoxic effects of silver nanoparticles on normal HEK-293 cells in comparison to cancerous HeLa cell line. *International journal of nanomedicine, 16*, 753.

201. Longo, L., Scardino, A., & Vasapollo, G. (2007). Identification and quantification of anthocyanins in the berries of Pistacia lentiscus L., Phillyrea latifolia L. and Rubia peregrina L. *Innovative Food Science & Emerging Technologies, 8*(3), 360-364.

202. Lovásová, E., Rácz, O., Cimboláková, I., Nováková, J., Dombrovský, P., & Ništiar, F. (2013). Effects of chronic low-dose cadmium exposure on selected biochemical and antioxidant parameters in rats. *Journal of Toxicology and Environmental Health, Part A, 76*(17), 1033-1038.

203. Lu, Z., Doulabi, B. Z., Wuisman, P., Bank, R., & Helder, M. (2007). Differentiation of adipose stem cells by nucleus pulposus cells: configuration effect. *Biochemical and biophysical research communications, 359*(4), 991-996.

204.M Carpi, F., Di Pietro, F., Vincenzetti, S., Mignini, F., & Napolioni, V. (2011). Human DNA extraction methods: patents and applications. *Recent Patents on DNA & Gene Sequences (Discontinued), 5*(1), 1-7.

205. Ma, Y., Gao, M., & Liu, D. (2015). Chlorogenic acid improves high fat diet-induced hepatic steatosis and insulin resistance in mice. *Pharmaceutical research, 32*(4), 1200-1209.

206. Mahmoud, M. E., & Elsoadaa, S. S. (2013). Protective effect of ascorbic acid, biopropolis and royal jelly against aluminum toxicity in rats. *Journal of Natural Sciences Research, 3*(1), 102-112.

207. Mahmoud, S. Y., & Alshammari, S. O. (2022). Bioactive compounds of methanolic extract of Helianthemum lippii grows in Hafr Al-Batin region, northeastern Saudi Arabia. *Acta Fytotechnica et zootechnica, 25*(1).

208. Mahmoudi, M., Lynch, I., Ejtehadi, M. R., Monopoli, M. P., Bombelli, F. B., & Laurent, S. (2011). Protein− nanoparticle interactions: opportunities and challenges. *Chemical reviews, 111*(9), 5610-5637.

209. Majeed, M., Hakeem, K. R., & Rehman, R. U. (2022). Synergistic effect of plant extract coupled silver nanoparticles in various therapeutic applications-present insights and bottlenecks. *Chemosphere, 288*, 132527.

210. Makarov, V., Love, A., Sinitsyna, O., Makarova, S., Yaminsky, I., Taliansky, M., & Kalinina, N. (2014). "Green" nanotechnologies: synthesis of metal nanoparticles using plants. *Acta Naturae (англоязычная версия), 6*(1 (20)), 35-44.

211. Mandaville, J. P. (2013). *Flora of Eastern Saudi Arabia*. Routledge.

212. Mandeel, Q. A., & Al-Laith, A. A. A. (2007). Ethnomycological aspects of the desert truffle among native Bahraini and non-Bahraini peoples of the Kingdom of Bahrain. *Journal of Ethnopharmacology, 110*(1), 118-129.

213. Mansouri, A., Embarek, G., Kokkalou, E., & Kefalas, P. (2005). Phenolic profile and antioxidant activity of the Algerian ripe date palm fruit (Phoenix dactylifera). *Food Chemistry, 89*(3), 411-420.

214. Marslin, G., Siram, K., Maqbool, Q., Selvakesavan, R. K., Kruszka, D., Kachlicki, P., & Franklin, G. (2018). Secondary metabolites in the green synthesis of metallic nanoparticles. *Materials, 11*(6), 940.

215. Maruthai, J., Muthukumarasamy, A., & Baskaran, B. (2019). Fabrication and characterisation of silver nanoparticles using bract extract of Musa paradisiaca for its synergistic combating effect on phytopathogens, free radical scavenging activity, and catalytic efficiency. *IET nanobiotechnology, 13*(2), 134-143.

216. Meckes, M., Calzada, F., Tapia-Contreras, A., & Cedillo-Rivera, R. (1999). Antiprotozoal properties of Helianthemum glomeratum. *Phytotherapy Research: An International Journal Devoted to Pharmacological and Toxicological Evaluation of Natural Product Derivatives, 13*(2), 102-105.

217. Mickymaray, S. (2019). Efficacy and mechanism of traditional medicinal plants and bioactive compounds against clinically important pathogens. *Antibiotics, 8*(4), 257.

218. Miller, W., & Neathery, M. (1971). Cadmium absorption, tissue and product distribution, toxicity effects and influence on metabolism of certain essential elements. *International Journal of Dairy Science, 58*(12), 1767-1178.

219. Miller, W. J. (1973). Dynamics of absorption rates, endogenous excretion, tissue turnover, and homeostatic control mechanisms of zinc, cadmium, manganese, and nickel in ruminants. Federation proceedings,

220. Miller, W. J., Blackmon, D. M., & Martin, Y. G. (1968). 109Cadmium absorption, excretion, and tissue distribution following single tracer oral and intravenous doses in young goats. *Journal of dairy science, 51*(11), 1836-1839.

221. Mitsumori, K., Shibutani, M., Sato, S., Onodera, H., Nakagawa, J., Hayashi, Y., & Ando, M. (1998). Relationship between the development of hepato-renal toxicity and cadmium accumulation in rats given minimum to large amounts of cadmium chloride in the long-term: preliminary study. *Archives of toxicology, 72*(9), 545-552.

222. Mittal, A. K., Tripathy, D., Choudhary, A., Aili, P. K., Chatterjee, A., Singh, I. P., & Banerjee, U. C. (2015). Bio-synthesis of silver nanoparticles using Potentilla fulgens Wall. ex Hook. and its therapeutic evaluation as anticancer and antimicrobial agent. *Materials Science and Engineering: C, 53*, 120-127.

223. Mogana, R., Adhikari, A., Tzar, M., Ramliza, R., & Wiart, C. (2020). Antibacterial activities of the extracts, fractions and isolated compounds from Canarium patentinervium Miq. against bacterial clinical isolates. *BMC complementary medicine and therapies, 20*(1), 1-11.

224. Mohamed, T. M., Salama, A. F., Nimr, T. M. E., & Gamal, D. M. E. (2015). Effects of phytate on thyroid gland of rats intoxicated with cadmium. *Toxicology and industrial health, 31*(12), 1258-1268.

225. Mohammad, S. I., Mustafa, I. A., & Abdulqader, S. Z. (2013). Ameliorative effect of the aqueous extract of Zingiber officinale on the cadmium-induced liver and kidney injury in females rats. *Jordan J Biol Sci, 6*(3), 231-234.

226. Morin, Y., Turmel, L., Grantham, H., & Fortier, J. (1963). Observations on the antihypertensive and sedative effects of mebutamate, meprobamate and reserpine. *Canadian Medical Association Journal, 89*(19), 980.

227. Murugan, K., Benelli, G., Ayyappan, S., Dinesh, D., Panneerselvam, C., Nicoletti, M., Hwang, J.-S., Kumar, P. M., Subramaniam, J., & Suresh, U. (2015). Toxicity of seaweed-synthesized silver nanoparticles against the filariasis vector Culex quinquefasciatus and its impact on predation efficiency of the cyclopoid crustacean Mesocyclops longisetus. *Parasitology research, 114*(6), 2243-2253.

228. Murugan, R., & Parimelazhagan, T. (2014). Comparative evaluation of different extraction methods for antioxidant and anti-inflammatory properties from Osbeckia parvifolia Arn.–An in vitro approach. *Journal of King Saud University-Science, 26*(4), 267-275.

229. Nagarajan, S., Kalaivani, G., Poongothai, E., Arul, M., & Natarajan, H. (2019). Characterization of silver nanoparticles synthesized from Catharanthus roseus (Vinca rosea) plant leaf extract and their antibacterial activity. *IJRAR, 6*(1), 680-685.

230. Nakazato, K., Nagamine, T., Suzuki, K., Kusakabe, T., Moon, H., Oikawa, M., Sakai, T., & Arakawa, K. (2008). Subcellular changes of essential metal shown by in-air micro-PIXE in oral cadmium-exposed mice. *Biometals, 21*(1), 83-91.

231. Nazima, B., Manoharan, V., & Miltonprabu, S. (2015). Grape seed proanthocyanidins ameliorates cadmium-induced renal injury and oxidative stress in experimental rats through the up-regulation of nuclear related factor 2 and antioxidant responsive elements. *Biochemistry and Cell Biology, 93*(3), 210-226.

232. Neathery, M., & Miller, W. (1975). Metabolism and toxicity of cadmium, mercury, and lead in animals: a review. *Journal of dairy science, 58*(12), 1767-1781.

233. Negro, C., Aprile, A., Luvisi, A., Nicolì, F., Nutricati, E., Vergine, M., Miceli, A., Blando, F., Sabella, E., & De Bellis, L. (2019). Phenolic profile and antioxidant activity of Italian monovarietal extra virgin olive oils. *Antioxidants, 8*(6), 161.

234. Neouze, M.-A. (2010). About the interactions between nanoparticles and imidazolium moieties: emergence of original hybrid materials. *Journal of Materials Chemistry, 20*(43), 9593-9607.

235. Niraimathi, K., Sudha, V., Lavanya, R., & Brindha, P. (2013). Biosynthesis of silver nanoparticles using Alternanthera sessilis (Linn.) extract and their antimicrobial, antioxidant activities. *Colloids and Surfaces B: Biointerfaces, 102*, 288-291.

236. Nishimura, F. d. C. Y., De Almeida, A. C., Ratti, B. A., Ueda-Nakamura, T., Nakamura, C. V., Ximenes, V. F., & Silva, S. d. O. (2013). Antioxidant effects of quercetin and naringenin are associated with impaired neutrophil microbicidal activity. *Evidence-Based Complementary and Alternative Medicine, 2013*.

237. Nithya Deva Krupa, A., & Raghavan, V. (2014). Biosynthesis of silver nanoparticles using Aegle marmelos (Bael) fruit extract and its application to prevent adhesion of bacteria: a strategy to control microfouling. *Bioinorganic chemistry and applications, 2014*.

238. Njateng, G. S. S., Du, Z., Gatsing, D., Mouokeu, R. S., Liu, Y., Zang, H.-X., Gu, J., Luo, X., & Kuiate, J.-R. (2017). Antibacterial and antioxidant properties of crude extract, fractions

and compounds from the stem bark of Polyscias fulva Hiern (Araliaceae). *BMC complementary and alternative medicine, 17*(1), 1-8.

239. Nna, V. U., Ujah, G. A., Mohamed, M., Etim, K. B., Igba, B. O., Augustine, E. R., & Osim, E. E. (2017). Cadmium chloride–induced testicular toxicity in male wistar rats; prophylactic effect of quercetin, and assessment of testicular recovery following cadmium chloride withdrawal. *Biomedicine & Pharmacotherapy, 94*, 109-123.

240. Nordberg, G. F., Garvey, J. S., & Chang, C. C. (1982). Metallothionein in plasma and urine of cadmium workers. *Environmental research, 28*(1), 179-182.

241. Nriagu, J. (1980). Production, uses, and properties of cadmium. *JOHN WILEY & SONS, 605 THIRD AVE., NEW YORK, NY 10016, USA.*, 35-70.

242. Oche, M., Oladigbolu, R., Ango, J., Okafoagu, N., & Ango, U. (2018). Work absenteeism amongst health care workers in a tertiary health institution in Sokoto, Nigeria. *Work, 26*(2).

243. Ognjanovic, B., Zikic, R., Stajn, A., Saicic, Z., Kostic, M., & Petrovic, V. (1995). The effects of selenium on the antioxidant defense system in the liver of rats exposed to cadmium. *Physiological Research, 44*, 293-300.

244. Olajide, J., Sanni, M., Achimugu, O., Suleiman, M., Jegede, E., & Sheneni, V. (2020). Effect of methanol extract of Trema orientalis leaf on some biochemical and histopathological indices of wistar albino rats with cadmium-induced-hepatotoxicity. *Scientific African, 10*, e00568.

245. Olayinka, E., Ore, A., Adeyemo, O., & Ola, O. (2016). Ameliorative effect of gallic acid on methotrexate-induced hepatotoxicity and nephrotoxicity in rat. *Journal of xenobiotics, 6*(1), 14-18.

246. Oraiza, M. (1986). Studies on product of browning reaction prepared from glucosamine. *Japanese J Nutr, 44*, 307-315.

247. Othman, A. I., & El Missiry, M. A. (1998). Role of selenium against lead toxicity in male rats. *Journal of Biochemical and Molecular Toxicology, 12*(6), 345-349.

248. Ozguner, F., Oktem, F., Ayata, A., Koyu, A., & Yilmaz, H. R. (2005). A novel antioxidant agent caffeic acid phenethyl ester prevents long-term mobile phone exposure-induced renal impairment in rat. *Molecular and cellular biochemistry, 277*(1), 73-80.

249. Pandey, A., & Negi, P. S. (2018). Phytochemical composition, in vitro antioxidant activity and antibacterial mechanisms of Neolamarckia cadamba fruits extracts. *Natural product research, 32*(10), 1189-1192.

250. Pari, L., Murugavel, P., Sitasawad, S., & Kumar, K. S. (2007). Cytoprotective and antioxidant role of diallyl tetrasulfide on cadmium induced renal injury: an in vivo and in vitro study. *Life sciences, 80*(7), 650-658.

251. Patil, M. P., & Kim, G.-D. (2017). Eco-friendly approach for nanoparticles synthesis and mechanism behind antibacterial activity of silver and anticancer activity of gold nanoparticles. *Applied microbiology and biotechnology, 101*(1), 79-92.

252. Patra, R., Swarup, D., Naresh, R., Kumar, P., Nandi, D., Shekhar, P., Roy, S., & Ali, S. (2007). Tail hair as an indicator of environmental exposure of cows to lead and cadmium in different industrial areas. *Ecotoxicology and Environmental Safety, 66*(1), 127-131.

253. Patterson, A. (1939). The Scherrer formula for X-ray particle size determination. *Physical review*, *56*(10), 978.

254. Peereboom-Stegeman, J. H. C., & Jongstra-Spaapen, E. J. (1979). The effect of a single sublethal administration of cadmium chloride on the microcirculation in the uterus of the rat. *Toxicology*, *13*, 199-213.

255. Peng, B. J., Qi, Z., Zhong, Y. L., Xu, S. H., & Zheng, W. (2015). Chlorogenic acid maintains glucose homeostasis through modulating the expression of SGLT-1, GLUT-2, and PLG in different intestinal segments of Sprague-Dawley rats fed a high-fat diet. *Biomedical and Environmental Sciences*, *28*(12), 894-903.

256.Pérez-García, F., & González-Benito, M. (2006). Seed germination of five Helianthemum species: Effect of temperature and presowing treatments. *Journal of Arid Environments*, *65*(4), 688-693.

257. Pinot, F., Kreps, S. E., Bachelet, M., Hainaut, P., Bakonyi, M., & Polla, B. S. (2000). Cadmium in the environment: sources, mechanisms of biotoxicity, and biomarkers. *Reviews on environmental health*, *15*(3), 299-324.

258. Piqueras, A., Olmos, E., Martinez-Solano, J., & Hellin, E. (1999). Cd-induced oxidative burst in tobacco BY2 cells: time course, subcellular location and antioxidant response. *Free Radical Research*, *31*(sup1), 33-38.

259. Pirtarighat, S., Ghannadnia, M., & Baghshahi, S. (2019). Green synthesis of silver nanoparticles using the plant extract of Salvia spinosa grown in vitro and their antibacterial activity assessment. *Journal of Nanostructure in Chemistry*, *9*(1), 1-9.

260. Plescia, F., Venturella, F., D'Anneo, A., Catania, V., Gargano, M. L., Polito, G., Schillaci, D., Palumbo Piccionello, A., Lauricella, M., & Venturella, G. (2022). Phytochemical-rich extracts of Helianthemum lippii possess antimicrobial, anticancer, and anti-biofilm activities. *Plant Biosystems-An International Journal Dealing with all Aspects of Plant Biology*, 1-11.

261. Pokhrel, B., Rijal, S., Raut, S., & Pandeya, A. (2015). Investigations of antioxidant and antibacterial activity of leaf extracts of Azadirachta indica. *African Journal of Biotechnology*, *14*(46), 3159-3163.

262. Poli, V., Madduru, R., Aparna, Y., Kandukuri, V., & Motireddy, S. R. (2022). Amelioration of Cadmium-Induced Oxidative Damage in Wistar Rats by Vitamin C, Zinc and N-Acetylcysteine. *Medical Sciences*, *10*(1), 7.

263. Poudel, M., & Rajbhandari, M. (2020). Phytochemical Analysis of Ampelopteris Prolifera (Retzius) Copeland. *Nepal Journal of Science and Technology*, *19*(1), 78-88.

264. Prasannaraj, G., & Venkatachalam, P. (2017). Hepatoprotective effect of engineered silver nanoparticles coated bioactive compounds against diethylnitrosamine induced hepatocarcinogenesis in experimental mice. *Journal of photochemistry and photobiology B: biology*, *167*, 309-320.

265. Price, C. W., Leslie, D. C., & Landers, J. P. (2009). Nucleic acid extraction techniques and application to the microchip. *Lab on a Chip*, *9*(17), 2484-2494.

266. Quig, D. (1998). Cysteine metabolism and metal toxicity. *Alternative Medicine Review*, *3*, 262-270.

267. Raghunandan, D., Ravishankar, B., Sharanbasava, G., Mahesh, D., Harsoor, V., Yalagatti, M. S., Bhagawanraju, M., & Venkataraman, A. (2011). Anti-cancer studies of noble metal nanoparticles synthesized using different plant extracts. *Cancer nanotechnology, 2*(1), 57-65.

268. Rahimzadeh, M. R., Rahimzadeh, M. R., Kazemi, S., & Moghadamnia, A.-a. (2017). Cadmium toxicity and treatment: An update. *Caspian journal of internal medicine, 8*(3), 135.

269. Rahman, M. (2017). *Bioaccumulation and toxicity of cadmium, chromium and lead to live fish food, the tubificid worms (Tubifex spp.)* University of Dhaka].

270. Raj, S., Mali, S. C., & Trivedi, R. (2018). Green synthesis and characterization of silver nanoparticles using Enicostemma axillare (Lam.) leaf extract. *Biochemical and biophysical research communications, 503*(4), 2814-2819.

271. Rajput, S., Kumar, D., & Agrawal, V. (2020). Green synthesis of silver nanoparticles using Indian Belladonna extract and their potential antioxidant, anti-inflammatory, anticancer and larvicidal activities. *Plant cell reports, 39*(7), 921-939.

272. Rather, M. A., Deori, P. J., Gupta, K., Daimary, N., Deka, D., Qureshi, A., Dutta, T. K., Joardar, S. N., & Mandal, M. (2022). Ecofriendly phytofabrication of silver nanoparticles using aqueous extract of Cuphea carthagenensis and their antioxidant potential and antibacterial activity against clinically important human pathogens. *Chemosphere, 300*, 134497.

273. Renugadevi, J., & Prabu, S. M. (2009). Naringenin protects against cadmium-induced oxidative renal dysfunction in rats. *Toxicology, 256*(1-2), 128-134.

274. Renugadevi, J., & Prabu, S. M. (2010a). Cadmium-induced hepatotoxicity in rats and the protective effect of naringenin. *Experimental and Toxicologic Pathology, 62*(2), 171-181.

275. Renugadevi, J., & Prabu, S. M. (2010b). Quercetin protects against oxidative stress-related renal dysfunction by cadmium in rats. *Experimental and Toxicologic Pathology, 62*(5), 471-481.

276. Rigat, M., Bonet, M. À., Garcia, S., Garnatje, T., & Valles, J. (2007). Studies on pharmaceutical ethnobotany in the high river Ter valley (Pyrenees, Catalonia, Iberian Peninsula). *Journal of Ethnopharmacology, 113*(2), 267-277.

277. Rivera, D., Obon, C., Inocencio, C., Heinrich, M., Verde, A., Fajardo, J., & Llorach, R. (2005). The ethnobotanical study of local Mediterranean food plants as medicinal resources in Southern Spain. *Journal of Physiology and Pharmacology. Supplement, 56*(1), 97-114.

278. Roy, S., & Das, T. K. (2015). Plant mediated green synthesis of silver nanoparticles-A. *Int. J. Plant Biol. Res, 3*, 1044-1055.

279. Rubio-Moraga, Á., Argandoña, J., Mota, B., Pérez, J., Verde, A., Fajardo, J., Gómez-Navarro, J., Castillo-López, R., Ahrazem, O., & Gómez-Gómez, L. (2013). Screening for polyphenols, antioxidant and antimicrobial activitiesof extracts from eleven Helianthemum taxa (Cistaceae) used in folk medicine in south-eastern Spain. *Journal of Ethnopharmacology, 148*(1), 287-296.

280. Sadhasivam, S., Shanmugam, P., & Yun, K. (2010). Biosynthesis of silver nanoparticles by Streptomyces hygroscopicus and antimicrobial activity against medically important pathogenic microorganisms. *Colloids and Surfaces B: Biointerfaces, 81*(1), 358-362.

281. Sainath, S., Meena, R., Supriya, C., Reddy, K. P., & Reddy, P. S. (2011). Protective role of Centella asiatica on lead-induced oxidative stress and suppressed reproductive health in male rats. *Environmental Toxicology and Pharmacology*, *32*(2), 146-154.

282. Saklani, S., Chandra, S., & Mishra, A. P. (2011). Evaluation of Nutritional profile, medicinal value and quantitative estimation in different parts of Pyrus pashia, Ficus palmata and Pyracantha crenulata. *JGTPS*, *2*(3), 350-354.

283. Sandoval, M., Okuhama, N., Zhang, X.-J., Condezo, L., Lao, J., Angeles, F., Musah, R., Bobrowski, P., & Miller, M. (2002). Anti-inflammatory and antioxidant activities of cat's claw (Uncaria tomentosa and Uncaria guianensis) are independent of their alkaloid content. *Phytomedicine*, *9*(4), 325-337.

284. Sankhalkar, S., & Vernekar, V. (2016). Quantitative and Qualitative analysis of Phenolic and Flavonoid content in Moringa oleifera Lam and Ocimum tenuiflorum L. *Pharmacognosy research*, *8*(1), 16.

285. Saranyaadevi, K., Subha, V., Ravindran, R. E., & Renganathan, S. (2014). Green synthesis and characterization of silver nanoparticle using leaf extract of Capparis zeylanica. *Asian J. Pharm. Clin. Res*, *7*, 44-48.

286. Sathishkumar, P., Vennila, K., Jayakumar, R., Yusoff, A. R. M., Hadibarata, T., & Palvannan, T. (2016). Phyto-synthesis of silver nanoparticles using Alternanthera tenella leaf extract: An effective inhibitor for the migration of human breast adenocarcinoma (MCF-7) cells. *Bioprocess and biosystems engineering*, *39*(4), 651-659.

287. Sauer, J.-M., Waalkes, M. P., Hooser, S. B., Kuester, R. K., McQueen, C. A., & Sipes, I. G. (1997). Suppression of Kupffer cell function prevents cadmium induced hepatocellular necrosis in the male Sprague-Dawley rat. *Toxicology*, *121*(2), 155-164.

288. Schutte, R., Nawrot, T. S., Richart, T., Thijs, L., Vanderschueren, D., Kuznetsova, T., Van Hecke, E., Roels, H. A., & Staessen, J. A. (2008). Bone resorption and environmental exposure to cadmium in women: a population study. *Environmental health perspectives*, *116*(6), 777-783.

289. Scoullos, M. J., Vonkeman, G. H., Thornton, I., & Makuch, Z. (2012). *Mercury—cadmium—lead handbook for sustainable heavy metals policy and regulation* (Vol. 31). Springer Science & Business Media.

290. Seif, M. M., Madboli, A.-N., Marrez, D. A., & Aboulthana, W. M. (2019). Hepato-renal protective effects of egyptian purslane extract against experimental cadmium toxicity in rats with special emphasis on the functional and histopathological changes. *Toxicology reports*, *6*, 625-631.

291. Shaikh, Z. A., Vu, T. T., & Zaman, K. (1999). Oxidative stress as a mechanism of chronic cadmium-induced hepatotoxicity and renal toxicity and protection by antioxidants. *Toxicology and applied pharmacology*, *154*(3), 256-263.

292. Shakhatreh, M. A. K., Al-Smadi, M. L., Khabour, O. F., Shuaibu, F. A., Hussein, E. I., & Alzoubi, K. H. (2016). Study of the antibacterial and antifungal activities of synthetic benzyl bromides, ketones, and corresponding chalcone derivatives. *Drug design, development and therapy*, *10*, 3653.

293. Shan, B., Cai, Y. Z., Sun, M., & Corke, H. (2005). Antioxidant capacity of 26 spice extracts and characterization of their phenolic constituents. *Journal of agricultural and food chemistry*, *53*(20), 7749-7759.

294. Shankar, S. S., Rai, A., Ahmad, A., & Sastry, M. (2005). Controlling the optical properties of lemongrass extract synthesized gold nanotriangles and potential application in infrared-absorbing optical coatings. *Chemistry of Materials*, *17*(3), 566-572.

295. Shanmuganathan, R., MubarakAli, D., Prabakar, D., Muthukumar, H., Thajuddin, N., Kumar, S. S., & Pugazhendhi, A. (2018). An enhancement of antimicrobial efficacy of biogenic and ceftriaxone-conjugated silver nanoparticles: green approach. *Environmental Science and Pollution Research*, *25*(11), 10362-10370.

296. Sharmin, S., Rahaman, M. M., Sarkar, C., Atolani, O., Islam, M. T., & Adeyemi, O. S. (2021). Nanoparticles as antimicrobial and antiviral agents: A literature-based perspective study. *Heliyon*, *7*(3), e06456.

297. Shih, C. M., Ko, W. C., Wu, J. S., Wei, Y. H., Wang, L. F., Chang, E. E., Lo, T. Y., Cheng, H. H., & Chen, C. T. (2004). Mediating of caspase-independent apoptosis by cadmium through the mitochondria-ROS pathway in MRC-5 fibroblasts. *Journal of cellular biochemistry*, *91*(2), 384-397.

298. Shin, W.-K., Cho, J., Kannan, A. G., Lee, Y.-S., & Kim, D.-W. (2016). Cross-linked composite gel polymer electrolyte using mesoporous methacrylate-functionalized SiO2 nanoparticles for lithium-ion polymer batteries. *Scientific reports*, *6*(1), 1-10.

299. Siddharthan, N., Kalaivani, G., Poongothai, E., Arul, M., & Hemalatha, N. (2019). CHARACTERIZATION OF SILVER NANOPARTICLES SYNTHESIZED FROM Catheranthus roseus (Vinca rosea) PLANT LEAF EXTRACT AND THEIR ANTIBACTERIAL ACTIVITY.

300. Simakin, A., Voronov, V., Kirichenko, N., & Shafeev, G. (2004). Nanoparticles produced by laser ablation of solids in liquid environment. *Applied Physics A*, *79*(4), 1127-1132.

301. Singh, A., Dar, M. Y., Joshi, B., Sharma, B., Shrivastava, S., & Shukla, S. (2018). Phytofabrication of silver nanoparticles: novel drug to overcome hepatocellular ailments. *Toxicology reports*, *5*, 333-342.

302. Sirajuddin, M., Ali, S., & Badshah, A. (2013). Drug–DNA interactions and their study by UV–Visible, fluorescence spectroscopies and cyclic voltametry. *Journal of photochemistry and photobiology B: biology*, *124*, 1-19.

303. Siu, E. R., Mruk, D. D., Porto, C. S., & Cheng, C. Y. (2009). Cadmium-induced testicular injury. *Toxicology and applied pharmacology*, *238*(3), 240-249.

304. Slinkard, K., & Singleton, V. L. (1977). Total phenol analysis: automation and comparison with manual methods. *American journal of enology and viticulture*, *28*(1), 49-55.

305. Sondi, I., & Salopek-Sondi, B. (2004). Silver nanoparticles as antimicrobial agent: a case study on E. coli as a model for Gram-negative bacteria. *Journal of colloid and interface science*, *275*(1), 177-182.

306. Southon, S., Gee, J. M., & Johnson, I. (1984). Hexose transport and mucosal morphology in the small intestine of the zinc-deficient rat. *British Journal of Nutrition*, *52*(2), 371-380.

307. Sriram, M. I., Kanth, S. B. M., Kalishwaralal, K., & Gurunathan, S. (2010). Antitumor activity of silver nanoparticles in Dalton's lymphoma ascites tumor model. *International journal of nanomedicine, 5*, 753.

308. Stirling, F., Naydich, A., Bramante, J., Barocio, R., Certo, M., Wellington, H., Redfield, E., O'Keefe, S., Gao, S., & Cusolito, A. (2020). Synthetic cassettes for pH-mediated sensing, counting, and containment. *Cell Reports, 30*(9), 3139-3148. e3134.

309. Sukirtha, R., Priyanka, K. M., Antony, J. J., Kamalakkannan, S., Thangam, R., Gunasekaran, P., Krishnan, M., & Achiraman, S. (2012). Cytotoxic effect of Green synthesized silver nanoparticles using Melia azedarach against in vitro HeLa cell lines and lymphoma mice model. *Process Biochemistry, 47*(2), 273-279.

310. Sumino, K., Hayakawa, K., Shibata, T., & Kitamura, S. (1975). Heavy metals in normal Japanese tissues: amounts of 15 heavy metals in 30 subjects. *Archives of Environmental Health: An International Journal, 30*(10), 487-494.

311. Sun, S., Murray, C. B., Weller, D., Folks, L., & Moser, A. (2000). Monodisperse FePt nanoparticles and ferromagnetic FePt nanocrystal superlattices. *science, 287*(5460), 1989-1992.

312. Suriyakalaa, U., Antony, J. J., Suganya, S., Siva, D., Sukirtha, R., Kamalakkannan, S., Pichiah, P. T., & Achiraman, S. (2013). Hepatocurative activity of biosynthesized silver nanoparticles fabricated using Andrographis paniculata. *Colloids and Surfaces B: Biointerfaces, 102*, 189-194.

313. Svartengren, M., Elinder, C. G., Friberg, L., & Lind, B. (1986). Distribution and concentration of cadmium in human kidney. *Environmental research, 39*(1), 1-7.

314. Taghavizadeh Yazdi, M. E., Amiri, M. S., Nourbakhsh, F., Rahnama, M., Forouzanfar, F., & Mousavi, S. H. (2021). Bio-indicators in cadmium toxicity: Role of HSP27 and HSP70. *Environmental Science and Pollution Research, 28*(21), 26359-26379.

315. Tamuly, C., Hazarika, M., Bordoloi, M., Bhattacharyya, P. K., & Kar, R. (2014). Biosynthesis of Ag nanoparticles using pedicellamide and its photocatalytic activity: an eco-friendly approach. *Spectrochimica Acta Part A: Molecular and Biomolecular Spectroscopy, 132*, 687-691.

316. Tarannum, N., & Gautam, Y. K. (2019). Facile green synthesis and applications of silver nanoparticles: a state-of-the-art review. *RSC advances, 9*(60), 34926-34948.

317. Tardío, J., Pardo-de-Santayana, M., & Morales, R. (2006). Ethnobotanical review of wild edible plants in Spain. *Botanical Journal of the Linnean Society, 152*(1), 27-71.

318. Thalib, I., Budianto, W. Y., & Suhartono, E. (2017). Effect of cadmium exposure on increasing risk of diabetes melitus through the measurement of blood glucose level and liver glucokinase activity in rats. *Berkala Kedokteran, 13*(2), 137-145.

319. Tian, J., Wong, K. K., Ho, C. M., Lok, C. N., Yu, W. Y., Che, C. M., Chiu, J. F., & Tam, P. K. (2007). Topical delivery of silver nanoparticles promotes wound healing. *ChemMedChem: Chemistry Enabling Drug Discovery, 2*(1), 129-136.

320. Tomaszewska, E., Soliwoda, K., Kadziola, K., Tkacz-Szczesna, B., Celichowski, G., Cichomski, M., Szmaja, W., & Grobelny, J. (2013). Detection limits of DLS and UV-Vis

spectroscopy in characterization of polydisperse nanoparticles colloids. *Journal of nanomaterials, 2013*.

321. Toppo, R., Roy, B. K., Gora, R. H., Baxla, S. L., & Kumar, P. (2015). Hepatoprotective activity of Moringa oleifera against cadmium toxicity in rats. *Veterinary world, 8*(4), 537.

322. Travlos, G., Morris, R., Elwell, M., Duke, A., Rosenblum, S., & Thompson, M. (1996). Frequency and relationships of clinical chemistry and liver and kidney histopathology findings in 13-week toxicity studies in rats. *Toxicology, 107*(1), 17-29.

323. Trease, G., & Evans, W. (1989). Pharmacognosy. 13th. *ELBS/Bailliere Tindall, London*, 345-346.

324.V. Le, A., E. Parks, S., H. Nguyen, M., & D. Roach, P. (2018). Improving the vanillin-sulphuric acid method for quantifying total saponins. *Technologies, 6*(3), 84.

325. Valko, M., Morris, H., & Cronin, M. (2005). Metals, toxicity and oxidative stress. *Current medicinal chemistry, 12*(10), 1161-1208.

326. Van Den Heuvel, R., Leppens, H., & Schoeters, G. (2001). Use of in vitro assays to assess hematotoxic effects of environmental compounds. *Cell biology and toxicology, 17*(2), 107-116.

327. Venturella, G., Gargano, M. L., Compagno, R., La Rosa, A., La Bella, S., Leto, C., & Tuttolomondo, T. (2015). Up-to-date report on the distribution of Helianthemum lippii (Cistaceae) in Italy. *Webbia, 70*(1), 151-154.

328. Verma, A., & Mehata, M. S. (2016). Controllable synthesis of silver nanoparticles using Neem leaves and their antimicrobial activity. *Journal of radiation research and applied sciences, 9*(1), 109-115.

329. Verma, D. K., Hasan, S. H., & Banik, R. M. (2016). Photo-catalyzed and phyto-mediated rapid green synthesis of silver nanoparticles using herbal extract of Salvinia molesta and its antimicrobial efficacy. *Journal of photochemistry and photobiology B: biology, 155*, 51-59.

330. Vesey, D. A. (2010). Transport pathways for cadmium in the intestine and kidney proximal tubule: focus on the interaction with essential metals. *Toxicology letters, 198*(1), 13-19.

331. Vinjamuri, S., Afshan, S., Shekar, S., & Saraswathi, V. (2015). Evaluation of hemolytic activity, ATPase inhibitory activity and antitumor activity of TLC extract of lemon grass (Cymbpogon citratus). *Int J Pharmacogn Phytochem Res, 7*(4), 785-788.

332. Von White, G., Kerscher, P., Brown, R. M., Morella, J. D., McAllister, W., Dean, D., & Kitchens, C. L. (2012). Green synthesis of robust, biocompatible silver nanoparticles using garlic extract. *Journal of nanomaterials, 2012*.

333. Vorobyova, V., Vasyliev, G., & Skiba, M. (2020). Eco-friendly "green" synthesis of silver nanoparticles with the black currant pomace extract and its antibacterial, electrochemical, and antioxidant activity. *Applied Nanoscience, 10*(12), 4523-4534.

334. Wadood, A., Ghufran, M., Jamal, S. B., Naeem, M., Khan, A., & Ghaffar, R. (2013). Phytochemical analysis of medicinal plants occurring in local area of Mardan. *Biochem anal biochem, 2*(4), 1-4.

335. Waisberg, M., Joseph, P., Hale, B., & Beyersmann, D. (2003). Molecular and cellular mechanisms of cadmium carcinogenesis. *Toxicology, 192*(2-3), 95-117.

336. Wang, L., Wu, Y., Xie, J., Wu, S., & Wu, Z. (2018). Characterization, antioxidant and antimicrobial activities of green synthesized silver nanoparticles from Psidium guajava L. leaf aqueous extracts. *Materials Science and Engineering: C, 86*, 1-8.

337. Wang, Y., Fang, J., Leonard, S. S., & Rao, K. M. K. (2004). Cadmium inhibits the electron transfer chain and induces reactive oxygen species. *Free Radical Biology and Medicine, 36*(11), 1434-1443.

338. Weckbecker, G., & Cory, J. G. (1988). Ribonucleotide reductase activity and growth of glutathione-depleted mouse leukemia L1210 cells in vitro. *Cancer letters, 40*(3), 257-264.

339. Weng, Y., Liu, J., Jin, S., Guo, W., Liang, X., & Hu, Z. (2017). Nanotechnology-based strategies for treatment of ocular disease. *Acta pharmaceutica sinica B, 7*(3), 281-291.

340. Winiarska-Mieczan, A., Krusiński, R., & Kwiecień, M. (2013). Tannic acid influence on lead and cadmium accumulation in the hearts and lungs of rats. *Advances in Clinical and Experimental Medicine, 22*(5), 615-620.

341. Wu, J., Bi, S.-Y., Sun, X.-Y., Zhao, R., Wang, J.-H., & Zhou, H.-F. (2019). Study on the interaction of fisetholz with BSA/HSA by multi-spectroscopic, cyclic voltammetric, and molecular docking technique. *Journal of Biomolecular Structure and Dynamics, 37*(13), 3496-3505.

342.https://www.floraofqatar.com/helianthemum_lippii.htm

343. Xu, Z., Bai, G., & Dong, C. (2005). Studies on interaction of an intramolecular charge transfer fluorescence probe: 4′-Dimethylamino-2, 5-dihydroxychalcone with DNA. *Bioorganic & medicinal chemistry, 13*(20), 5694-5699.

344. Xu, Z. P., Zeng, Q. H., Lu, G. Q., & Yu, A. B. (2006). Inorganic nanoparticles as carriers for efficient cellular delivery. *Chemical Engineering Science, 61*(3), 1027-1040.

345. Yaki, K. (1976). A simple fluorometric assay for lipoprotein in blood plasma. *Biochem Med, 15*, 212-217.

346. Yam, M. F., Ang, L. F., Ameer, O. Z., Salman, I. M., Aziz, H. A., & Asmawi, M. Z. (2009). Anti-inflammatory and analgesic effects of Elephantopus tomentosus ethanolic extract. *Journal of Acupuncture and Meridian Studies, 2*(4), 280-287.

347. Yan, Y., Zhou, X., Guo, K., Zhou, F., & Yang, H. (2020). Use of chlorogenic acid against diabetes mellitus and its complications. *Journal of Immunology Research, 2020*.

348. Yang, Y., Matsubara, S., Xiong, L., Hayakawa, T., & Nogami, M. (2007). Solvothermal synthesis of multiple shapes of silver nanoparticles and their SERS properties. *The Journal of Physical Chemistry C, 111*(26), 9095-9104.

349. Ye, X., Qian, H., Xu, P., Zhu, L., Longnecker, M. P., & Fu, H. (2009). Nephrotoxicity, neurotoxicity, and mercury exposure among children with and without dental amalgam fillings. *International journal of hygiene and environmental health, 212*(4), 378-386.

350. Yee, W., Selvaduray, G., & Hawkins, B. (2016). Characterization of silver nanoparticle-infused tissue adhesive for ophthalmic use. *Journal of the mechanical behavior of biomedical materials*, *55*, 67-74.

351. Yesilot, S., & Aydin, C. (2019). Silver nanoparticles; a new hope in cancer therapy? *Eastern Journal of Medicine*, *24*(1), 111-116.

352. Yesmin, S., Paul, A., Naz, T., Rahman, A., Akhter, S. F., Wahed, M. I. I., Emran, T. B., & Siddiqui, S. A. (2020). Membrane stabilization as a mechanism of the anti-inflammatory activity of ethanolic root extract of Choi (Piper chaba). *Clinical Phytoscience*, *6*(1), 1-10.

353. Yiin, S., & Lin, T. (1995). Lead-catalyzed peroxidation of essential unsaturated fatty acid. *Biological trace element research*, *50*(2), 167-172.

354. Youngs, H. L., Sundaramoorthy, M., & Gold, M. H. (2000). Effects of cadmium on manganese peroxidase: competitive inhibition of MnII oxidation and thermal stabilization of the enzyme. *European journal of biochemistry*, *267*(6), 1761-1769.

355. Yousaf, H., Mehmood, A., Ahmad, K. S., & Raffi, M. (2020). Green synthesis of silver nanoparticles and their applications as an alternative antibacterial and antioxidant agents. *Materials Science and Engineering: C*, *112*, 110901.

356. Yousif, A. S., & Ahmed, A. A. (2009). Effects of cadmium (Cd) and lead (Pb) on the structure and function of thyroid gland. *Afr J Environ Sci Technol*, *3*(3), 78-85.

357. Zargar, M., Hamid, A. A., Bakar, F. A., Shamsudin, M. N., Shameli, K., Jahanshiri, F., & Farahani, F. (2011). Green synthesis and antibacterial effect of silver nanoparticles using Vitex negundo L. *Molecules*, *16*(8), 6667-6676.

358. Zhang, H., Jacob, J. A., Jiang, Z., Xu, S., Sun, K., Zhong, Z., Varadharaju, N., & Shanmugam, A. (2019). Hepatoprotective effect of silver nanoparticles synthesized using aqueous leaf extract of Rhizophora apiculata. *International journal of nanomedicine*, *14*, 3517.

359. Zhang, W., Zhi, J., Cui, Y., Zhang, F., Habyarimana, A., Cambier, C., & Gustin, P. (2014). Potentiated interaction between ineffective doses of budesonide and formoterol to control the inhaled cadmium-induced up-regulation of metalloproteinases and acute pulmonary inflammation in rats. *Plos one*, *9*(10), e109136.

Annex

Annex 01: Calibration curve for estimation of phytochemicals compounds

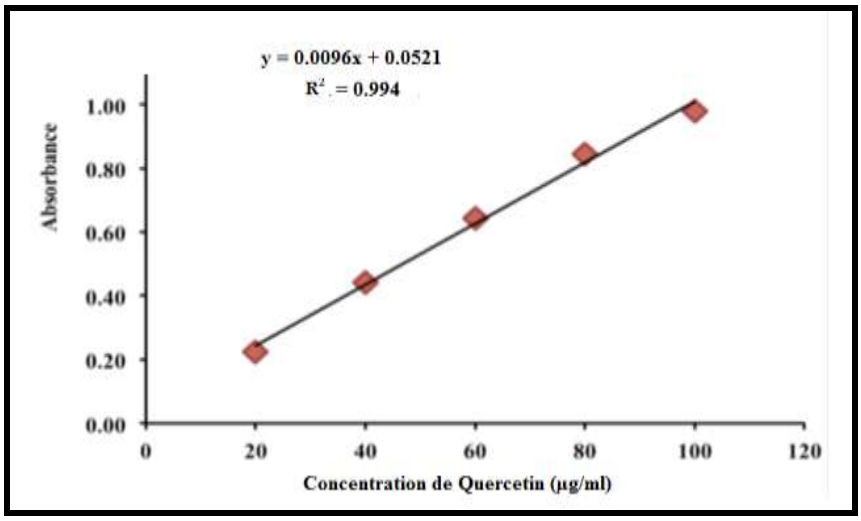

Figure: Calibration curve of Quercitin for determination of total flavonoids content.

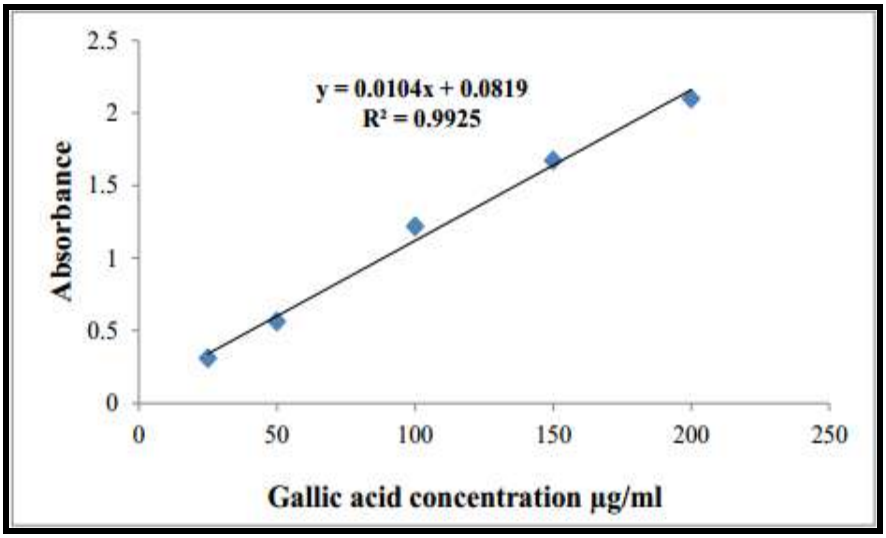

Figure: Calibration curve of Gallic acid for determination of total phenolic content.

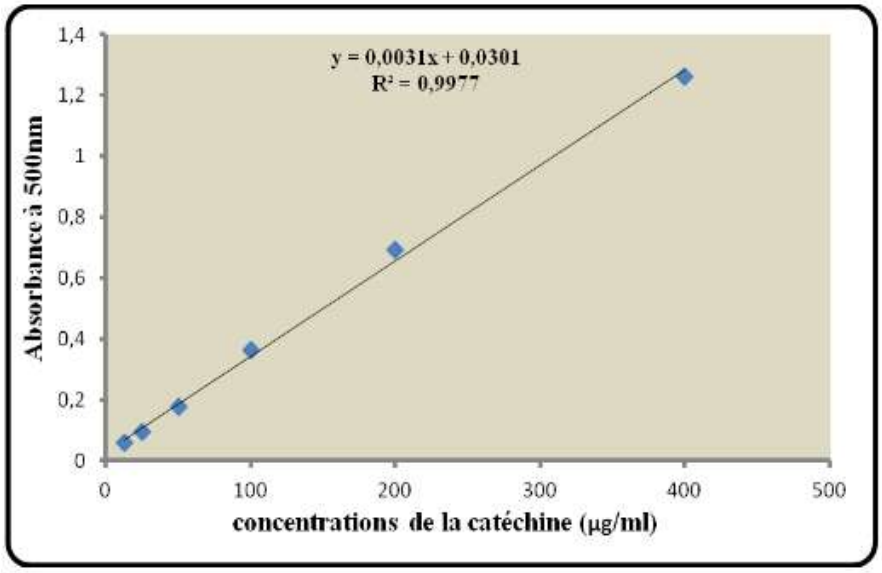

Figure: Calibration curve of Catechin for determination of condensed tannins content.

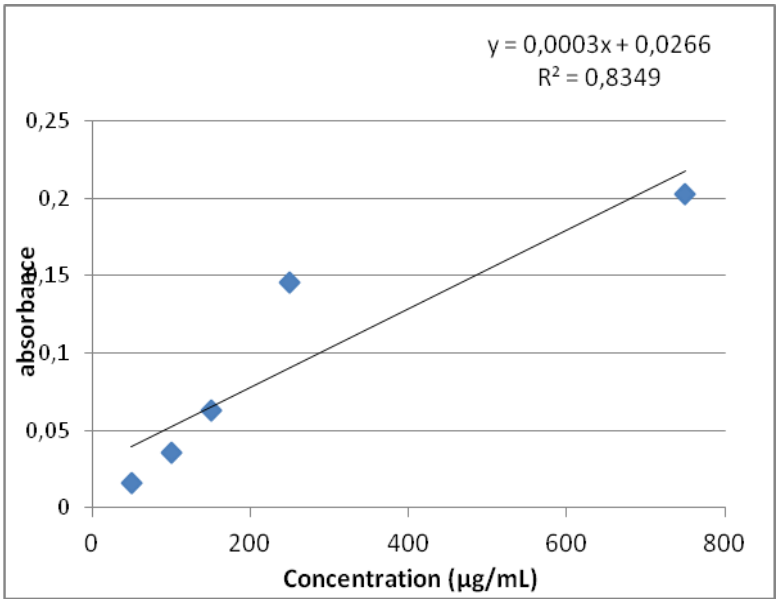

Figure: Calibration curve of tannic acid for determination of total Tannins hydrolyzble

Annex 02: Calibration curve for determination of capacity antioxidant of samples

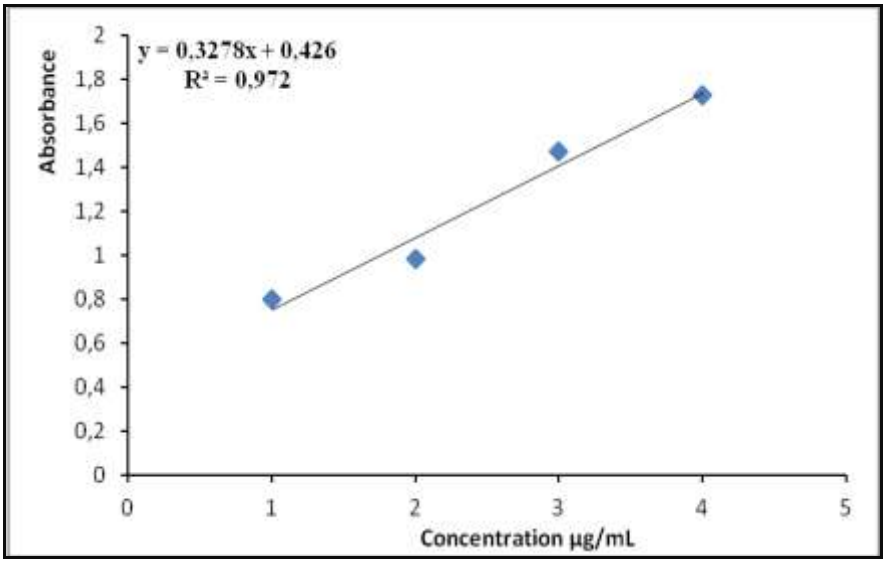

Figure: Calibration curve of Ascorbic Acid for determination of reducing power capacity

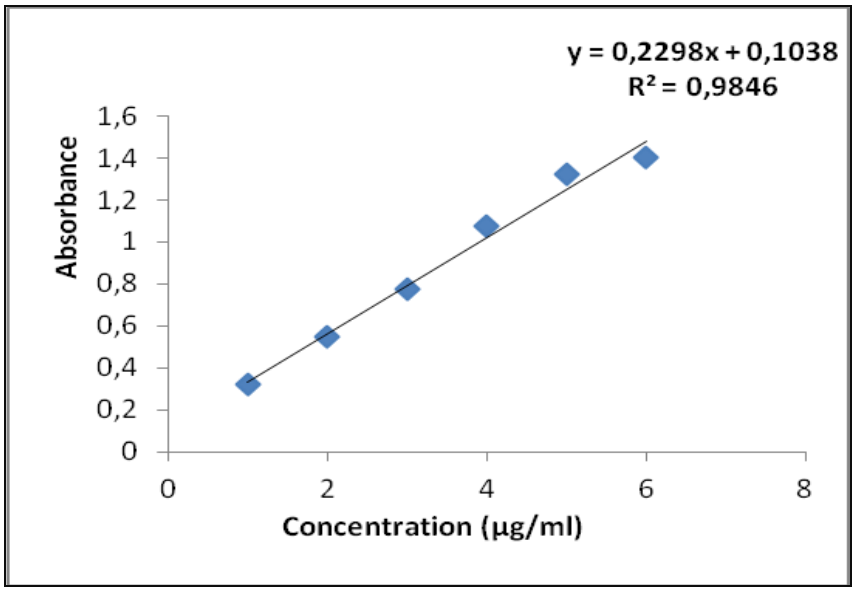

Figure: Calibration curve of *H.lippii* extract for determination of reducing power capacity

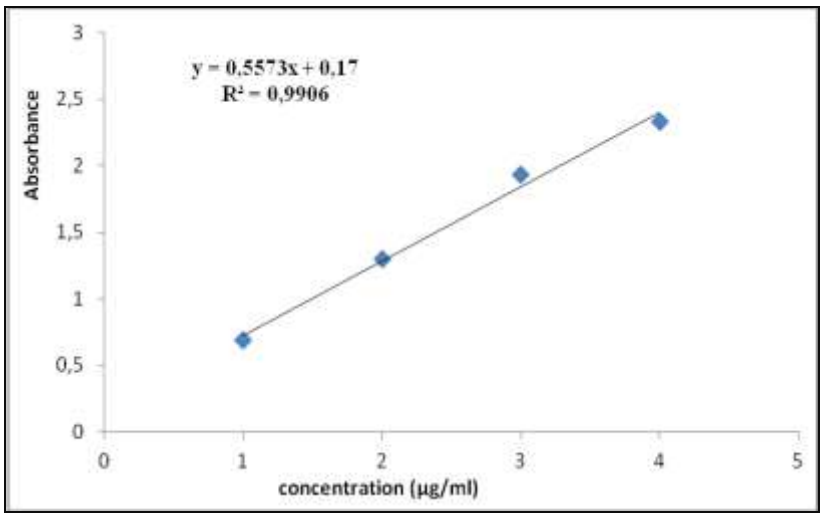

Figure: Calibration curve of dichloromethane fraction for determination of reducing power capacity

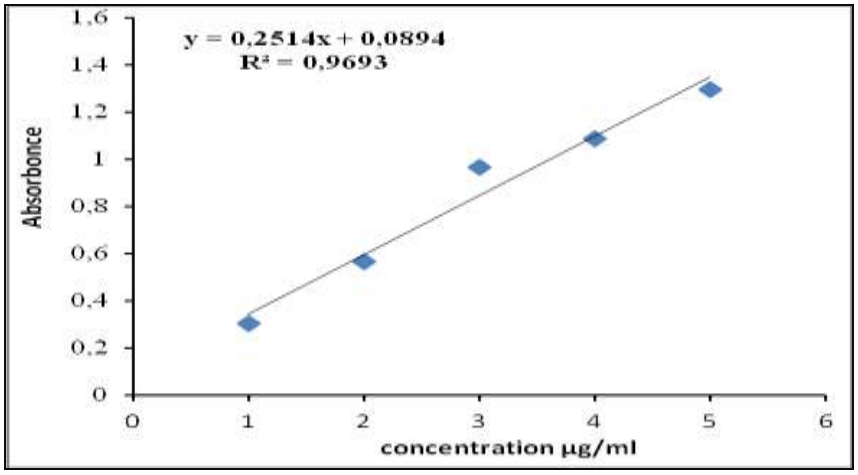

Figure: Calibration curve of Anthocyanin fraction for determination of reducing power capacity

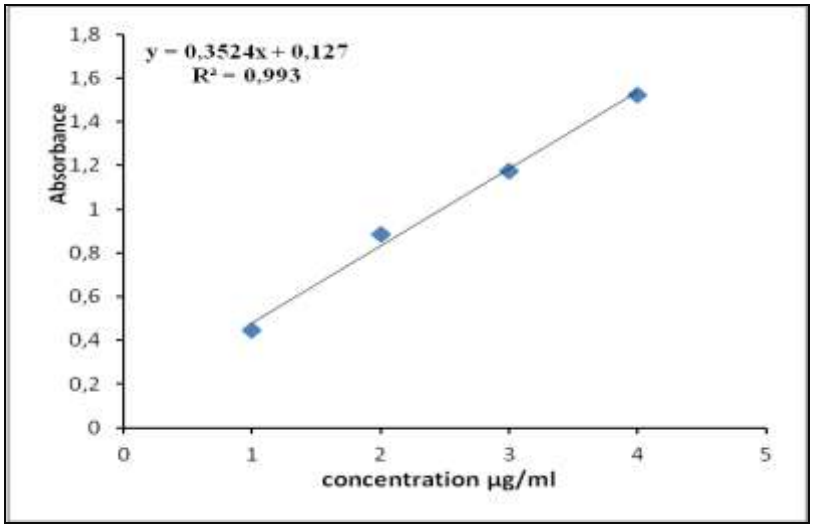

Figure: Calibration curve of ethyl acetate fraction for determination of reducing power capacity

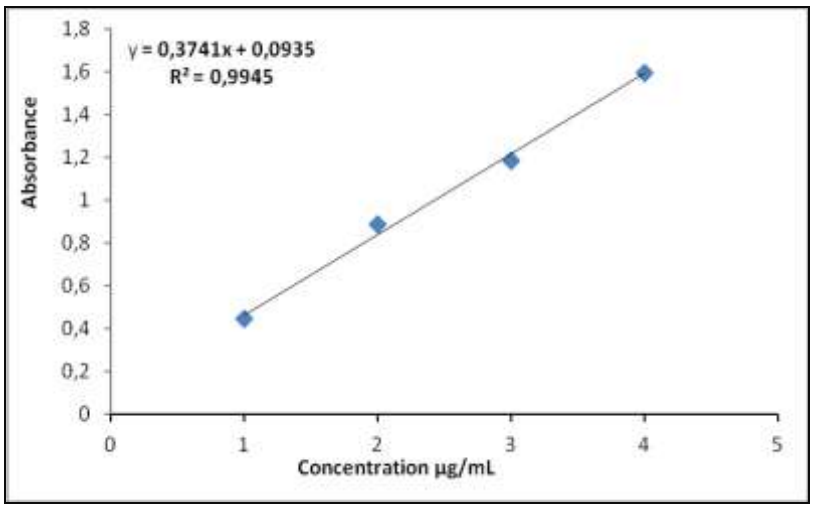

Figure: Calibration curve of n-butanol fraction for determination of reducing power capacity

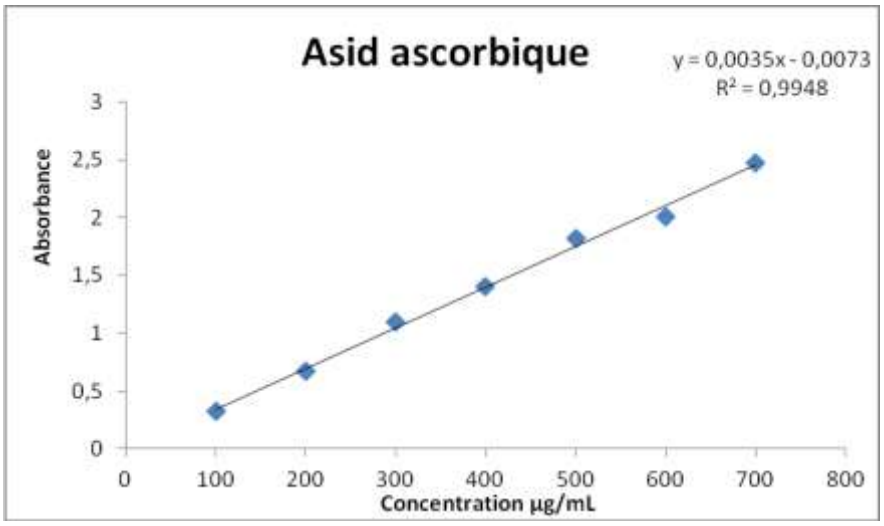

Figure: Calibration curve of Ascorbic acid for determination of total antioxidant capacity

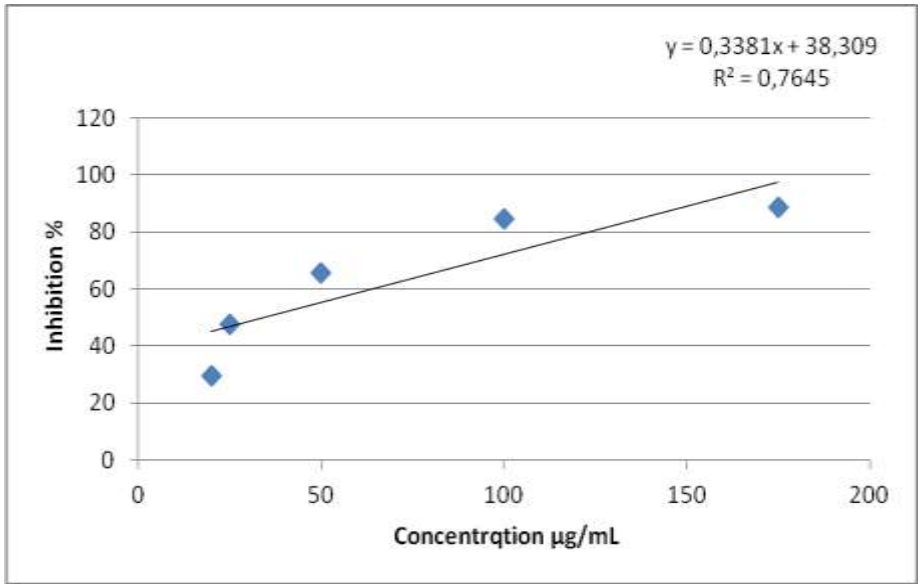

Figure: Percentage inhibition of DPPH radical by *H.lippii*

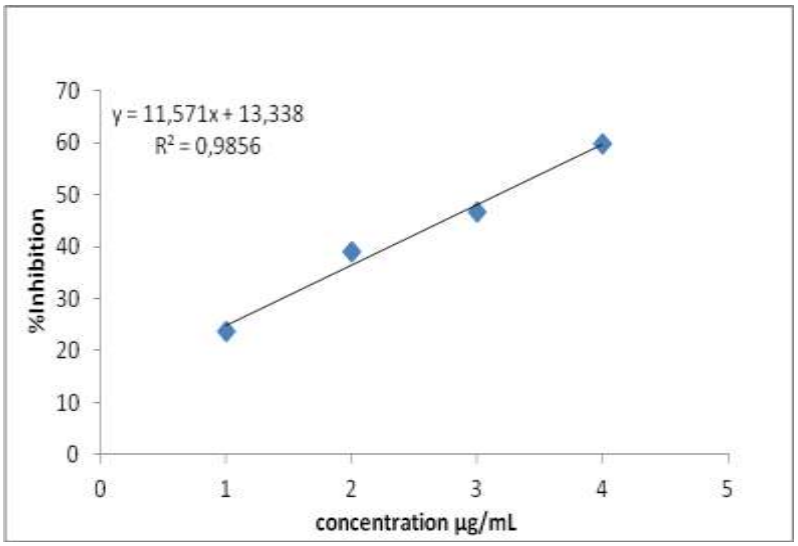

Figure: Percentage inhibition of DPPH radical by silver nanoparticule

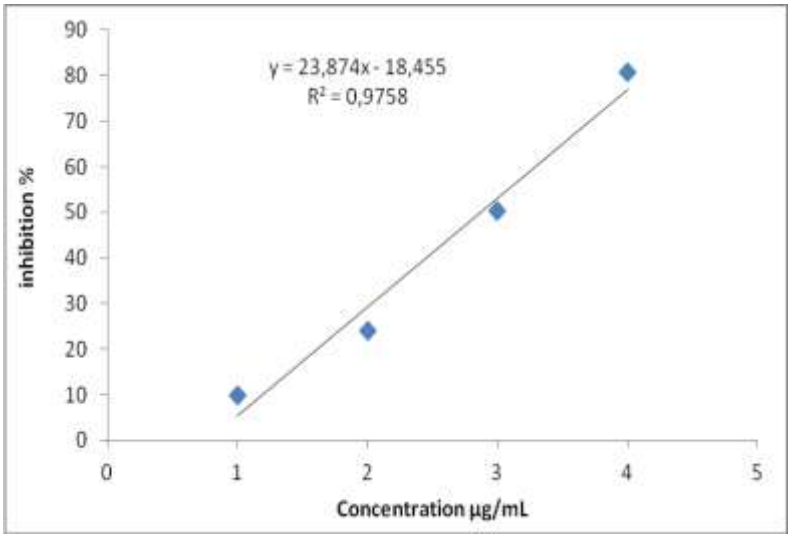

Figure: Percentage inhibition of DPPH radical by Anthocyanin

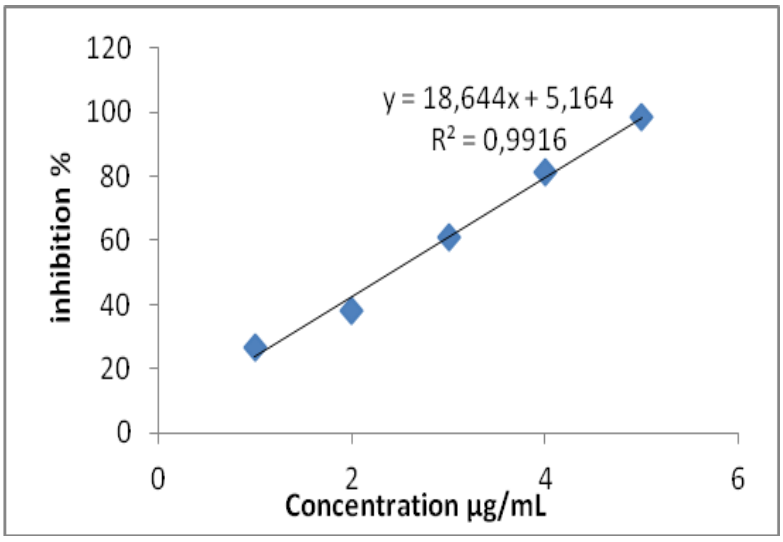

Figure: Percentage inhibition of DPPH radical by dichloromethane fraction

Annex 03: Calibration curve of BSA for determination of protein level

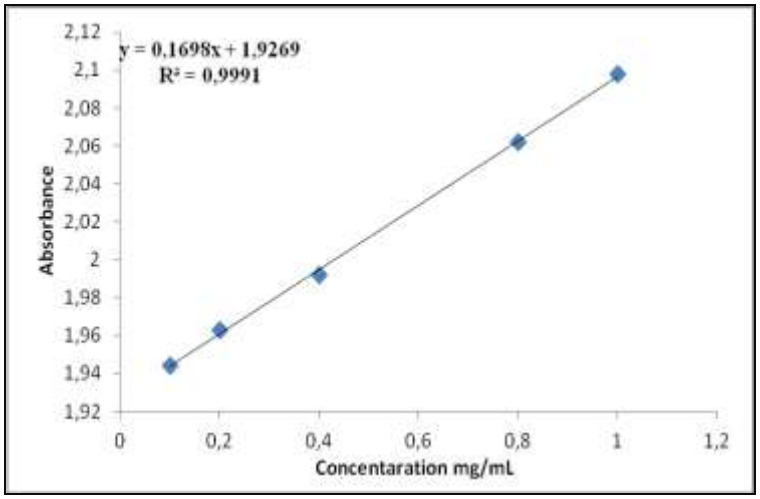

Figure: Calibration curve of BSA for determination of protein level.

Annex 04: Biochemical parameters analysis

SPINREACT

CE GLUCOSE -HK

Glucose-HK

Hexokinase. Enzymatic - UV

Quantitative determination of glucose
IVD

Store at 2-8 °C

PRINCIPLE OF THE METHOD

Hexoquinase (HK) catalyzes the phosphorylation of glucose to glucose-6-phosphate (G6P) by ATP. The formed glucose-6-phosphate is reduced to 6-phosphogluconate in the presence of glucose-6-phosphate dehydrogenase (G6P-DH) with the subsequent reduction of NAD to NADH:

$$\text{Glucose} + \text{ATP} \xrightarrow{\text{HK}} \text{Glucose-6-phosphate} + \text{ADP}$$

$$\text{G6P} + \text{NAD}^+ \xrightarrow{\text{G6P-DH}} \text{6-Phosphogluconate} + \text{NADH} + \text{H}^+$$

The increase in concentration of NADH is proportional to the glucose concentration in the sample[1,2].

CLINICAL SIGNIFICANCE

Glucose is a major source of energy for most cells of the body; insulin facilitates glucose entry into the cells.
Diabetes is a disease manifested by hyperglycemia; patients with diabetes demonstrate an inability to produce insulin[1,5,6].
Clinical diagnosis should not be made on a single test result; it should integrate clinical and other laboratory data.

REAGENTS

R 1 Buffer	TRIS pH 7,5	4 mmol/L
	ATP	2,1 mmol/L
	Mg^{2+}	0,8 mmol/L
R 2 Enzymes	NAD^+	2 mmol/L
	Hexoquinase (HK)	1000 U/L
	Glucose-6-phosphate (G6P-DH)	1000 U/L
GLUCOSE CAL	Glucose aqueous primary standard 100 mg/dL	

PREPARATION

Working reagent (WR): Dissolve (→) the contents of one vial of R 2 Enzymes in one bottle of R 1 Buffer.
Cap and mix gently to dissolve contents.
The reagent is stable after reconstitution 1 month in the refrigerator (2-8°C) or 7 days at room temperature (15-25°C).

STORAGE AND STABILITY

All the components of the kit are stable until the expiration date on the label when stored tightly closed at 2-8°C, protected from light and contaminations prevented during their use.
Do not use reagents over the expiration date.
Signs of reagent deterioration:
- Presence of particles and turbidity.
- Blank absorbance (A) at 340 nm ≥ 0.30.

4. Mix and incubate for 5 min. at 37°C or 10 min. at room temperature (15-25°C).
5. Read the absorbance (A) of the samples and calibrator, against the Blank.

CALCULATIONS

$$\frac{(A)\text{Sample} - (A)\text{Blank}}{(A)\text{Standard} - (A)\text{Blank}} \times 100\ (\text{Standard conc.}) = \text{mg/dL glucose in the sample}$$

Conversion factor: mg/dL x 0,0555= mmol/L.

QUALITY CONTROL

Control sera are recommended to monitor the performance of assay procedures: SPINTROL H Normal and Pathologic (Ref. 1002120 and 1002210).
If control values are found outside the defined range, check the instrument, reagents and calibrator for problems.
Each laboratory should establish its own Quality Control scheme and corrective actions if controls do not meet the acceptable tolerances.

REFERENCE VALUES[1]

Serum or plasma:

60 – 110 mg/dL ≈ 3,33 – 6,10 mmol/L

These values are for orientation purpose; each laboratory should establish its own reference range.

PERFORMANCE CHARACTERISTICS

Measuring range: From *detection limit* of 0,16 mg/dL to *linearity limit* of 600 mg/dL.
If the results obtained were greater than linearity limit, dilute the sample 1/2 with NaCl 9 g/L and multiply the result by 2.
Precision:

	Intra-assay (n=20)		Inter-assay (n=20)	
Mean (mg/dL)	98	251	99	253
SD	1,05	4,15	1,51	2,42
CV (%)	1,07	1,66	1,52	0,96

Sensitivity: 1 mg/dL = 0,0036 A.
Accuracy: Results obtained using SPINREACT reagents (y) did not show systematic differences when compared with other commercial reagents (x).
The results obtained using 50 samples were the following:
Correlation coefficient (r^2): 0,99
Regression equation: y=1,0146x + 5,5029.
The results of the performance characteristics depend on the analyzer used.

INTERFERENCES

Hemoglobin up to 19 g/L and bilirubin up to 100 mg/L, do not interfere[1].
A list of drugs and other interfering substances with glucose determination has been reported by Young et. al[3,4].

NOTES

1. GLUCOSE CAL: Proceed carefully with this product because due its nature it can get contaminated easily.

SPINREACT

CE CREATININE -J

Creatinina

Jaffé. Colorimétrico - cinético

Determinación cuantitativa de creatinina

IVD

Conservar a 2-8°C

PRINCIPIO DEL MÉTODO

El ensayo de la creatinina esta basado en la reacción de la creatinina con el picrato de sodio descrito por Jaffé.

La creatinina reacciona con el picrato alcalino formando un complejo rojizo. El intervalo de tiempo escogido para las lecturas permite eliminar gran parte de las interferencias conocidas del método.

La intensidad del color formado es proporcional a la concentración de creatinina en la muestra ensayada[1].

SIGNIFICADO CLÍNICO

La creatinina es el resultado de la degradación de la creatina, componente de los músculos y puede ser transformada en ATP, fuente de energía para las células.

La producción de creatinina depende de la modificación de la masa muscular. Varía poco y los niveles suelen ser muy estables.

Se elimina a través del riñón. En una insuficiencia renal progresiva hay una retención en sangre de urea, creatinina y ácido úrico.

Niveles altos de creatinina son indicativos de patología renal[1,2]

El diagnóstico clínico debe realizarse teniendo en cuenta todos los datos clínicos y de laboratorio.

REACTIVOS

R 1 Reactivo Pícrico	Ácido pícrico	17,5 mmol/L
R 2 Reactivo Alcalinizante	Hidróxido sódico	0,29 mol/L
CREATININE CAL	Patrón primario acuoso de Creatinina	2 mg/dL

PRECAUCIONES

R1/ R2: H314-Provoca quemaduras graves en la piel y lesiones oculares graves.

CAL: H290-Puede ser corrosivo para los metales.

Seguir los consejos de prudencia indicados en la FDS y etiqueta del producto.

PREPARACIÓN

Reactivo de trabajo (RT): Mezclar volúmenes iguales de R1 Reactivo Pícrico y de R2 Reactivo Alcalinizante.

Estabilidad del reactivo de trabajo: 15 días a 2-8°C o 7 días a temperatura ambiente (15-25°C).

CONSERVACIÓN Y ESTABILIDAD

Todos los componentes del kit son estables, hasta la fecha de caducidad indicada en la etiqueta, cuando se mantienen los frascos bien cerrados a 2-8°C, protegidos de la luz y se evita su contaminación. No usar reactivos

4. Mezclar y poner en marcha el cronómetro.
5. Leer la absorbancia (A_1) al cabo de 30 segundos y al cabo de 90 segundos (A_2) de la adición de la muestra.
6. Calcular: $\Delta A = A_2 - A_1$.

CÁLCULOS

$$\frac{\Delta A \text{ Muestra} - \Delta A \text{ Blanco}}{\Delta A \text{ Patrón} - \Delta A \text{ Blanco}} \times 2 \text{ (Conc. Patrón)} = \text{mg/dL de creatinina en la muestra}$$

Factor de conversión: mg/dL x 88,4 = µmol/L

CONTROL DE CALIDAD

Es conveniente analizar junto con las muestras sueros control valorados: SPINTROL H Normal y Patológico (Ref. 1002120 y 1002210).

Si los valores hallados se encuentran fuera del rango de tolerancia, revisar el instrumento, los reactivos y el calibrador.

Cada laboratorio debe disponer su propio Control de Calidad y establecer correcciones en el caso de que los controles no cumplan con las tolerancias.

VALORES DE REFERENCIA[1]

Suero o plasma:

Hombres	0,7 - 1,4 mg/dL	≅ 61,8 - 123,7 µmol/L
Mujeres	0,6 - 1,1 mg/dL	≅ 53,0 - 97,2 µmol/L

Orina: 15-25 mg/Kg/24 h

Hombres	10 - 20 mg/Kg/24 h
Mujeres	8 - 18 mg/Kg/24 h

Estos valores son orientativos. Es recomendable que cada laboratorio establezca sus propios valores de referencia.

CARACTERÍSTICAS DEL MÉTODO

Rango de medida: Desde el *límite de detección* de 0,000 mg/dL hasta el *límite de linealidad* de 35 mg/dL.

Si la concentración es superior al límite de linealidad, diluir la muestra 1/2 con ClNa 9 g/L y multiplicar el resultado final por 2.

Precisión:

	Intraserie (n=20)		Interserie (n=20)	
Media (mg/dL)	0,92	3,43	0,96	3,50
SD	0,03	0,07	0,04	0,09
CV (%)	2,76	1,90	3,97	2,51

Sensibilidad analítica: 1 mg/dL = 0,0407 ΔA/min.

Exactitud: Los reactivos de SPINREACT (y) no muestran diferencias sistemáticas significativas cuando se comparan con otros reactivos comerciales (x).

Los resultados obtenidos con 50 muestras fueron los siguientes:

Coeficiente de correlación $(r)^2$: 0,99584

Ecuación de la recta de regresión: y= 0,953x + 0,075

Las características del método pueden variar según el analizador utilizado.

SPINREACT

CE UREA-UV

Urea-UV

Ureasa -GLDH. Cinético UV

Determinación cuantitativa de urea
IVD

Conservar a 2-8°C

PRINCIPIO DEL METODO

La ureasa cataliza la hidrólisis de la urea, presente en la muestra, en amoniaco (NH_3) y anhídrido carbónico (CO_2).

El amoniaco formado se incorporan al α-cetoglutarato por acción de la glutamato deshidrogenasa (GLDH) con oxidación paralela de NADH a NAD^+:

$$\text{Urea} + H_2O + 2\,H^+ \xrightarrow{\text{Ureasa}} 2\,NH_3 + CO_2$$

$$2\,NH_3 + \alpha\text{-Cetoglutarato} + NADH \xrightarrow{\text{GLDH}} H_2O + NAD^+ + \text{L-Glutamato}$$

La disminución de la concentración de NAD^+ en el medio es proporcional a la concentración de urea de la muestra ensayada[1].

SIGNIFICADO CLINICO

La urea es el resultado final del metabolismo de las proteínas; se forma en el hígado a partir de su destrucción.

Puede aparecer la urea elevada en sangre (uremia) en dietas con exceso de proteínas, enfermedades renales, insuficiencia cardiaca, hemorragias gástricas, hipovolemia y obstrucciones renales [1,4,5].

El diagnóstico clínico debe realizarse teniendo en cuenta todos los datos clínicos y de laboratorio.

REACTIVOS

R 1 Tampón	TRIS pH 7,8	80 mmol/L
	α-Cetoglutarato	6 mmol/L
R 2 Enzimas	Ureasa	3750 U/L
	Glutamato deshidrogenasa (GLDH)	6000 U/L
	NADH	0,32 mmol/L
UREA CAL	Patrón primario acuoso de Urea	50 mg/dL

PREPARACION

Reactivo de trabajo (RT): Disolver (→) el contenido de un vial de R 2 Enzimas en un frasco de R 1 Tampón.

Tapar y mezclar suavemente hasta disolver su contenido.

Estabilidad: 6 semanas a 2-8°C o 7 días a 15-25°C.

CONSERVACION Y ESTABILIDAD

Todos los componentes del kit son estables, hasta la fecha de caducidad indicada en la etiqueta, cuando se mantienen los frascos bien cerrados a 2-8°C, protegidos de la luz y se evita su contaminación. No usar reactivos fuera de la fecha indicada.

Indicadores de deterioro de los reactivos:

- Presencia de partículas y turbidez.
- Absorbancia (A) del blanco a 340 nm < 1,00.

MATERIAL ADICIONAL

- Espectrofotómetro o analizador para lecturas a 340 nm.

CALCULOS

$$\frac{(A1\text{-}A2)\ \text{Muestra} - (A1\text{-}A2)\ \text{Blanco}}{(A1\text{-}A2)\ \text{Patrón} - (A1\text{-}A2)\ \text{Blanco}} \times 50\ (\text{Conc. Patrón}) = \text{mg/dL de urea en la muestra}$$

mg/dL urea x 0,466 = mg/dL de urea BUN (Blood Urea Nitrogen)[1]

Factor de conversión: mg/dL x 0,1665 = mmol/L.

CONTROL DE CALIDAD

Es conveniente analizar junto con las muestras sueros control valorados: SPINTROL H Normal y Patológico (Ref. 1002120 y 1002210).

Si los valores hallados se encuentran fuera del rango de tolerancia, revisar el instrumento, los reactivos y el calibrador.

Cada laboratorio debe disponer su propio Control de Calidad y establecer correcciones en el caso de que los controles no cumplan con las tolerancias.

VALORES DE REFERENCIA[1]

Suero: de 15 a 45 mg/dL (2,49-7,49 mmol/L)

Orina: de 20 a 35 gr/24 horas

Estos valores son orientativos. Es recomendable que cada laboratorio establezca sus propios valores de referencia.

CARACTERISTICAS DEL METODO

Rango de medida: Desde el *límite de detección* de 1,241 mg/dL hasta el *límite de linealidad* de 530 mg/dL.

Si la concentración es superior al límite de linealidad, diluir la muestra 1/2 con ClNa 9 g/L y multiplicar el resultado final por 2.

Precisión:

	Intraserie (n=20)		Interserie (n=20)	
Media (mg/dL)	40,7	130	40,5	128
SD	0,88	1,02	1,19	2,07
CV (%)	2,16	0,78	2,94	1,61

Sensibilidad analítica: 1 mg/dL = 0,00080 ΔA.

Exactitud: Los reactivos SPINREACT (y) no muestran diferencias sistemáticas significativas cuando se comparan con otros reactivos comerciales (x).

Los resultados obtenidos con 50 muestras fueron los siguientes:

Coeficiente de correlación (r)²: 0,998.

Ecuación de la recta de regresión: y= 1,5759x + 1,1577.

Las características del método pueden variar según el analizador utilizado.

INTERFERENCIAS

Como anticoagulante se recomienda la heparina. En ningún caso deben utilizarse sales de amonio o fluoruro[1].

Se han descrito varias drogas y otras substancias que interfieren en la determinación de la urea[2,3].

NOTAS

SPINREACT

CE URIC ACID

Ácido úrico

Uricasa -POD. Enzimático colorimétrico

Determinación cuantitativa de ácido úrico
IVD

Conservar a 2-8ºC

PRINCIPIO DEL MÉTODO

El ácido úrico es oxidado por la uricasa a alantoína y peróxido de hidrógeno ($2H_2O_2$) que en presencia de peroxidasa (POD), 4-aminofenazona (4-AF) y 2-4 Diclorofenol Sulfonato (DCPS) forma un compuesto rosáceo:

$$\text{Ácido úrico} + 2H_2O + O_2 \xrightarrow{\text{Uricasa}} \text{Alantoína} + CO_2 + 2H_2O_2$$

$$2H_2O_2 + \text{4-AF} + \text{DCPS} \xrightarrow{\text{POD}} \text{Quinonaimina} + 4H_2O$$

La intensidad de quinonaimina roja formada es proporcional a la concentración de ácido úrico presente en la muestra ensayada[1,2].

SIGNIFICADO CLÍNICO

El ácido úrico y sus sales son el producto final del metabolismo de las purinas. En una insuficiencia renal progresiva hay una retención en sangre de urea, creatinina y ácido úrico.
Niveles altos de ácido úrico son indicativos de patología renal y generalmente se asocia con la gota[1,3,4].
El diagnóstico clínico debe realizarse teniendo en cuenta todos los datos clínicos y de laboratorio.

REACTIVOS

R 1 Tampón	Fosfatos pH 7,4	50 mmol/L
	2-4 Diclorofenol Sulfonato (DCPS)	4 mmol/L
R 2 Enzimas	Uricasa	60 U/L
	Peroxidasa (POD)	660 U/L
	Ascorbato oxidasa	200 U/L
	4 - Aminofenazona (4-AF)	1 mmol/L
URIC ACID CAL	Patrón primario acuoso de Ácido úrico	6 mg/dL

PREPARACIÓN

Reactivo de trabajo (RT): Disolver (⇒) el contenido de un vial de R 2 Enzimas en un frasco de R 1 Tampón. Tapar y mezclar suavemente hasta disolver su contenido. Estabilidad: 1 mes en nevera (2-8ºC) o 10 días a temperatura ambiente.

CONSERVACIÓN Y ESTABILIDAD

Todos los componentes del kit son estables, hasta la fecha de caducidad indicada en la etiqueta, cuando se mantienen los frascos bien cerrados a 2-8ºC, protegidos de la luz y se evita su contaminación. No usar reactivos fuera de la fecha indicada.

Indicadores de deterioro de los reactivos:

- Presencia de partículas y turbidez.
- Absorbancia (A) del blanco a 520 nm ≥ 0,16.

MATERIAL ADICIONAL

- Espectrofotómetro o analizador para lecturas a 520 nm.
- Cubetas de 1 cm de paso de luz.

CÁLCULOS

Suero o plasma

$$\frac{\text{(A) Muestra - (A) Blanco}}{\text{(A) Patrón - (A) Blanco}} \times 6\ (\text{Conc. Patrón}) = \text{mg/dL de ácido úrico en la muestra}$$

Orina 24 h

$$\frac{\text{(A) Muestra - (A) Blanco}}{\text{(A) Patrón - (A) Blanco}} \times 6 \times \text{vol. (dL) orina/24h} = \text{mg/24 h de ácido úrico}$$

Factor de conversión: mg/dL x 59,5= µmol/L.

CONTROL DE CALIDAD

Es conveniente analizar junto con las muestras sueros control valorados: SPINTROL H Normal y Patológico (Ref. 1002120 y 1002210).
Si los valores hallados se encuentran fuera del rango de tolerancia, revisar el instrumento, los reactivos y el calibrador.
Cada laboratorio debe disponer su propio Control de Calidad y establecer correcciones en el caso de que los controles no cumplan con las tolerancias.

VALORES DE REFERENCIA[1]

Suero o plasma:

Mujeres	2,5 - 6,8 mg/dL	= 149 – 405 µmol/L
Hombres	3,6 - 7,7 mg/dL	= 214 – 458 µmol/L
Orina:	250 - 750 mg/24 h	= 1,49 - 4,5 mmol/24 h

Estos valores son orientativos. Es recomendable que cada laboratorio establezca sus propios valores de referencia.

CARACTERÍSTICAS DEL MÉTODO

Rango de medida: Desde el *límite de detección* de 0,00 mg/dL hasta el *límite de linealidad* de 40 mg/dL.
Si la concentración es superior al límite de linealidad, diluir la muestra 1/2 con NaCl 9 g/L y multiplicar el resultado final por 2.

Precisión:

	Intraserie (n=20)		Interserie (n=20)	
Media (mg/dL)	4,74	10,55	4,73	10,50
SD	0,02	0,03	0,13	0,29
CV (%)	0,50	0,30	2,67	2,77

Sensibilidad analítica: 1 mg/dL = 0,02930 A.
Exactitud: Los reactivos SPINREACT (y) no muestran diferencias sistemáticas significativas cuando se comparan con otros reactivos comerciales (x).
Los resultados obtenidos con 50 muestras fueron los siguientes:
Coeficiente de correlación (r^2): 0,97137.
Ecuación de la recta de regresión: y=1,162x + 0,14156.
Las características del método pueden variar según el analizador utilizado.

INTERFERENCIAS

No se han observado interferencias con bilirrubina hasta 170 µmol/L, hemoglobina hasta 130 mg/dL y ácido ascórbico hasta 570 µmol/L[2].
Se han descrito varias drogas y otras substancias que interfieren en la

CE CHOLESTEROL

Cholestérol

CHOD-POD. Enzymatique chlorimétrique

Détermination quantitative de cholestérol
IVD

Conserver à 2-8°C

PRINCIPE DE LA METHODE

Le cholestérol présent dans l'échantillon donne lieu à un composé coloré, suivant la réaction suivante:

$$\text{Cholestérol ester} + H_2O \xrightarrow{CHE} \text{Cholestérol} + \text{Acides gras}$$

$$\text{Cholestérol} + O_2 \xrightarrow{CHOD} \text{4-Cholestènone} + H_2O_2$$

$$2\,H_2O_2 + \text{Phénol} + \text{4-Aminophénazone} \xrightarrow{POD} \text{Quinonimine} + 4H_2O$$

L'intensité de la couleur formée est proportionnelle à la concentration de cholestérol présent dans l'échantillon testé[1, 2].

SIGNIFICATION CLINIQUE

Le cholestérol est une substance grasse présente dans toutes les cellules de l'organisme. Le foie produit naturellement tout le cholestérol dont il a besoin pour former les membranes cellulaires et pour produire certaines hormones. La détermination du cholestérol est l'un des outils les plus importants pour diagnostiquer et classifier les lipémies. L'augmentation du niveau de cholestérol est l'un des facteurs de risques cardiovasculaires possibles[5, 6].
Le diagnostic clinique doit tenir compte des données cliniques et de laboratoire.

REACTIFS

R 1 Tampon	PIPES pH 6,9 phénol	90 mmol/L 26 mmol/L
R 2 (Remarque 2) Enzymes	Cholestérol estérase (CHE) Cholestérol oxydase (CHOD) Peroxydase (POD) 4 - Aminophénazone (4-AF)	300 U/L 300 U/L 1250 U/L 0,4 mmol/L
CHOLESTEROL CAL	Patron primaire de détection du cholestérol 200 mg/dL. Contient Triton X-114 10-15%.	

PRÉCAUTIONS

CAL : H225- Liquide et vapeurs très inflammables. H318- Provoque des lésions oculaires graves. H412- Nocif pour les organismes aquatiques, entraîne des effets néfastes à long terme.
Suivez les conseils de prudence donnés en SDS et étiquette.

PREPARATION

Réactif de travail (RT): Dissoudre (→) le contenu d'une capsule d'enzymes R 2 dans un 1 flacon de tampon R 1.
Refermer et mélanger doucement jusqu'à ce que le contenu soit dissout

4. Mélanger et incuber pendant exactement 5 minutes à 37°C ou 10 min. at température ambiante.
5. Lire l'absorbation (A) du patron et l'échantillon, en comparaison avec le blanc du réactif. La couleur reste stable pendant au moins 60 minutes.

CALCULS

$$\frac{(A)\text{Échantillon} - (A)\text{Blanc}}{(A)\text{Etalon} - (A)\text{Blanc}} \times 200\ (\text{étalon conc.}) = \text{mg/dL de cholestérol dans l'échantillon}$$

Facteur de conversion: mg/dL x 0,0258= mmol/L.

CONTROLE DE QUALITE

Il est conseillé d'analyser conjointement les échantillons de sérum dont les valeurs ont été contrôlées: SPINTROL H Normal et pathologique (Réf. 1002120 et 1002210).
Si les valeurs se trouvent en dehors des valeurs tolérées, analyser l'instrument, les réactifs et le calibreur.
Chaque laboratoire doit disposer de son propre contrôle de qualité et déterminer les mesures correctives à mettre en place dans le cas où les vérifications ne correspondraient pas aux attentes.

VALEURS DE REFERENCE

Evaluation du risque[5, 6]:

Moins de 200 mg/dL	Normal
200-239 mg/dL	Modéré
≥ 240	Elevé

Ces valeurs sont données à titre d'information. Il est conseillé à chaque laboratoire de définir ses propres valeurs de référence.

CARACTERISTIQUES DE LA METHODE

Gamme de mesures: Depuis la limite de détection de 0 mg/dL jusqu'à la limite de linéarité de 900 mg/dL.
Si la concentration de l'échantillon est supérieure à la limite de linéarité, diluer 1/2 avec du ClNa 9 g/L et multiplier le résultat final par 2.
Précision:

	Intra-série (n=20)		Inter-série (n=20)	
Moyenne (mg/dL)	90,4	187	92,8	193
SD	1,15	1,01	1,98	2,39
CV (%)	1,27	0,54	2,14	1,24

Sensibilité analytique: 1 mg/dL = 0,00152 A.
Exactitude: Les réactifs SPINREACT (y) ne montrent pas de différences systématiques significatives lorsqu'on les compare à d'autres réactifs commerciaux (x).
Les résultats obtenus avec 50 échantillons ont été les suivants:
Coefficient de corrélation $(r)^2$: 0,99541.
Equation de la Coubre de régression: y=0,95293x – 3,020.
Les caractéristiques de la méthode peuvent varier suivant l'analyseur employé.

INTERFERENCES

Aucune interférence d'hémoglobine n'a été constaté jusqu'à 5 g/L et bilirubine

SPINREACT

CE TRIGLYCERIDES

Triglycérides

GPO-POD. Enzymatique colorimétrique

Détermination quantitative de triglycérides
IVD

Conserver à 2-8°C

PRINCIPE DE LA METHODE

Les triglycérides incubés avec de la lipoprotéinlipase (LPL) libèrent du glycérol et des acides gras libres. Le glycérol est phosphorilasé par du glycérophosphate déshydrogénase (GPO) et de l'ATP en présence de glycérol kinase (GK) pour produire du glycérol-3-phosphate (G3P) et de l'adénosine-5-di phosphate (ADP). Le G3P est alors transformé en dihydroxiacétone phosphate (DAP) et en peroxyde d'hydrogène (H_2O_2) par le GPO.

Au final, le peroxyde d'hydrogène (H_2O_2) réagit avec du 4-aminophénazone (4-AF) et du p-chlorophénol, réaction catalysée par la peroxydase (POD), ce qui donne une couleur rouge:

$$\text{Triglycérides} + H_2O \xrightarrow{LPL} \text{Glycérol} + \text{Acides gras libres}$$

$$\text{Glycérol} + \text{ATP} \xrightarrow{\text{Glycérolkinase}} \text{G3P} + \text{ADP}$$

$$\text{G3P} + O_2 \xrightarrow{GPO} \text{DAP} + H_2O_2$$

$$H_2O_2 + \text{4-AF} + \text{p-Chlorophénol} \xrightarrow{POD} \text{Quinone} + H_2O$$

L'intensité de la couleur formée est proportionnelle à la concentration de triglycérides présents dans l'échantillon testé [1,2,3].

SIGNIFICATION CLINIQUE

Les triglycérides sont des graisses qui fournissent à la cellule son énergie. Tout comme le cholestérol, ils sont transportés vers les cellules de l'organisme par les lipoprotéines du sang.

Un régime fort en graisses saturés ou en carbohydrates peut élever les niveaux de triglycérides.

Leur augmentation est relativement neutre. Diverses maladies, telles que certaines dysfonctions hépatiques (cirrhose, hépatite, obstruction biliaire) ou diabètes mellitus, peuvent être associées à des hausses de triglycérides [3 & 1].

Le diagnostique clinique doit tenir compte des données cliniques et de laboratoire.

REACTIFS

R 1 Tampon	GOOD pH 7,5 p-Chlorophénol	50 mmol/L 2 mmol/L
R 2 Enzymes	Lipoprotéine lipase (LPL) Glycérol kinase (GK) Glycérol-3-oxydase (GPO) Peroxydase(POD) 4 – Aminophénazone (4-AF) ATP	150000 U/L 500 U/L 2500 U/L 440 U/L 0,1 mmol/L 0,1 mmol/L
TRIGLYCERIDES CAL	Patron primaire de détection de triglycérides 200 mg/dL	

PREPARATION

Réactif de travail (RT): Dissoudre (→) le contenu d'une capsule d'enzymes R 2 et un flacon de tampon R 1.

Réf: 1001310 Réactif de travail (RT): Reconstituer (→) le contenu d'une capsule d'enzymes R 2 dans 40 mL de tampon R 1.

	Blanc	Modèle	Echantillon
RT (mL)	1,0	1,0	1,0
Modèle [Remarque 1, 2] (µL)	–	10	–
Echantillon (µL)	–	–	10

4. Mélanger et incuber 5 minutes a 37°C ou 10 min. à température ambiante.
5. Lire l'absorbation (A) du patron et l'échantillon, en comparaison avec le blanc du réactif. La couleur reste stable pendant au moins 30 minutes.

CALCULS

$$\frac{(A)\text{Echantillon}}{(A)\text{Modèle}} \times 200\ (\text{modèle conc.}) = \text{mg/dL de triglycéride dans l'échantillon}$$

Facteur de conversion: mg/dL x 0,0113 = mmol/L.

CONTROLE DE QUALITE

Il est conseillé d'analyser conjointement les échantillons de sérum dont les valeurs ont été contrôlées: SPINTROL H Normal et pathologique (Réf. 1002120 et 1002210).

Si les valeurs se trouvent en dehors des valeurs tolérées, analyser l'instrument, les réactifs et le calibreur.

Chaque laboratoire doit disposer de son propre contrôle de qualité et déterminer les mesures correctives à mettre en place dans le cas où les vérifications ne correspondraient pas aux attentes.

VALEURS DE REFERENCE

Hommes: 40 – 160 mg/dL
Femmes: 35 – 135 mg/dL

Ces valeurs sont données à titre d'information. Il est conseillé à chaque laboratoire de définir ses propres valeurs de référence.

CARACTERISTIQUES DE LA METHODE

Gamme de mesures: Depuis la limite de détection de 0,000 mg/dL jusqu'à la limite de linéarité de 2200 mg/dL.

Si la concentration de l'échantillon est supérieure à la limite de linéarité, diluer 1/2 avec du ClNa 9 g/L et multiplier le résultat final par 2.

Précision:

	Intra-série (n=20)		Inter-série (n=20)	
Moyenne (mg/dL)	103	219	103	217
SD	0,41	0,93	3,74	7,80
CV (%)	0,39	0,43	3,62	3,59

Sensibilité analytique: 1 mg/dL = 0,00137 A.

Exactitude: Les réactifs SPINREACT (y) ne montrent pas de différences systématiques significatives lorsqu'on les compare à d'autres réactifs commerciaux (x).

Les résultats obtenus avec 50 échantillons ont été les suivants:

Coefficient de corrélation (r): 0,99760.

Equation de la Coubre de régression: y=0,905x +10,77.

Les caractéristiques de la méthode peuvent varier suivant l'analyseur employé.

INTERFERENCES

Aucune interférence n'a été relevée avec bilirubine jusqu'à 170 µmol/L et hémoglobine jusqu'à 10 g/L [2].

Différentes drogues ont été décrites ainsi que d'autres substances qui peuvent interférer lors de la détermination de la triglycérides [4,5].

SPINREACT

CE CALCIUM-A III

Calcium

Arsénazo III. colorimétrique

Détermination quantitative de calcium
IVD

Conserver à 2-8°C

PRINCIPE DE LA METHODE

Le calcium, en milieu neutre, forme un complexe de couleur bleu avec l'arsénazo III (acide 1,8-dihidroxi-3,6-disulfo-2,7-naftalenen-bis (azo)-dibenzénarsonique).
L'intensité de couleur est directement proportionnelle à la quantité de calcium présent dans l'échantillon testé[1, 2,3].

SIGNIFICATION CLINIQUE

Le calcium est le minéral le plus abondant et le plus important du corps humain. Il est présent à 99 % dans les os.
Une réduction des niveaux d'albumine provoque une réduction du calcium dans le sérum. Des niveaux bas de calcium peuvent être dus à un hypoparatiroïdisme, à un pseudohypoparatiroïdisme, à un déficit de vitamine D, à de la malnutrition ou à un problème d'absorption.
La majorité des causes d'hypercalcémie sont dues à des maladies oncologiques, à des intoxications par la vitamine D, à une augmentation de la rétention rénale, à une ostéoporose, à une sarcoïdose, à une tirotoxicose et à un hyperparatiroïdisme[1,6,7].
Le diagnostic doit prendre en compte les données cliniques et de laboratoire.

REACTIFS

R Arsénazo III	Tampon imidazole pH 6,5 Arsénazo III	100 mmol/L 120 mmol/L
CALCIUM CAL	Patron primaire de détection	10 mg/dL

PREPARATION

Le réactif et le modèle sont prêts à l'emploi.

CONSERVATION ET STABILITE

Tous les composants du kit sont stables jusqu'à la date de péremption indiquée sur l'étiquette du flacon, et si les flacons sont maintenus hermétiquement fermés à 2-8°C, à l'abri de la lumière et des sources de contamination. Ne pas utiliser les réactifs en dehors de la date indiquée.
Indices de détérioration des réactifs:

- Présence de particules et turbidité.
- Absorbation (A) du blanc à 650 nm ≥ 0,50.

MATERIEL SUPPLEMENTAIRE

- Spectrophotomètre ou analyseur pour les lectures à 650 nm.
- Cuvettes de 1,0 cm d'éclairage.
- Equipement classique de laboratoire (Remarque 2,3).

ECHANTILLONS

- Sérum ou plasma[1]: Séparé dès que possible des hématies. Ne pas

Urine 24 h $\frac{(A)\text{Échantillon} - (A)\text{Blanc}}{(A)\text{Étalon} - (A)\text{Blanc}}$ x 10 x vol. (dL) urine/24h = mg/24 h de calcium

Facteur de conversion: mg/dL x 0,25= mmol/L.

CONTROLE DE QUALITE

Il est conseillé d'analyser conjointement les échantillons de sérum dont les valeurs ont été contrôlées: SPINTROL H Normal et pathologique (Réf. 1002120 et 1002210).
Si les valeurs se trouvent en dehors des valeurs tolérées, analyser l'instrument, le réactif et le matériel d'étalonnage.
Chaque laboratoire doit disposer de son propre contrôle de qualité et déterminer les mesures correctives à mettre en place dans le cas où les vérifications ne correspondraient pas aux attentes.

VALEURS DE REFERENCE[1]

Sérum ou plasma:		
Adultes	8,5-10,5 mg /dL	≅ 2,1-2,6 mmol/L
Enfants	10-12 mg/dL	≅ 2,5-3,0 mmol/L
Nouveau-nées	8-13 mg/dL	≅ 2,00-3,25 mmol/L
Urine:		
Adultes	50-300 mg/24 h	≅ 1,25-7,50 mmol/24 h
Enfants	80-160 mg/24 h	≅ 2-4 mmol/24 h

Ces valeurs sont données à titre d'information. Il est conseillé à chaque laboratoire de définir ses propres valeurs de référence.

CARACTERISTIQUES DE LA METHODE

Gamme de mesures: Depuis la *limite de détection* de 0,026 mg/dL jusqu'à la *limite de linéarité* de 32 mg/dL.
Si la concentration de l'échantillon est supérieure à la limite de linéarité, diluer 1/2 avec du ClNa 9 g/L et multiplier le résultat final par 2.
Précision:

	Intra-série (n=20)		Inter-série (n=20)	
Moyenne (mg/dL)	8,35	14,28	8,58	14,57
SD	0,08	0,08	0,19	0,34
CV (%)	0,95	0,59	2,24	2,31

Sensibilité analytique: 1 mg/dL = 0,0316 A.
Exactitude: Les réactifs SPINREACT (y) ne montrent pas de différences systématiques significatives lorsqu'on les compare à d'autres réactifs commerciaux (x).
Les résultats obtenus avec 50 échantillons ont été les suivants:
Coefficient de corrélation (r): 0,9506.
Equation de la Coubre de régression: y=0,8944x + 1,3421.
Les caractéristiques de la méthode peuvent varier suivant l'analyseur employé.

INTERFERENCES

Triglycérides ≤1,25 g/L, n'interfèrent pas[1].
Différentes drogues ont été décrites ainsi que d'autres substances qui interfèrent dans la détermination du calcium[4, 5].

SPINREACT

CE ALBUMIN

Albumine

Vert de bromocrésol. Colorimétrique

Détermination quantitative de l'albumine
IVD

Conserver à 2-8°C

PRINCIPE DE LA METHODE

L'albumine se combine au vert de bromocrésol, à pH légèrement acide, entraînant un changement de couleur de l'indice, passant du jaune-vert au vert-bleuté, et proportionnel à la concentration d'albumine présente dans l'échantillon testé[1, 2, 3, 4].

SIGNIFICATION CLINIQUE

L'albumine est l'une des protéines plasmatiques les plus importantes produite par le foie.
Parmi ses multiples fonctions, on retiendra la nutrition, l'entretien de la pression oncotique et le transport des substances telles que la Ca^{++}, la bilirubine, les acides gras, les drogues et les stéroïdes.
Des perturbations dans les valeurs de l'albumine signalent des maladies du foie, une malnutrition, des lésions de la peau telles que de la dermatite, des brûlures importantes ou une déhydratation[1, 7,8].
Le diagnostic clinique doit tenir compte des données cliniques et des données de laboratoire.

REACTIFS

R	Vert de bromocrésol pH 4,2	0,12 mmol/L
ALBUMINE CAL	Étalon primaire de détection de l'albumine 5 g/dL	

PREPARATION

Le réactif et le étalon sont prêts à l'emploi.

CONSERVATION ET STABILITE

Tous les composants du kit sont stables jusqu'à la date de péremption indiquée sur l'étiquette du flacon, et si les flacons sont maintenus hermétiquement fermés à 2-8°C, à l'abri de la lumière et des sources de contamination. Ne pas utiliser les réactifs en dehors de la date indiquée.
Indices de détérioration des réactifs:

- Présence de particules et turbidité.
- Absorbation du blanc à 630 nm $\geq$ 0,40.

MATERIEL SUPPLEMENTAIRE

- Spectrophotomètre ou analyseur pour les lectures à 630 nm.
- Cuvettes de 1,0 cm d'éclairage.
- Equipement classique de laboratoire.

ECHANTILLONS

Sérum ou plasma sans hemolysis[1]: Stabilité 1 mois à 2-8°C ou 1 semaine à 15-25°C.

CONTROLE DE QUALITE

Il est conseillé d'analyser conjointement les échantillons de sérum dont les valeurs ont été contrôlées: SPINTROL H Normal et pathologique (Réf. 1002120 et 1002210).
Si les valeurs se trouvent en dehors des valeurs tolérées, analyser l'instrument, les réactifs et le calibreur.
Chaque laboratoire doit disposer de son propre contrôle de qualité et déterminer les mesures correctives à mettre en place dans le cas où les vérifications ne correspondraient pas aux attentes.

VALEURS DE REFERENCE

3,5 à 5,0 g/dL[1].
Ces valeurs sont données à titre d'information. Il est conseillé à chaque laboratoire de définir ses propres valeurs de référence.

CARACTERISTIQUES DE LA METHODE

Gamme de mesures: Depuis la limite de détection de 0,0349 mg/dL jusqu'à la limite de linéarité de 6 mg/dL.
Si la concentration de l'échantillon est supérieure à la limite de linéarité, diluer 1/2 avec du ClNa 9 g/L et multiplier le résultat final par 2.
Précision:

	Intra-série (n= 20)		Inter-série (n= 20)	
Moyenne (g/dL)	4,17	2,84	4,56	3,07
SD	0,02	0,01	0,28	0,18
CV (%)	0,42	0,53	6,20	5,90

Sensibilité analytique: 1 g/dL = 0,2003 A.
Exactitude: Les réactifs SPINREACT (y) ne montrent pas de différences systématiques significatives lorsqu'on les compare à d'autres réactifs commerciaux (x).
Les résultats obtenus avec 50 échantillons ont été les suivants:
Coefficient de corrélation $(r)^2$: 0,99169.
Equation de la Coubre de régression: y=1,045x – 0,028.
Les caractéristiques de la méthode peuvent varier suivant l'analyseur employé.

INTERFERENCES

La bilirubine jusqu'à 110 mg/L, l'hémoglobine jusqu'à 1 g/L et a lipémie jusqu'à 10 g/L, interfèrent [1,4].
Différentes drogues ont été décrites ainsi que d'autres substances qui interfèrent dans la détermination de l'albumine[5, 6].

REMARQUES

1. ALBUMINE CAL: Etant donné la nature du produit, il est conseillé de le manipuler avec précaution. En effet, il peut être facilement contaminé.
2. Le calibrage au moyen du patron de détection peut donner lieu à des erreurs systématiques lors de méthodes automatiques. Dans de tels cas, il est conseillé d'utiliser des calibrages sériques
3. Utiliser des embouts de pipettes jetables propres pour diffuser le produit.
4. **SPINREACT dispose de consignes détaillées pour l'application de ce réactif dans différents analyseurs.**

SPINREACT

CE GPT (ALT)-LQ

GPT (ALT)

NADH. Cinétique UV. IFCC rec. liquide

Détermination quantitative d'alanine amino transférase GPT (ALT)
IVD

Conserver à 2-8°C

PRINCIPE DE LA METHODE

L'alanine amino transférase (ALT) initialement appelée transaminase glutamique pyruvique (GPT) catalyse le transfert réversible d'un groupe animique d'alanine vers l'alpha-cétoglutarate à formation de glutamate et de pyruvate. Le pyruvate produit est réduit en lactate en présence de lactate déshydrogénase (LDH) et NADH:

$$\text{Alanine} + \alpha\text{-Cétoglutarate} \xrightarrow{\text{ALT}} \text{Glutamate} + \text{Pyruvate}$$

$$\text{Pyruvate} + \text{NADH} + \text{H}^+ \xrightarrow{\text{LDH}} \text{Lactate} + \text{NAD}^+$$

La vitesse de réduction de la concentration en NADH au centre, déterminée photométriquement, est proportionnelle à la concentration catalytique d'ALT dans l'échantillon[1].

SIGNIFICATION CLINIQUE

L'ALT est une enzyme intracellulaire, qui se trouve principalement dans les cellules du foie et des reins.
Son meilleur avantage est le diagnostic de maladies du foie.
On l'observe en grandes quantités dans le cadre de maladies hépatiques, telles que l'hépatite, les maladies du muscles et des infarctus du cœur, étant donné que la valeur de l'ALT reste dans les limites standards et augmente dans les niveaux de AST[1, 4, 3].
La diagnostique clinique doit être réalisée en prenant en compte les données cliniques et de laboratoire.

REACTIFS

R 1 Tampon	TRIS pH 7,8 Lactate déshydrogénase (LDH) L-Alanine	100 mmol/L 1200 U/L 500 mmol/L
R 2 Substrats	NADH α-Cétoglutarate	0,18 mmol/L 15 mmol/L

PRECAUTIONS

R1 : H290- Peut être corrosif pour les métaux.
Suivez les conseils de prudence donnés en SDS et étiquette.

PREPARATION

Réactif de travail (RT):
Mélanger: 1 vol. de (R2) Substrats + 4 vol. (R1) Tampon.
Stabilité: 21 jours à 2-8°C ou 72 heures à température ambiante (15-25°C).

CONSERVATION ET STABILITE

Tous les composants du kit sont stables jusqu'à la date de péremption indiquée sur l'étiquette, et si les flacons sont maintenus hermétiquement fermés à 2-8°C, à l'abri de la lumière et des sources de contamination. Ne pas utiliser les réactifs en dehors de la date indiquée.
Indices de détérioration des réactifs:
- Présence de particules et turbidité.

CALCULS

ΔA/min x 1750 = U/L d'ALT

Unités: L'unité internationale (UI) correspond à la quantité d'enzymes qui converti 1 µmol de substrats par minute, dans des conditions standard. La concentration est exprimée en unité/litre (U/L).

Facteurs de conversion de températures
Les résultats peuvent se transformer à d'autres températures, en multipliant par:

Température de mesure	Facteur de conversion à		
	25°C	30°C	37°C
25°C	1,00	1,32	1,82
30°C	0,76	1,00	1,39
37°C	0,55	0,72	1,00

CONTROLE DE QUALITE

Il est conseillé d'analyser conjointement les échantillons de sérum dont les valeurs ont été contrôlées: SPINTROL H Normal et pathologique (Réf. 1002120 et 1002210).
Si les valeurs se trouvent en dehors des valeurs tolérées, analyser l'instrument, les réactifs et le calibreur.
Chaque laboratoire doit disposer de son propre contrôle de qualité et déterminer les mesures correctives à mettre en place dans le cas où les vérifications ne correspondraient pas aux attentes.

VALEURS DE REFERENCE[4, 5]

	25°C	30°C	37°C
Hommes	Jusqu'à 22 U/L	29 U/L	40 U/L
Femmes	Jusqu'à 18 U/L	22 U/L	32 U/L

Chez les nouveau-nés en bon état de santé, on a détecté des valeurs presque doublés par rapport à celle relevées chez les adultes, état donné leur maturité hépatique, ces valeurs redeviennent normales dans les trois mois.
Ces valeurs sont données à titre d'information. Il est conseillé à chaque laboratoire de définir ses propres valeurs de référence.

CARACTERISTIQUES DE LA METHODE

Gamme de mesures: Depuis la *limite de détection* de 0 U/L, jusqu'à la *limite de linéarité* de 400 U/L.
Si la concentration de l'échantillon est supérieure à la limite de linéarité, diluer 1/10 avec du ClNa 9 g/L et multiplier le résultat final par 10.
Précision:

	Intra-série (n= 20)		Inter-série (n= 20)	
Moyenne (U/L)	42,0	116	41,1	115
SD	0,47	0,42	0,76	1,61
CV (%)	1,11	0,36	1,85	1,40

Sensibilité analytique: 1 U/L = 0,00052 *ΔA /min*
Exactitude: Les réactifs SPINREACT (y) ne montrent pas de différences systématiques significatives lorsqu'on les compare à d'autres réactifs commerciaux (x).
Les résultats obtenus avec 50 échantillons ont été les suivants:
Coefficient de corrélation $(r)^2$: 0,99597.
Equation de la Coubre de régression: y=1,1209x + 1,390.
Les caractéristiques de la méthode peuvent varier suivant l'analyseur employé

SPINREACT

CE GOT (AST)

GOT (AST)

NADH. Cinétique UV. IFCC rec.

Détermination quantitative d'aspartate amino transférase
GOT (AST)
IVD

Conserver à 2-8°C

PRINCIPE DE LA METHODE

L'aspartate amino transférase (AST), initialement appelée transaminase glutamate oxaloacétique (GOT) catalyse le transfert réversible d'un groupe animique de l'aspartate vers l'alpha-cétoglutarate à formation de glutamate et d'oxalacétate. L'oxalacétate produit est réduit en malate en présence de déshydrogénées (MDH) et NADH:

$$\text{Aspartate} + \alpha\text{-Cétoglutarate} \xrightarrow{\text{AST}} \text{Glutamate} + \text{Oxalacétate}$$

$$\text{Oxalacétate} + \text{NADH} + \text{H}^+ \xrightarrow{\text{MDH}} \text{Malate} + \text{NAD}^+$$

La vitesse de réduction de la concentration en NADH au centre, déterminée photo numériquement, est proportionnelle à la concentration catalytique d'AST dans l'échantillon[1].

SIGNIFICATION CLINIQUE

L'AST est une enzyme intracellulaire, qui se trouve en grandes quantités dans les muscles du cœur, les cellules du foie, les cellules du muscle squelettique et en plus faibles quantités dans les autres tissus.
Bien qu'un niveau élevé d'AST dans le sérum ne soit pas caractéristique d'une maladie hépatique, elle s'emploie principalement pour les diagnostics et le suivi, avec d'autres enzymes telles que l'ALT et l'ALP. Elle s'utilise également dans le cadre du contrôle post-infarctus, chez les patients souffrant de troubles musculaires du squelette et dans certains autres cas[1-4,5].

Le diagnostic clinique doit être réalisé en prenant en compte les données cliniques et les données de laboratoire.

REACTIFS

R 1 Tampon	TRIS pH 7,8	80 mmol/L
	L-aspartate	200 mmol/L
R 2 Substrats	NADH	0,18 mmol/L
	Lactate déshydrogéné (LDH)	800 U/L
	Malate déshydrogénisé (MDH)	600 U/L
	α-cétoglutarate	12 mmol/L

PREPARATION

Réactif de travail (RT):
Réf: 1001160 Dissoudre (→) une tablette de substrats R2 dans une dose (ampoule) R1.
Réf: 1001161 Dissoudre (→) une tablette de substrats R2 dans 15 mL de R1.
Réf: 1001162 Dissoudre (→) une tablette de substrats de R2 dans 50 mL de R1.
Refermer et mélanger doucement, jusqu'à ce que le contenu soit totalement dissout.
Stabilité: 21 jours à 2-8°C ou 72 heures à température ambiante (15-25°C).

CONSERVATION ET STABILITE

5. Lire l'absorbation (A) initiale de l'échantillon, mettre en route le chronomètre et lire l'absorbation à chaque minute pendant 3 minutes.
6. Calculer la moyenne de l'augmentation d'absorbation par minute (ΔA/min).

CALCULS

ΔA/min x 1750 = U/L de AST

Unités: L'unité internationale (UI) correspond à la quantité d'enzymes qui converti 1 µmol de substrats par minute, dans des conditions standard. La concentration est exprimée en unité/litre (U/L).

Facteurs de conversion de températures

Les résultats peuvent se transformer à d'autres températures, en multipliant par:

Température de mesure	Facteur de conversion à		
	25°C	30°C	37°C
25°C	1,00	1,37	2,08
30°C	0,73	1,00	1,54
37°C	0,48	0,65	1,00

CONTROLE DE QUALITE

Il est conseillé d'analyser conjointement les échantillons de sérum dont les valeurs ont été contrôlées: SPINTROL H Normal et pathologique (Réf. 1002120 et 1002210).
Si les valeurs se trouvent en dehors des valeurs tolérées, analyser l'instrument, les réactifs et le calibreur.
Chaque laboratoire doit disposer de son propre contrôle de qualité et déterminer les mesures correctives à mettre en place dans le cas où les vérifications ne correspondraient pas aux attentes.

VALEURS DE REFERENCE[1]

	25°C	30°C	37°C
Hommes	Jusqu'à 19 U/L	26 U/L	38 U/L
Femmes	Jusqu'à 16 U/L	22 U/L	31 U/L

Ces valeurs sont données à titre d'information. Il est conseillé à chaque laboratoire de définir ses propres valeurs de référence.

CARACTERISTIQUES DE LA METHODE

Gamme de mesures: Depuis la limite de détection 0 U/L jusqu'à la limite de linéarité 360 U/L.
Si la concentration de l'échantillon est supérieure à la limite de linéarité diluer 1/10 avec du ClNa 9 g/L et multiplier le résultat final par 10.

Précision:

	Intra-série (n= 20)		Inter-série (n= 20)	
Moyenne (U/L)	55,5	165	55,0	162
SD	1,30	3,44	0,92	2,52
CV (%)	2,35	2,07	1,68	1,55

Sensibilité analytique: 1 U/L = 0,00051 ΔA /min
Exactitude: Les réactifs SPINREACT (y) ne montrent pas de différences systématiques significatives lorsqu'on les compare à d'autres réactifs commerciaux (x).
Les résultats obtenus avec 50 échantillons ont été les suivants:
Coefficient de corrélation $(r)^2$: 0,98277.
Equation de la Coubre de régression: y= 0,9259x - 5,1685.
Les caractéristiques de la méthode peuvent varier suivant l'analyseur employé.

SPINREACT

CE LDH

LDH

Piruvato. Cinética UV. DGKC

Determinación cuantitativa de lactato deshidrogenasa (LDH)
IVD

Conservar a 2-8ºC

PRINCIPIO DEL MÉTODO

La lactato deshidrogenasa (LDH) cataliza la reducción del piruvato por el NADH, según la siguiente reacción:

$$\text{Piruvato} + \text{NADH} + \text{H}^+ \xrightarrow{\text{LDH}} \text{L-lactato} + \text{NAD}^+$$

La velocidad de disminución de la concentración de NADH en el medio determinado fotometricamente, es proporcional a la concentración catalítica de LDH en la muestra ensayada[1].

SIGNIFICADO CLÍNICO

La lactato deshidrogenasa (LDH) es una enzima, distribuida por todo el organismo humano. Las mayores concentraciones de LDH se encuentran en el hígado, corazón, riñón, músculo esquelético y eritrocitos.

El nivel de LDH en suero esta elevado en pacientes con enfermedades del hígado, infartos de miocardio, alteraciones renales, distrofias musculares y anemias[1,4,5].

El diagnostico clínico debe realizarse teniendo en cuenta todos los datos clínicos y de laboratorio.

REACTIVOS

R 1 Tampón	Imidazol Piruvato	65 mmol/L 0,6 mmol/L
R 2 Substrato	NADH	0,18 mmol/L

PRECAUCIONES

R1: H360-Puede perjudicar la fertilidad o dañar al feto.
Seguir los consejos de prudencia indicados en la FDS y etiqueta del producto.

PREPARACIÓN

Reactivo de trabajo (RT):
Disolver (→) 1 comprimido de R2 en un vial de R1.
Tapar y mezclar suavemente hasta disolver su contenido.
Estabilidad: 2 días a 2-8ºC o 12 horas a temperatura ambiente (15-25ºC).

CONSERVACIÓN Y ESTABILIDAD

Todos los componentes del kit son estables, hasta la fecha de caducidad indicada en la etiqueta, cuando se mantienen los frascos bien cerrados a 2-8ºC, protegidos de la luz y se evita su contaminación.
No usar las tabletas si aparecen fragmentadas.
No usar reactivos fuera de la fecha indicada.
Indicadores de deterioro de los reactivos:
- Presencia de partículas y turbidez.

6. Calcular el promedio del incremento de absorbancia por minuto (ΔA/min).

CÁLCULOS

25º- 30ºC ΔA/min x 4925 = U/L LDH

37ºC ΔA/min x 9690 = U/L LDH

Unidades: La unidad internacional (UI) es la cantidad de enzima que convierte 1 µmol de substrato por minuto, en condiciones estándar. La concentración se expresa en unidades por litro (U/L).

Factores de conversión de temperaturas
Los resultados pueden transformarse a otras temperaturas multiplicando por:

Temperatura de medición	Factor par a convertir a		
	25ºC	30ºC	37ºC
25ºC	1,00	1,33	1,92
30ºC	0,75	1,00	1,43
37ºC	0,52	0,70	1,00

CONTROL DE CALIDAD

Es conveniente analizar junto con las muestras sueros control valorados: SPINTROL H Normal y Patológico (Ref. 1002120 y 1002210).
Si los valores hallados se encuentran fuera del rango de tolerancia, se debe revisar el instrumento, los reactivos y la técnica.
Cada laboratorio debe disponer su propio Control de Calidad y establecer correcciones en el caso de que los controles no cumplan con las tolerancias.

VALORES DE REFERENCIA[1]

25ºC	30ºC	37ºC
120-240 U/L	160-320 U/L	230-460 U/L

Estos valores son orientativos. Es recomendable que cada laboratorio establezca sus propios valores de referencia.

CARACTERÍSTICAS DEL MÉTODO

Rango de medida: Desde el límite de detección 2 U/L hasta el *límite de linealidad* 1500 U/L.
Si la concentración de la muestra es superior al límite de linealidad, diluir 1/10 con ClNa 9 g/L y multiplicar el resultado final por 10.
Precisión:

	Intraserie (n= 20)		Interserie (n= 20)	
Media (U/L)	388	731	402	757
SD	7,44	12,49	12,45	16,96
CV (%)	1,92	1,71	3,10	2,24

Sensibilidad analítica: 1 U/L = 0,00010 ΔA/min.
Exactitud: Los reactivos SPINREACT (y) no muestran diferencias sistemáticas significativas cuando se comparan con otros reactivos comerciales (x).
Los resultados obtenidos con 50 muestras fueron los siguientes:
Coeficiente de regresión $(r)^2$: 0,987.

Abstract

In this context, The main objective of this work is to green synthesis of AgNPs from *H.lippii* aqueous extract and to evaluate the biological effects of *H.lippii* plant and silver nanoparticles *in vitro* and as well as *in vivo* in order to look into their potential therapeutic effects against the physiological and biochemical changes brought on by sub-chronic exposure to cadmium chloride in rats. For this purpose, quantitative, qualitative, and extraction bioactive compounds standard procedures were applied. While identification and quantification of individual phenolic compounds were performed by HPLC analysis. On the other hand, has been of AgNPs green synthesis and characterization by different methods (UV, FTIR, XRD, and SEM). In addition, *in vitro* activities Evaluation has been done via antioxidant, anti-inflammatory, Hemolytic, and antibacterial activities, Meanwhile, Spectrophotometric, Voltammetric studies of the binding interaction of AgNPs with deoxyribonucleic acid and bovine serum albumin under similar condition. In regards to studying in vivo, 35 Wistar male rats were divided into seven groups (5 rats in each): Control, *H.lippii*, $CdCl_2$, $CdCl_2$+*H.lippii*, AgNPs, $CdCl_2$+AgNPs, and $CdCl_2$+*H.lippii*+AgNPs. $CdCl_2$ (50mg/Kg) was added in drinking water for 35 day. The therapeutic systems were received intragastrically for *H.lippii* (100 mg/kg b.w) and AgNPs were supplemented intraperitoneally at 0.1mg/kg for the last 15 days. Some biochemical, hematological, oxidative stress markers and histopathology were observed

The phytochemical analysis revealed the presence of most of the phenolic compounds, Further, *H. lippii* had high levels of total phenolics (183.12±2.84mg GA eq/g dry Ex) and flavonoid contents (72.00±1.03 mg QE/mg Ex), as well as saponins (82.2± 33.00 mg DO eq/g dry Ex), and of tannins (Total hydrolyzable tannin; 2.818±0.138mgTA eq/g dry Ex, Condensed tannin; (5.88±1.58 mg Ca eq/g dry Ex) and anthocyanins (4.256±0.590 mg C-3-GE/g dry Ex). HPLC analysis identified six phenolic compounds in high concentration, mainly gallic acid and chlorogenic acid. According to, the absorption peak at 428 nm characterized the synthesized silver nanoparticles, the crystalline nature of AgNP was confirmed by XRD patterns, and SEM analysis revealed that the majority of the nanoparticles were spherical in shape. While investigations using FT-IR technique confirmed the presence of many functional groups that are involved in covering and reducing AgNPs. In addition, *H.lippii* and AgNPs demonstrated strong efficiency as antioxidant, and anti-inflammatory, while providing moderate protection for red blood cells. On the other hand, they showed good antibacterial activity against six types of selected bacteria. Moreover, the results show that there is a spontaneous interaction between AgNPs and DNA as well as BSA via electrostatic interactions, translated by parameters K and ΔG. On the other hand, according to the results obtained *in vivo*, there was a decrease in the body weight gain. An increase in the relative weight of the liver, kidneys, heart and brain, with a decrease in the absolute and relative weight of the testicle. Moreover, the findings in cadmium chloride-treated rats induced significant changes in hematological and biochemical, hormonal parameters, hepatic enzyme markers, and renal function compared to the control group. These changes were accompanied by a decrease in antioxidant defense (GSH, SOD, and CAT) and an increase in MDA levels. The data clearly showed the deterioration of the structure of the studied tissues in comparison with the control group, including severe deterioration of liver and kidney cells, while testicular tissues showed severe necrosis. However, the treatment with *H.lippii* and/or AgNPs mitigated most of toxic effects and the restored all previous variable parameters.

In conclusion, this study demonstrated the promising biological activity of *H.lippii* and AgNPs, Meanwhile, it is worth noting the strong therapeutic potential of *H.lippii* and AgNPs against cadmium chloride-induced toxicity in rats, which opens new avenues for the use of phytotherapy and nanotherapy and enhances their application in approaches medical.

Keywords: *Helianthemum lippii*, silver nanoparticles, green synthesis, biological activities, cadmium chloride.

الملخص

في هذا السياق ، الهدف الرئيسي من هذا العمل هو تخليق الأخضر لجسيمات الفضة النانوية من مستخلص السمهري وتقييم الآثار البيولوجية لنبات السمهري وجسيمات الفضة النانوية في المختبر وكذلك في الجسم الحي من أجل النظر في التأثيرات العلاجية المحتملة ضد التغيرات الفسيولوجية والكيميائية الحيوية الناجمة عن التعرض شبه المزمن لكلوريد الكادميوم في الفئران. لهذا الغرض ، تم تطبيق الإجراءات القياسية الكمية والنوعية واستخراج المركبات النشطة بيولوجيا. بينما تم إجراء تحديد وتقدير المركبات الفينولية الفردية عن طريق تحليل HPLC. من ناحية أخرى ، تم التوليف الأخضر وتوصيف AgNPs بطرق مختلفة (UV و FTIR و XRD و SEM). بالإضافة إلى ذلك ، تم تقييم النشاط في المختبر عن طريق مضادات الأكسدة ، ومضادات الالتهاب ، وانحلال الدم ، ومضاد البكتيريا ، وفي الوقت نفسه ، دراسات قياس الطيف الضوئي ، الفولتميترية للتفاعل الملزم لـ AgNPs مع الحمض النووي المنقوص الاوكسجين وألبومين المصل البقري تحت ظروف مماثلة.

بالنسبة للدراسة في الجسم الحي، تم تقسيم 35 جرذًا من الجرذان البيضاء إلى سبع مجموعات من 5 فئران لكل منها: الشاهد، *H.lippi*، $CdCl_2$، $CdCl_2$ + *H.lippii* ، AgNPs، $CdCl_2$+AgNPs ، و $CdCl_2$+*H.lippii*+AgNPs. تمت إضافة كلوريد الكادميوم (50 ملغ/ كلغ) في ماء الشرب لمدة 5 أسابيع. تم تلقي الأنظمة العلاجية (100 ملغ/كغ من وزن الجسم) داخل المعدة من السمهري وتم استعمال الجسيمات الفضة النانوية داخل الصفاق بجرعة(0.1 ملغ/ كلغ) خلال آخر 15 يومًا. تم تحديد بعض مؤشرات الإجهاد الكيميائي الحيوي، الدموي، والاجهاد التأكسدي. كما تمت الملاحظة المجهرية للانسجة من الكبد الكلى والخصية

أظهر التحليل الكيميائي النباتي وجود معظم المركبات الفينولية ، علاوة على ذلك ، كان لدى السمهري مستويات عالية من إجمالي الفينولات (183.12 ± 2.84 ملغ مكافئ حمض الغاليك/ غ من المادة الجافة) ومحتويات الفلافونويد (72.00 ± 1.03 ملغ مكافئ من الكيرسيتين / غ من المادة الجافة) ، بالإضافة إلى الصابونين (82.2 ± 33.00 ملغ DO مكافئ /غ من المادة الجافة) ، ومستويات منخفضة من التانين (إجمالي التانين المتحلل بالماء ؛ 2.818 ± 0.138 ملغ مكافئ لحمض التانيك/ غ من المادة الجافة ، مكثف التانين ؛ (5.88 ± 1.58ملغ مكافئ كاتيشين / غ من المادة الجافة) والأنثوسيانين (4.256 ± 0.590 ملغ مكافئ من سيانيدين 3 جلوكوزيد C-3-GE /غ من المادة الجافة) . فيما حدد تحليل HPLC ستة مركبات فينولية بتركيز مرتفع، خاصة حمض الجاليك وحمض الكلوروجينيك. بينما تميزت الجسيمات النانوية الفضية المركبة بذروة الامتصاص عند 428 نانومتر، تم تأكيد الطبيعة البلورية لـ AgNP بواسطة أنماط XRD، وكشف تحليل SEM أن غالبية الجسيمات النانوية كانت كروية الشكل. بينما أكدت التحقيقات باستخدام تقنية FT-IR وجود العديد من المجموعات الوظيفية التي تشارك في تغطية وتقليل AgNPs. بالإضافة إلى ذلك، أوضح السمهري و جسيمات الفضة النانوية فعالية قوية كمضاد للأكسدة، ومضاد للالتهابات، بينما يوفر حماية معتدلة لخلايا الدم الحمراء. من ناحية أخرى، أظهرا نشاطًا مضادًا للبكتيريا جيدًا ضد ستة أنواع من البكتيريا المنتقاة. علاوة على ذلك، تظهر النتائج أن هناك تفاعلًا تلقائيًا بين AgNPs والحمض النووي وكذلك BSA عبر التفاعلات الكهروستاتيكية، المترجمة بواسطة معلمات ال ثابت K وطاقة الترابط. من جهة اخرى ووفقًا للنتائج التي تم الحصول عليها في الجسم الحي، كان هناك انخفاض في زيادة وزن الجسم بسبب تلوث الكادميوم وزيادة الوزن النسبي للكبد والكلى والقلب والدماغ، مع انخفاض الوزن المطلق والنسبي للخصية. علاوة على ذلك، فإن النتائج التي توصلت إليها الفئران المعالجة ب كلوريد الكادميوم تسببت في حدوث تغيرات معنوية في المعلمات الدموية والكيميائية الحيوية، المعلمات الهرمونية, وعلامات الإنزيمات الكبدية، ووظيفة الكلى مقارنة بالمجموعة الضابطة. ترافقت هذه التغييرات مع انخفاض في الدفاع المضاد للأكسدة (GSH وSOD وCAT) وزيادة في مستويات MDA. أظهرت البيانات بوضوح تدهور بنية الأنسجة المدروسة بالمقارنة مع المجموعة الضابطة، بما في ذلك تدهور شديد في خلايا الكبد والكلى، بينما أظهرت أنسجة الخصية نخرًا شديدًا. ومع ذلك، فان النظام العلاج مع السمهري و / أو AgNPs خفف من معظم الآثار السمية وأعاد النظام العلاجي جميع المعلمات المتغيرة السابقة.

في الختام، أظهرت هذه الدراسة النشاط البيولوجي الواعد لنبات السمهري و جسيمات الفضة النانوية ، وفي الوقت نفسه، تجدر الإشارة إلى الإمكانات العلاجية القوية ل نبات السمهري وAgNPs ضد السمية المستحثة بواسطة كلوريد الكادميوم في الفئران، مما يفتح آفاقًا جديدة لاستخدام العلاج بالنباتات والعلاج بالنانو ويعزز تطبيقهما في النهج الطبي

الكلمات المفتاحية: نبات السمهري، الجسيمات الفضة النانوية، التوليف الأخضر، الأنشطة البيولوجية، كلوريد الكادميوم، فئران Wistar